Neutron Stars in the Multi-Messenger Era

Sanjay Reddy
Institute for Nuclear Theory,
University of Washington, Seattle

Lecture 1: Basic notions of dense matter. Nuclear interactions and nuclear matter, effective field theory.

Lecture 2: Mass and radius. Linear response, proto-neutron star evolution, supernova neutrino emission and detection.

Lecture 3: Late neutron star cooling: Thermal and transport properties of degenerate matter, cooling of isolated neutron stars, heating and cooling in accreting neutron stars. Observational constraints.

Lecture 4: Neutron stars as laboratories for particle physics:Dark matter candidates (axions and other light weakly interacting particles, WIMPs, compact dark objects). Constraints from observations of neutron star masses, radii and cooling.

INSTITUTE for
NUCLEAR THEORY

Why is matter heterogeneous at sub-nuclear density?

Thinking Grand

$$P(\mu, T) = -\epsilon + \mu\, n + s\, T = -\frac{\Omega}{V}$$

pressure | energy density | number density | entropy density | free energy

The vacuum responds to a chemical potential and finite temperature and by producing a finite density of particles with the lowest free energy.

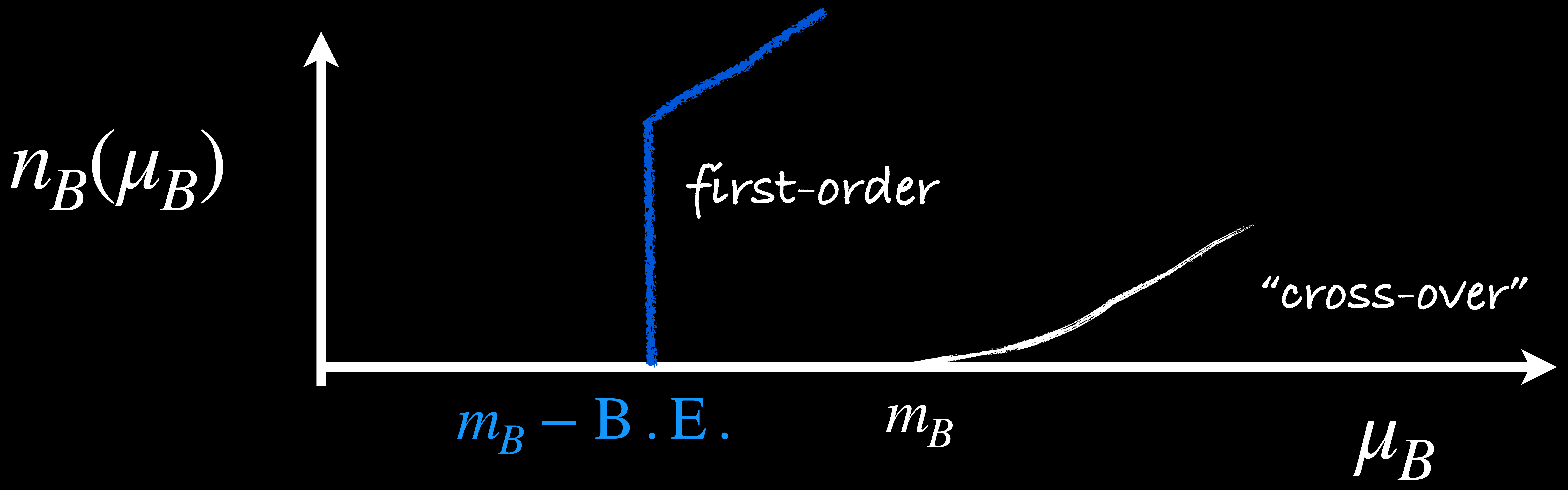

Thinking Grand Canonically

$$P(\mu, T) = -\epsilon + \mu\, n + s\, T = -\frac{\Omega}{V}$$

pressure

energy density

number density

entropy density

free energy

The vacuum responds to a chemical potential and finite temperature and by producing a finite density of particles with the lowest free energy.

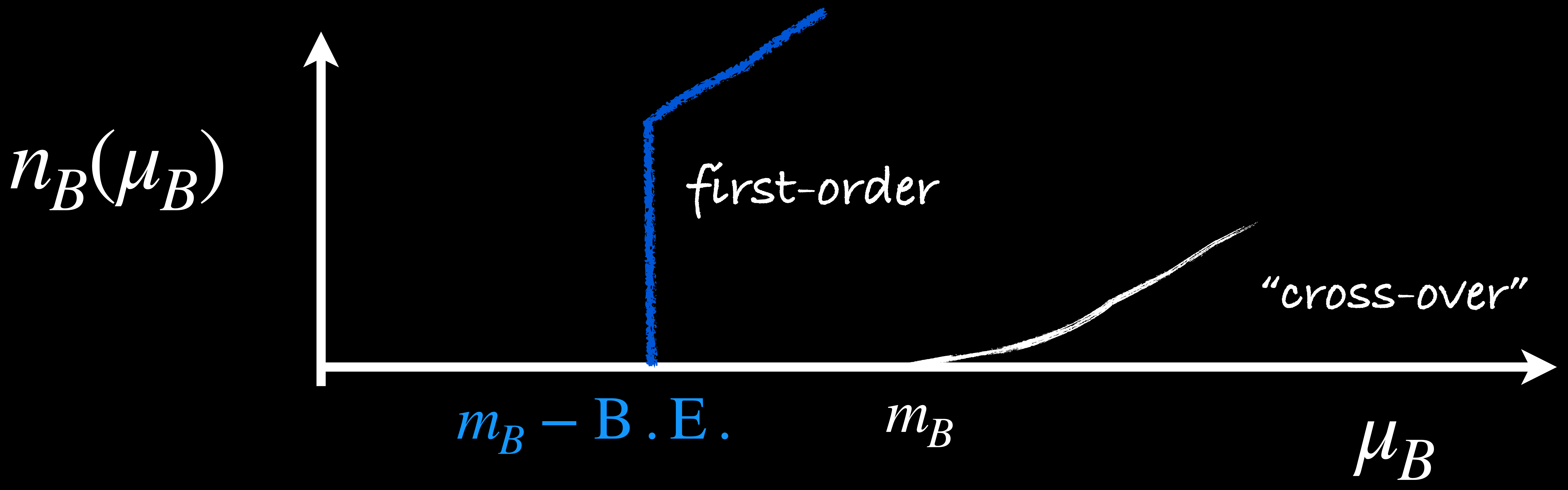

First-order transitions with 2 conserved Charges

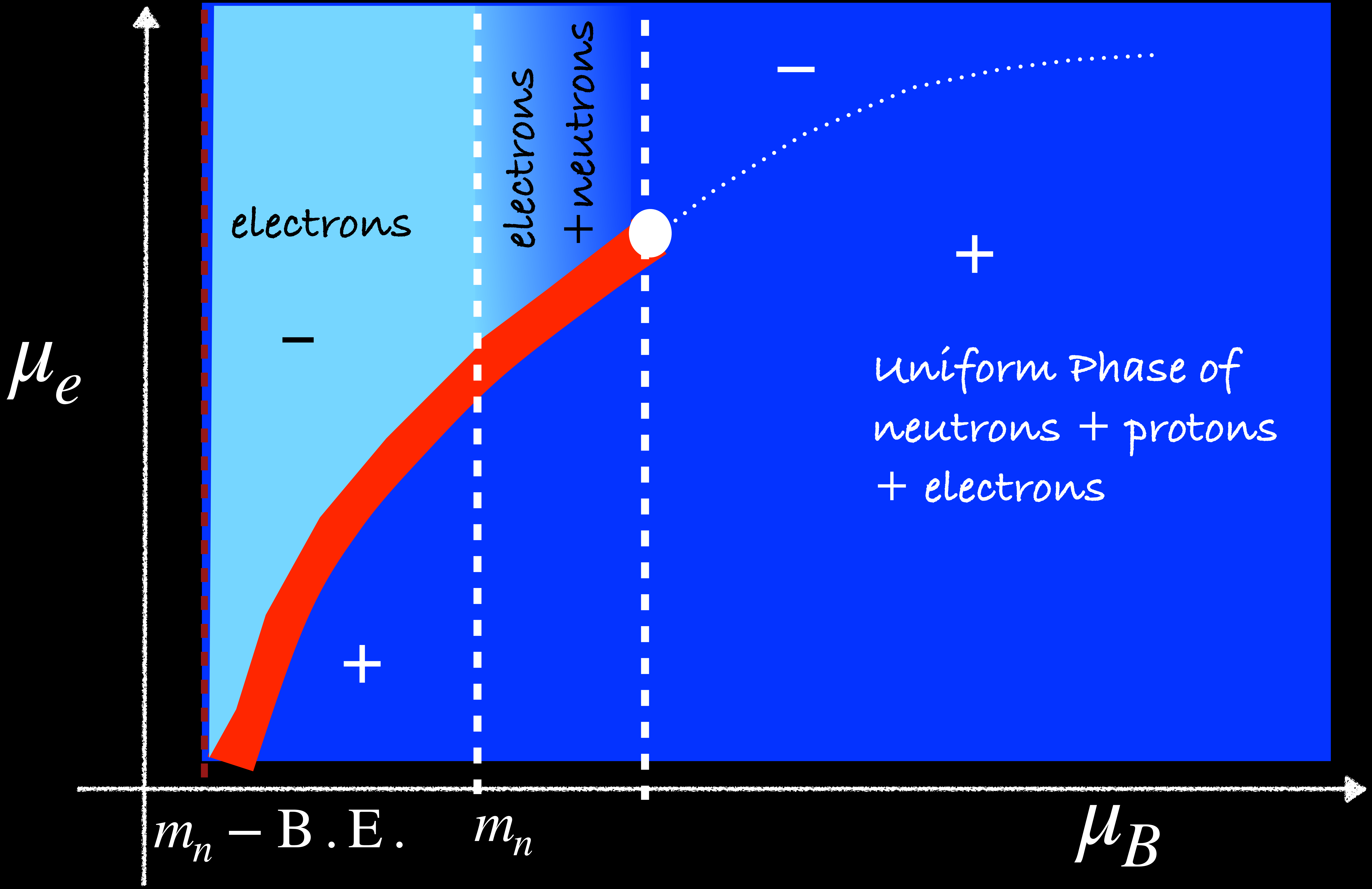

Global charge neutrality

Local charge neutrality

Energy cost due to Coulomb
and surface energies.

Surface and Coulomb Energies

$$E_S = 4\pi\sigma\ R^2 \qquad E_C = \frac{3}{5}\alpha_{\rm em}\ \frac{Z^2}{R} = \frac{3}{5}x_p^2\alpha_{\rm em}\ \frac{A^2}{R}$$

Constant density : $R = r_0 A^{1/3}$ $\qquad r_0 = \left(\frac{3}{4\pi\ n_0}\right)^{1/3} \simeq 1.14\ \text{fm}$

$$\boxed{\frac{E_S}{A} = 4\pi\ r_0^2\ \sigma\ \ A^{-1/3}} \qquad \boxed{\frac{E_C}{A} = \frac{3\ \alpha_{\rm em}\ x_p^2}{5\ r_0}\ A^{2/3}}$$

At the minimum : $$\frac{2}{3}E_C - \frac{1}{3}E_S = 0$$

or : $$E_S = 2E_C$$

Most favored nucleus has $A \simeq \left(\frac{r_0}{1.2\ \text{fm}}\right)^3 \left(\frac{\sigma}{1\ \text{MeV/fm}^2}\right)\ \frac{4\pi}{x_p^2}$

Neutron-rich nuclei

At fixed A:

(i) The nuclear symmetry energy favors small (N-Z).

(ii) Coulomb energy favors small Z.

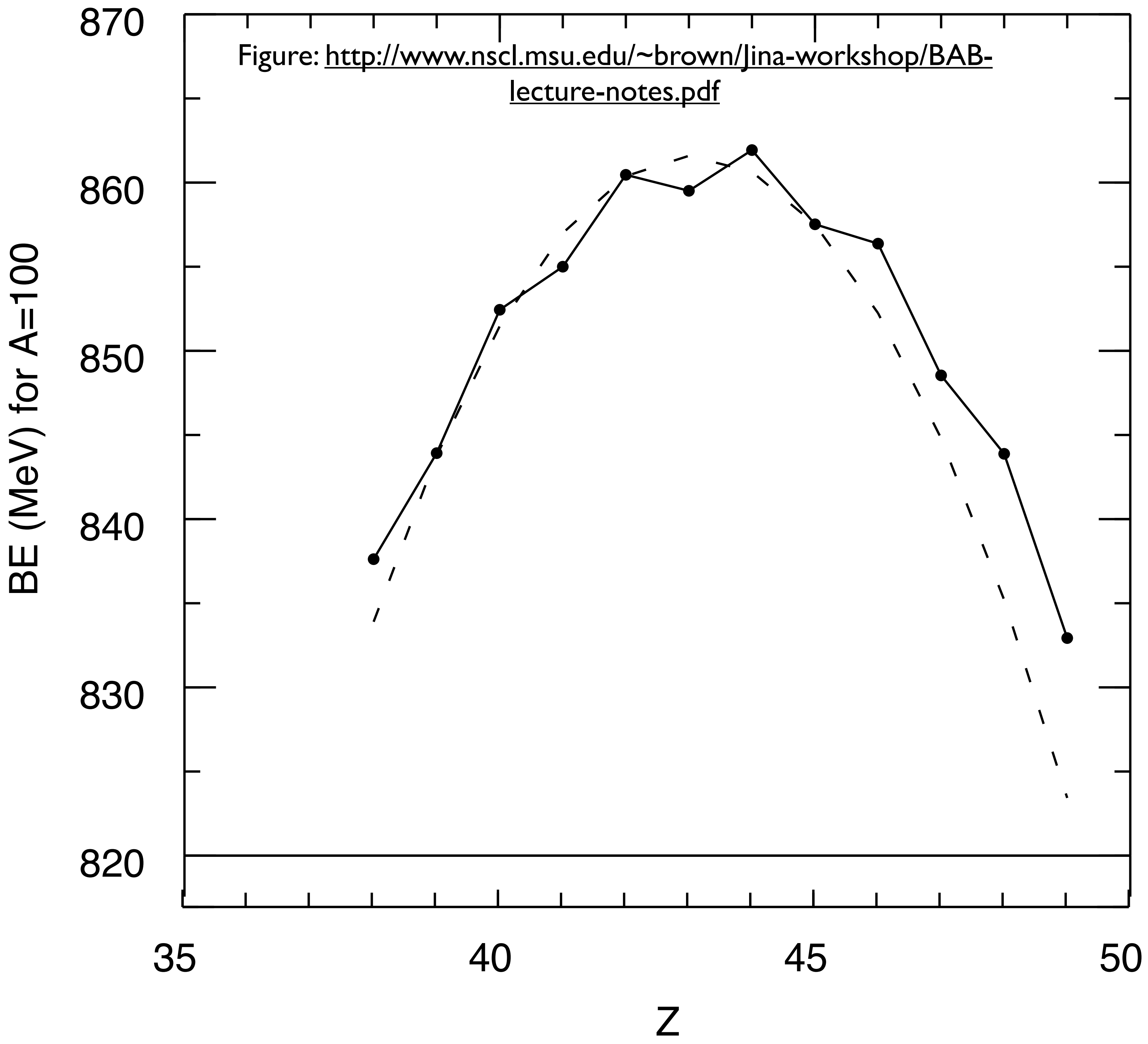

nuclei with "excess" neutrons or protons are unstable to weak interactions.

$$\hat{\mu} = \mu_n - \mu_p = \frac{\partial \text{ B.E}(A,Z)}{\partial Z} + (m_n - m_p)$$

$$= 4\alpha_{\text{sym}} \; (1 - 2\frac{Z}{A}) - 2\alpha_C \; \frac{Z}{A^{1/3}} + (m_n - m_p)$$

Problem : Show that for A=100, Z=44 is the most stable nucleus.

Use: $\alpha_{\text{sym}} = 28 \text{ MeV} \qquad \alpha_C = 0.697 \text{ MeV}$

Nuclei immersed in a dense electron gas

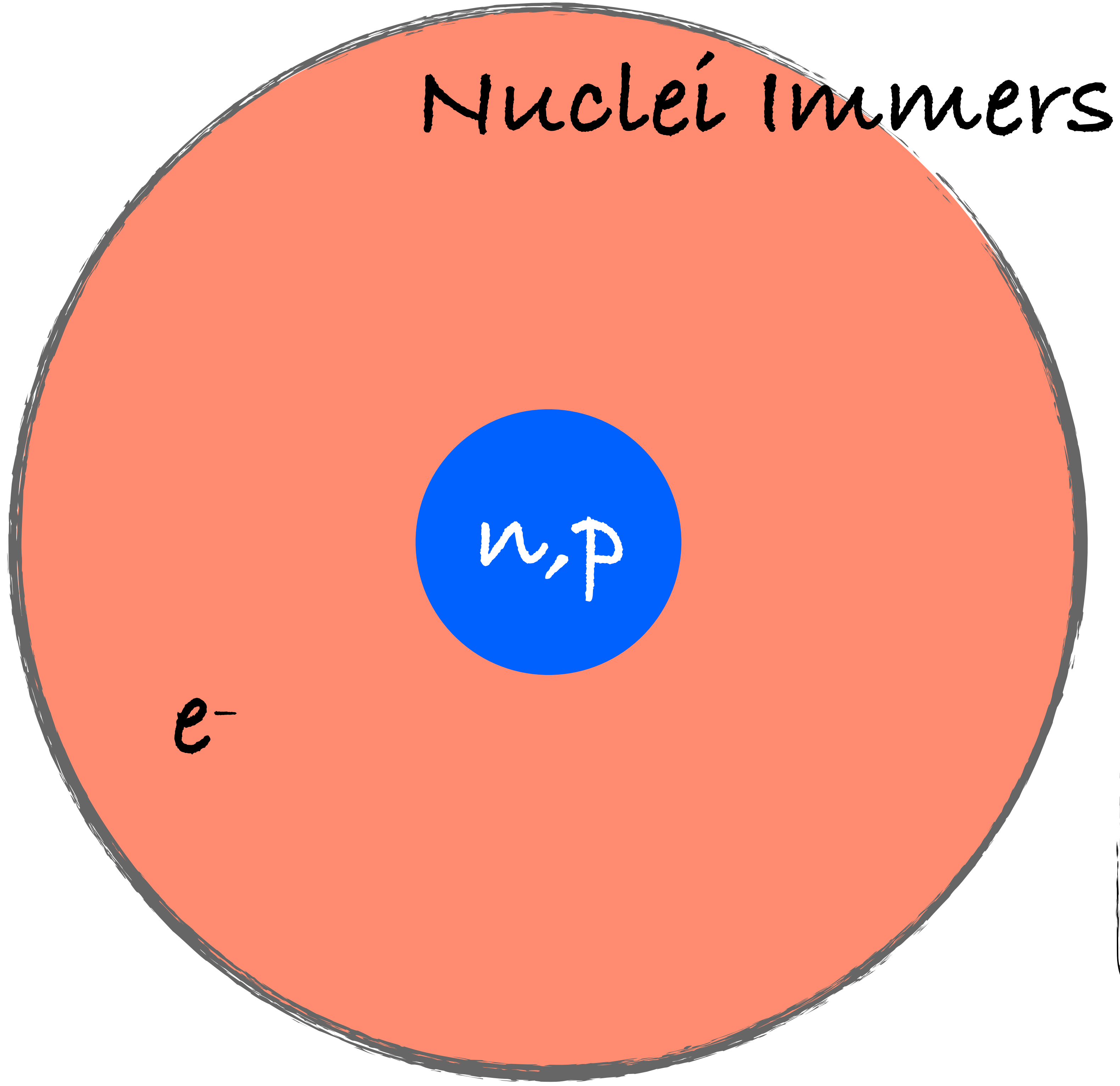

Beta Equilibrium:

$$e^- + p \to n + \nu_e, \qquad n \to p + e^- + \bar{\nu}_e$$

$$\mu_n - \mu_p = \mu_e \simeq 4\ \alpha_{\rm sym}(1 - 2\ x_p)$$

$$\boxed{x_p \simeq \frac{1}{2}\left(1 - \frac{\mu_e}{4\ \alpha_{\rm sym}}\right)\left(1 + \frac{\alpha_{\rm C}\ A^{2/3}}{4\ \alpha_{\rm sym}}\right)^{-1}}$$

Neutron Fermi levels rise : $\mu_n \simeq -\alpha_{\rm bulk} + 2\alpha_{\rm sym}[(1 - 2x_p) - \frac{1}{2}(1 - 2x_p)^2]$

Nuclei immersed in a dense electron gas

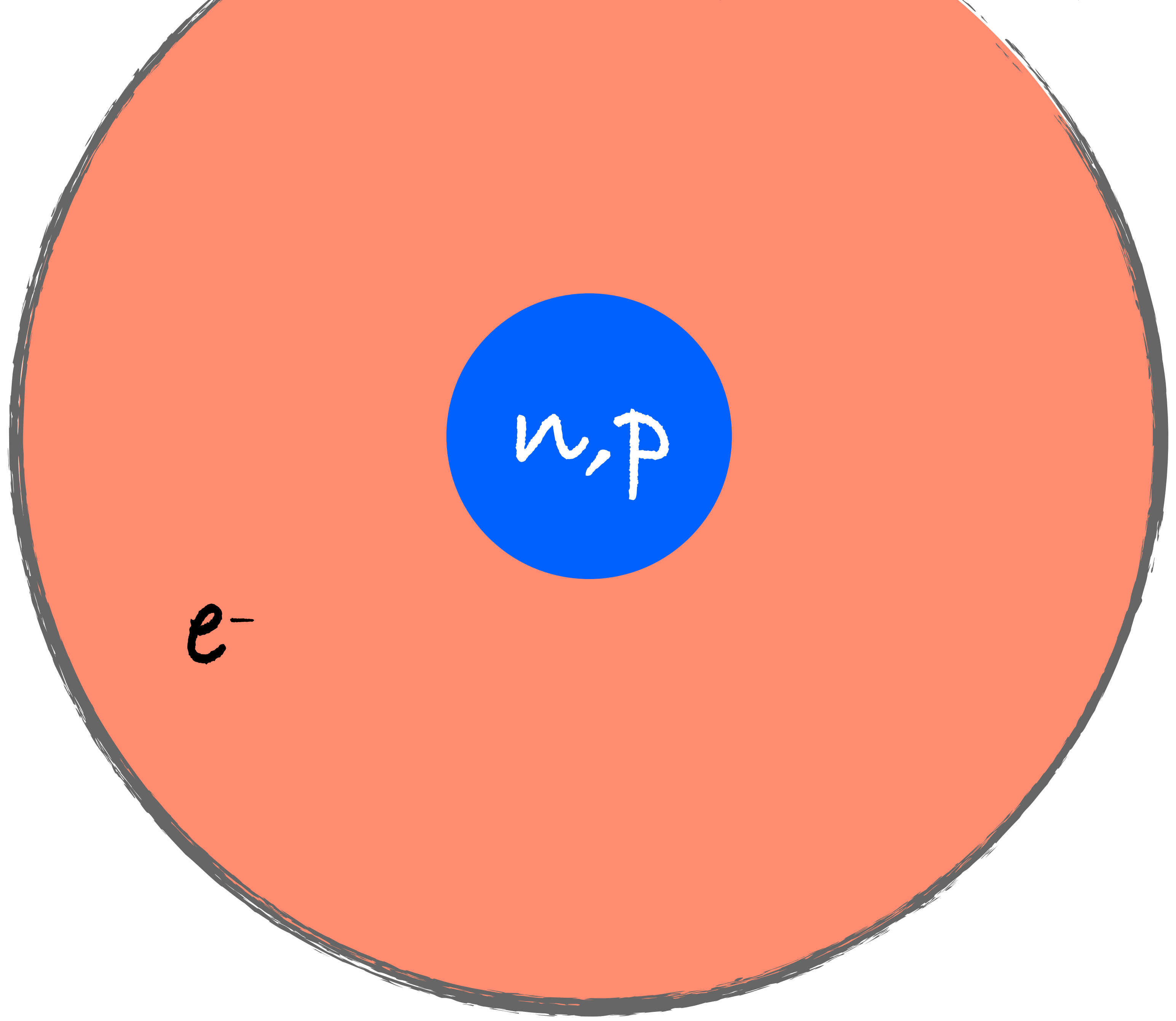

Beta Equilibrium:

$$e^- + p \to n + \nu_e, \quad n \to p + e^- + \bar{\nu}_e$$

$$\mu_n - \mu_p = \mu_e \simeq 4\ \alpha_{\rm sym}(1 - 2\ x_p)$$

$$x_p \simeq \frac{1}{2}\left(1 - \frac{\mu_e}{4\ \alpha_{\rm sym}}\right)\left(1 + \frac{\alpha_C\ A^{2/3}}{4\ \alpha_{\rm sym}}\right)^{-1}$$

Neutron Fermi levels rise : $\mu_n \simeq -\alpha_{\rm bulk} + 2\alpha_{\rm sym}[(1 - 2x_p) - \frac{1}{2}(1 - 2x_p)^2]$

Neutrons drip at : $x_p \simeq \frac{1}{2}\sqrt{1 - \frac{\alpha_{\rm bulk}}{\alpha_{\rm sym}}} \approx 0.34$

What have we ignored thus far ?

- Shell structure - Magic numbers

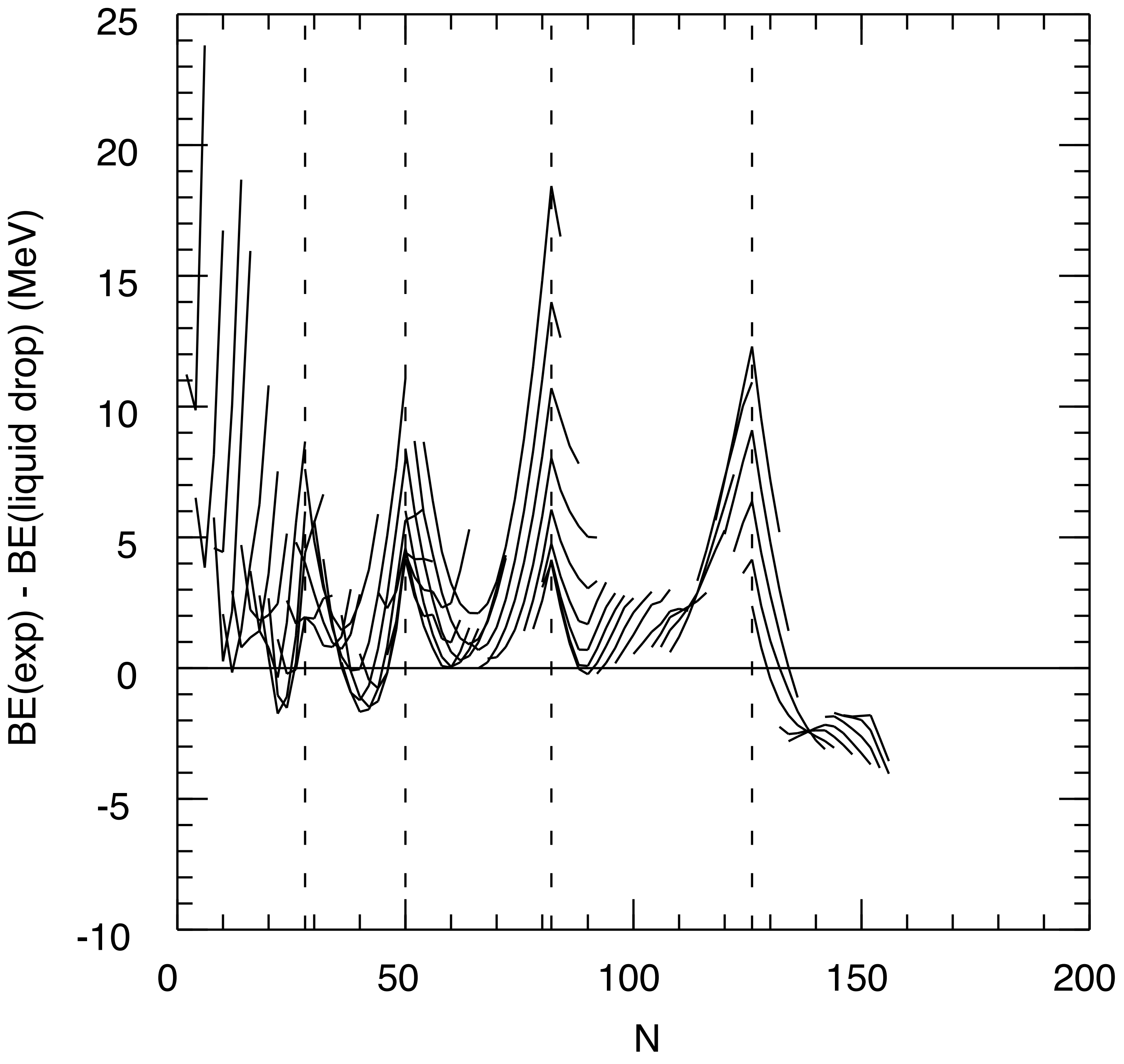

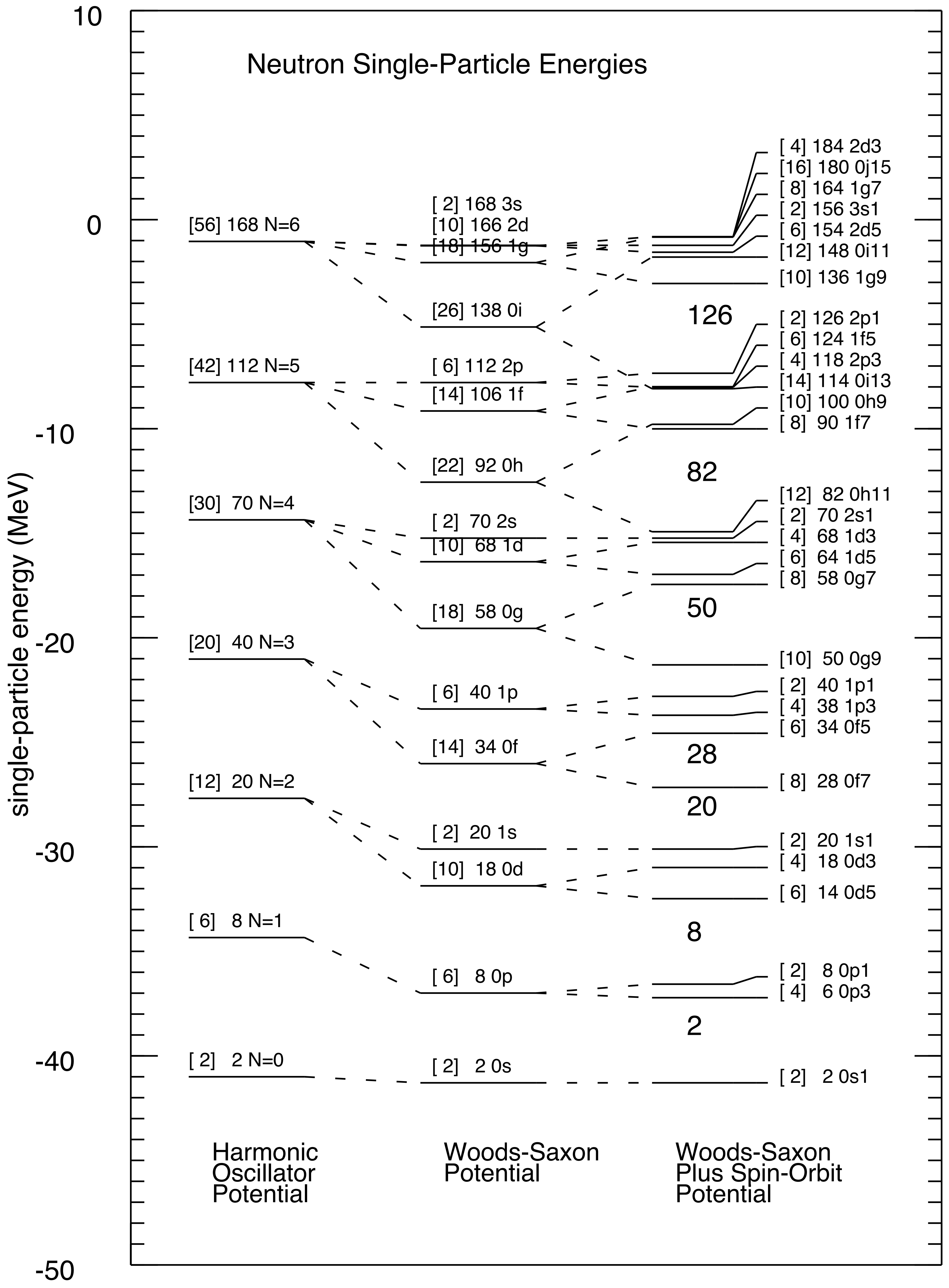

Figures: http://www.nscl.msu.edu/~brown/Jina-workshop/BAB-lecture-notes.pdf

Pairing

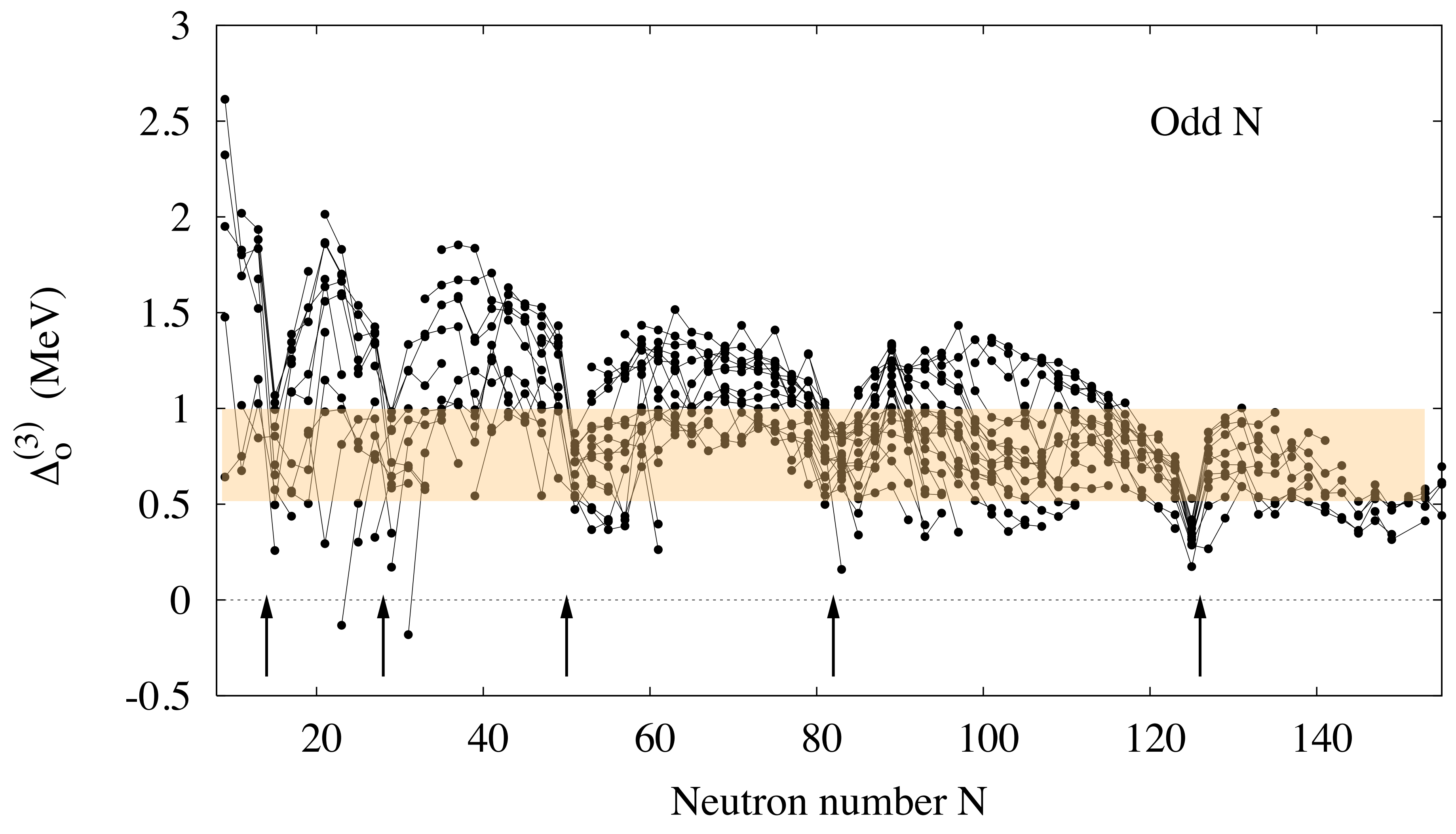

Bertsch, arXiv:1203.5529

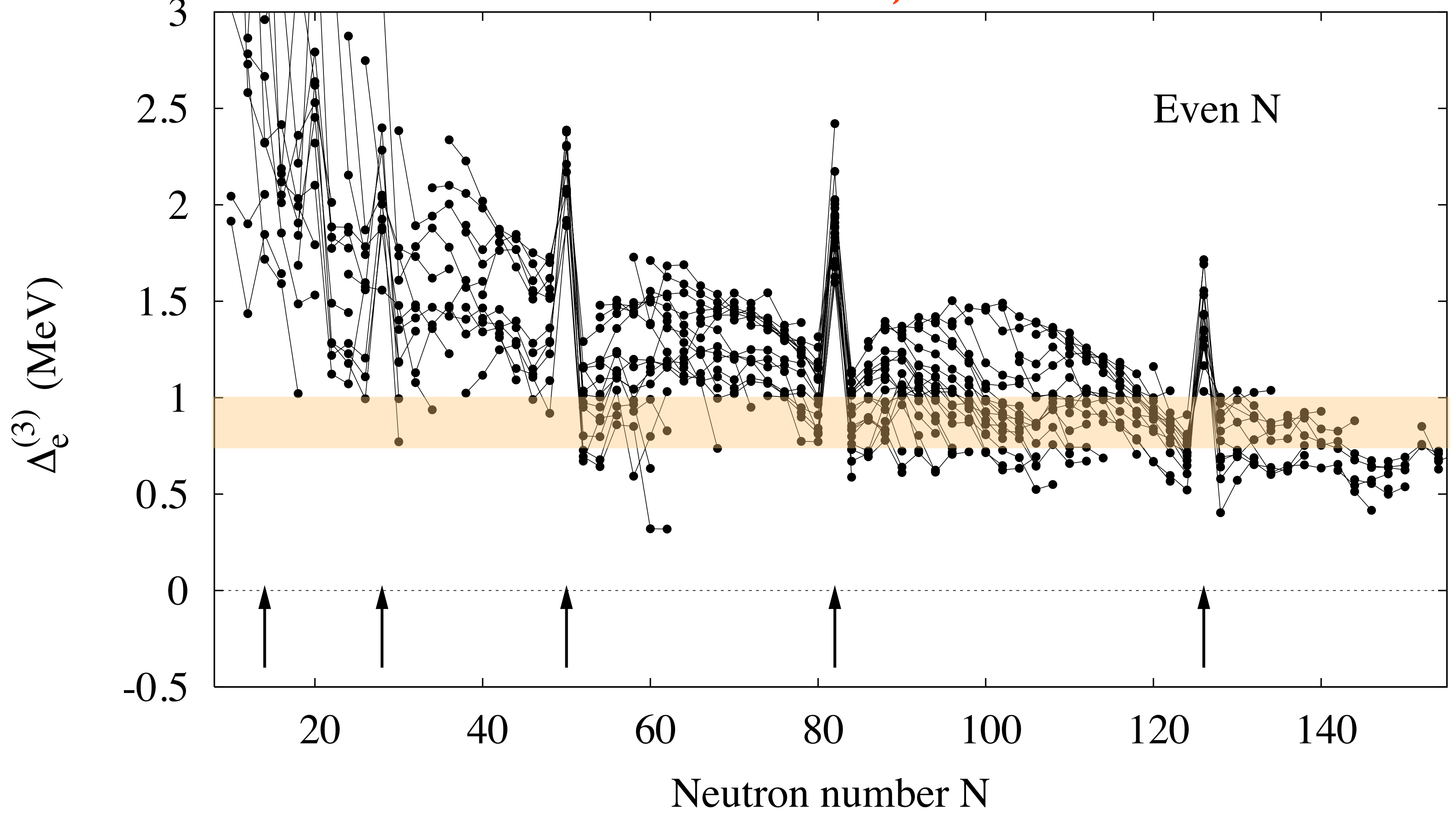

$$\Delta^{(3)}_{o,Z}(N) = \frac{1}{2}(E_b(Z,N+1) - 2E_b(Z,N) + E_b(Z,N-1))$$

$$\Delta^{(3)}_{e,Z}(N) = -\frac{1}{2}(E_b(Z,N+1) - 2E_b(Z,N) + E_b(Z,N-1))$$

There is a gap in the single particle spectrum
Systems with odd number of neutrons or protons
have lower relative binding energy.

Sequence of nuclei encountered in the neutron star outer crust.

From ^{56}Fe to ^{118}Kr

Table 1 Nuclides in the ground state of cold matter as a function of density, from Haensel & Pichon (21)

Element	Z	N	Z/A	ρ_{max}^{a} (g cm^{-3})	μ_e^{b} (MeV)	$\Delta\rho/\rho^{c}$ (%)
Using experimental nuclear masses						
^{56}Fe	26	30	0.4643	$7.96\ 10^{6}$	0.95	2.9
^{62}Ni	28	34	0.4516	$2.71\ 10^{8}$	2.61	3.1
^{64}Ni	28	36	0.4375	$1.30\ 10^{9}$	4.31	3.1
^{66}Ni	28	38	0.4242	$1.48\ 10^{9}$	4.45	2.0
^{86}Kr	36	50	0.4186	$3.12\ 10^{9}$	5.66	3.3
^{84}Se	34	50	0.4048	$1.10\ 10^{10}$	8.49	3.6
^{82}Ge	32	50	0.3902	$2.80\ 10^{10}$	11.44	3.9
^{80}Zn	30	50	0.3750	$5.44\ 10^{10}$	14.08	4.3
^{78}Ni	28	50	0.3590	$9.64\ 10^{10}$	16.78	4.0
From the mass formula of Möller (1992), unpublished results						
^{126}Ru	44	82	0.3492	$1.29\ 10^{11}$	18.34	3.0
^{124}Mo	42	82	0.3387	$1.88\ 10^{11}$	20.56	3.2
^{122}Zr	40	82	0.3279	$2.67\ 10^{11}$	22.86	3.4
^{120}Sr	38	82	0.3167	$3.79\ 10^{11}$	25.38	3.6
^{118}Kr	36	82	0.3051	$(4.33\ 10^{11})^{d}$	(26.19)	

[a] ρ_{max} is the maximum density at which the nuclide is present.
[b] μ_e is the electron chemical potential (including electron rest mass) at that density.
[c] $\Delta\rho/\rho$ is the fractional increase in the mass density in the transition to the next nuclide.
[d] The lines with ρ_{max} in parentheses correspond to the neutron drip point.

Electron-nucleus Interaction and Lattice Energy

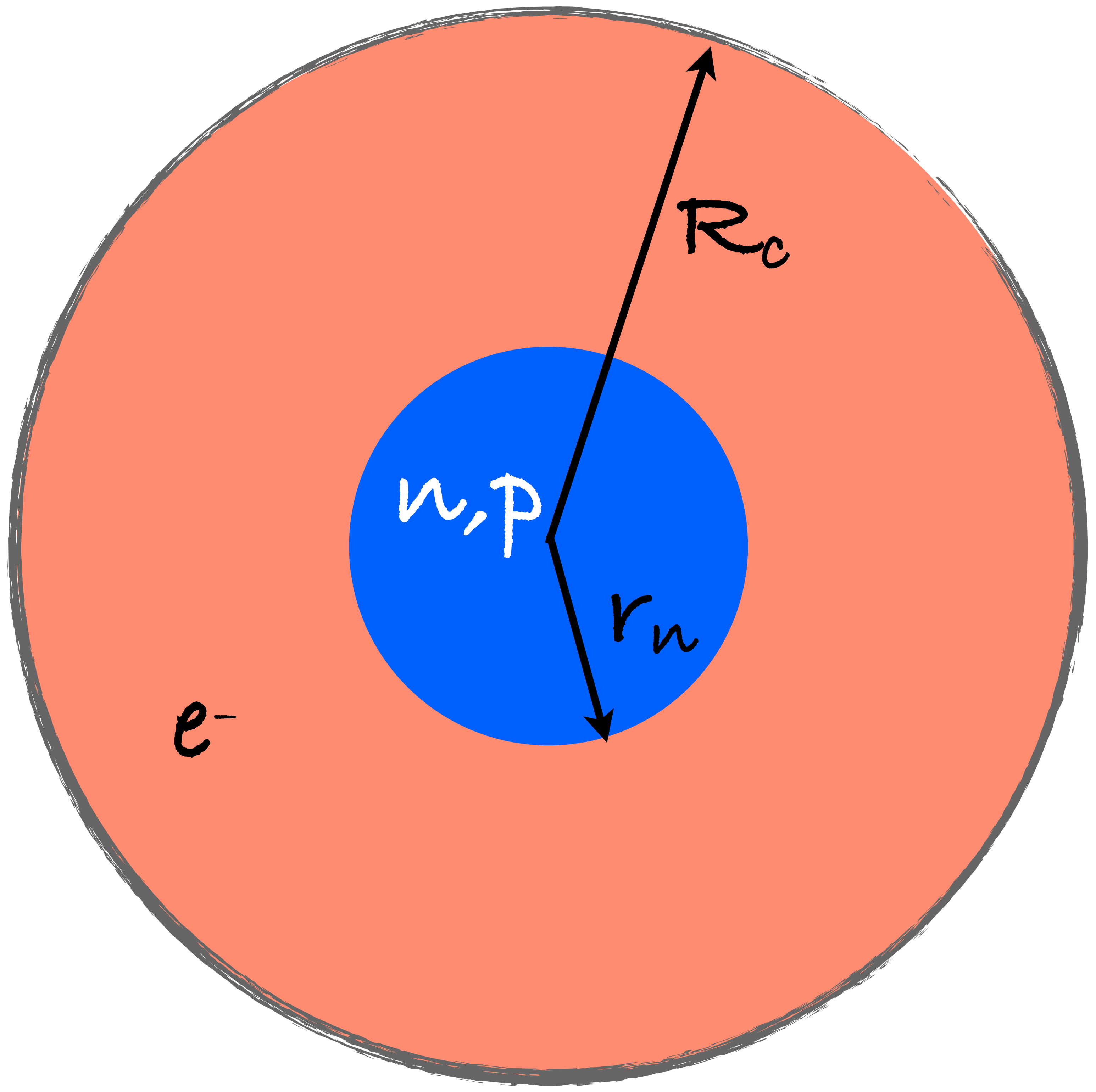

unit cell

To good approximation, electron charge distribution is uniform.

$$E_C = \frac{3}{5}\frac{Z^2\alpha}{r}\left(1 - \frac{3}{2}\frac{r}{R} + \frac{1}{2}\frac{r^3}{R^3}\right)$$

Nucleus becomes unstable to deformations when

$$E_C^0 = \frac{3}{5}\frac{Z^2\alpha}{r} > 2\ E_S$$

or $\left(1 - \frac{3}{2}\frac{r}{R} + \frac{1}{2}\frac{r^3}{R^3}\right) < \frac{1}{4}$ or $\frac{r}{R} > 0.56$

Bohr-Wheeler (1938)

Non-spherical nuclei or Pasta

For spherical nuclei $$E_{\rm C} = \frac{3}{5}\frac{Z^2\alpha}{r}\left(1 - \frac{3}{2}\frac{r}{R} + \frac{1}{2}\frac{r^3}{R^3}\right)$$

For "d" dimensional structures:

$$\boxed{\frac{E_C}{V} = 2\pi\ \alpha\ n_p^2\ r^2\ u\ f_d(u)}$$

$$\boxed{\frac{E_S}{V} = \frac{d\ u\ \sigma}{r}}$$

where:

$$f_3(u) = \frac{1}{5}(2 - 3u^{1/3} + u) \simeq \frac{2}{5},$$

$$f_2(u) = \frac{1}{4}\left(\ln\frac{1}{u} - 1 + u\right) \simeq \frac{1}{4}\ln\frac{1}{eu}$$

$$f_1(u) = \frac{1}{3}\left(\frac{1}{u} - 2 + u\right) \simeq \frac{1}{3u}.$$

For small surface tension Pasta is favored.

Baym, Bethe, Pethick (1971)

Energy gain is modest and model dependent

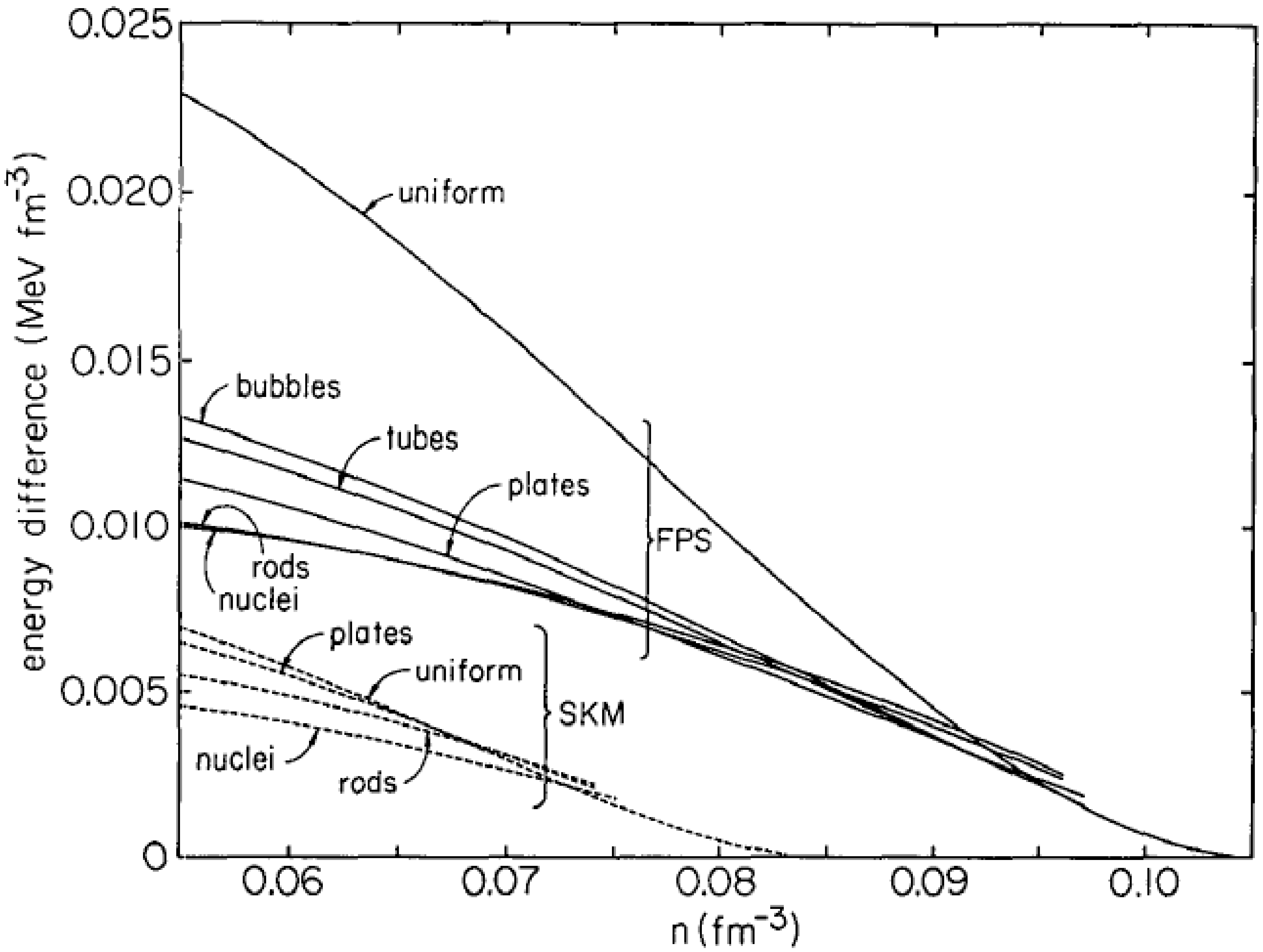

Baym, Bethe, Pethick (1971)

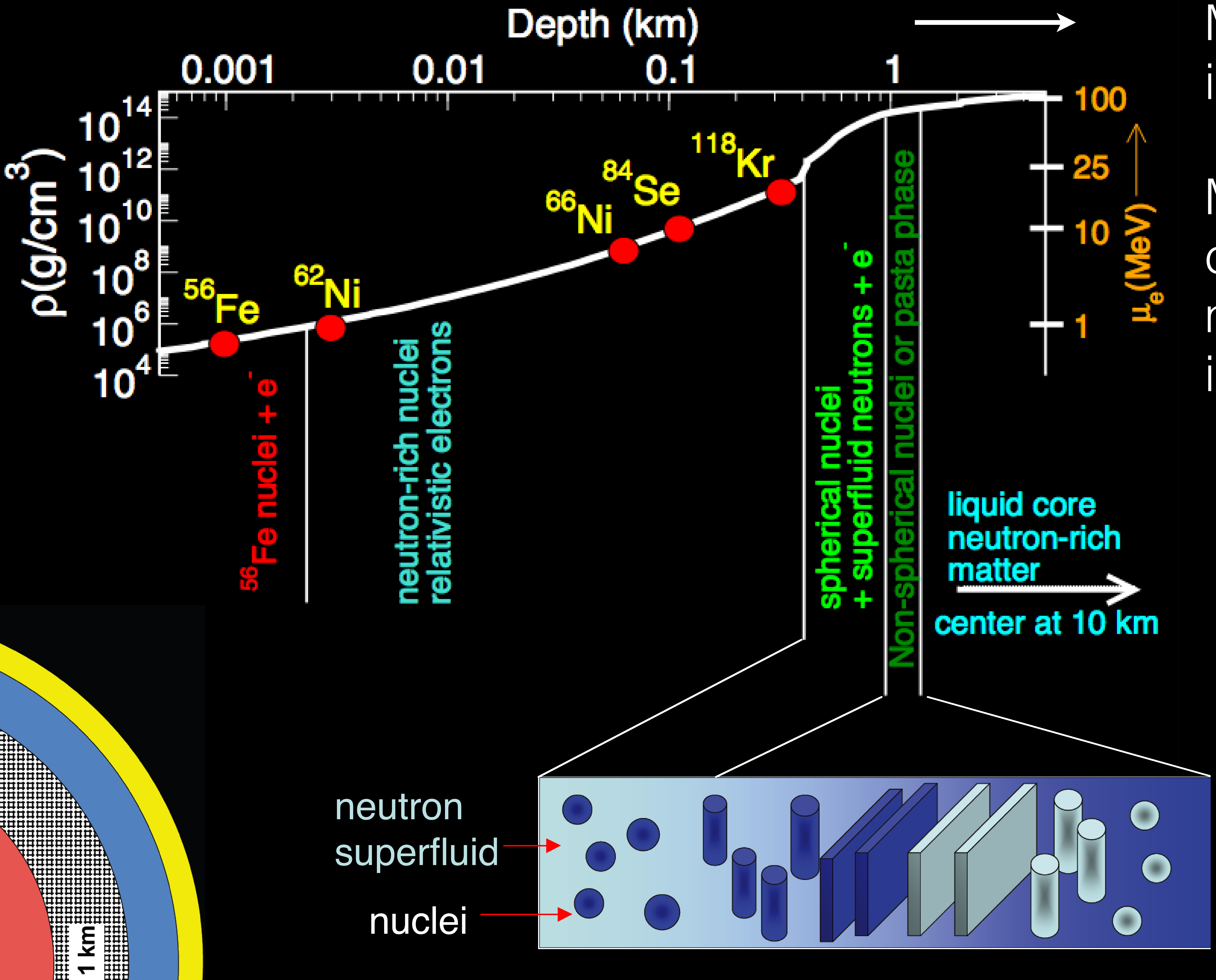

Mass contained in the crust is small ~ few percent.

Most of it is in the inner-crust as either spherical or non-spherical nuclei immersed in a neutron fluid.

Neutron Fraction:

Outer Crust < 70%.
Inner Crust ~ 90%.
Outer Core: > 90%

Equation of State and Neutron Star Structure

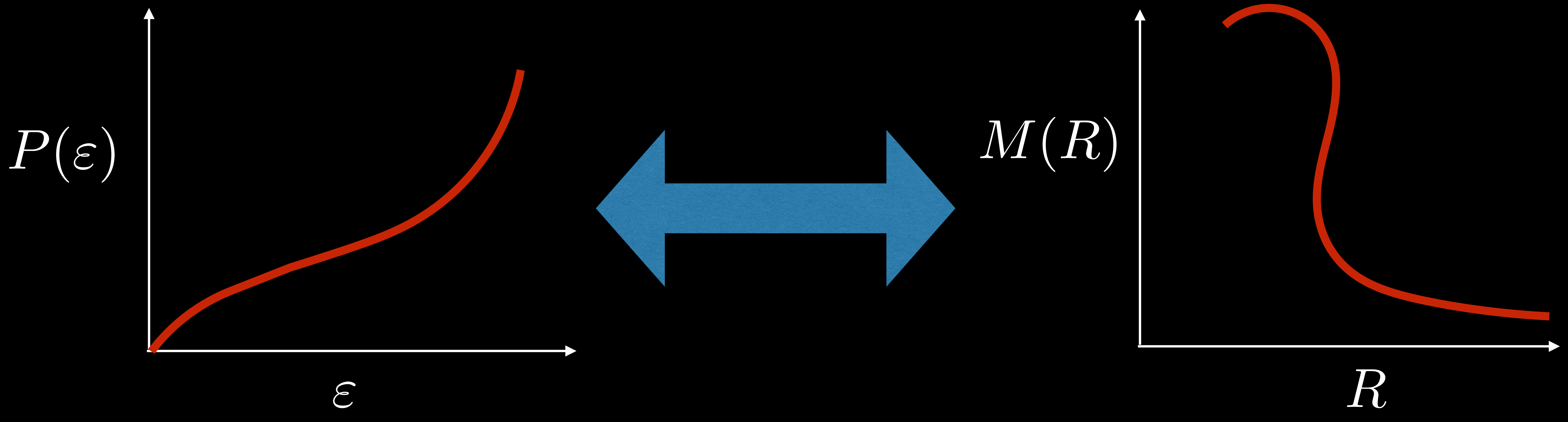

$$P(\varepsilon) + \text{Gen.Rel.} = M(R)$$

Equation of State and Neutron Star Structure

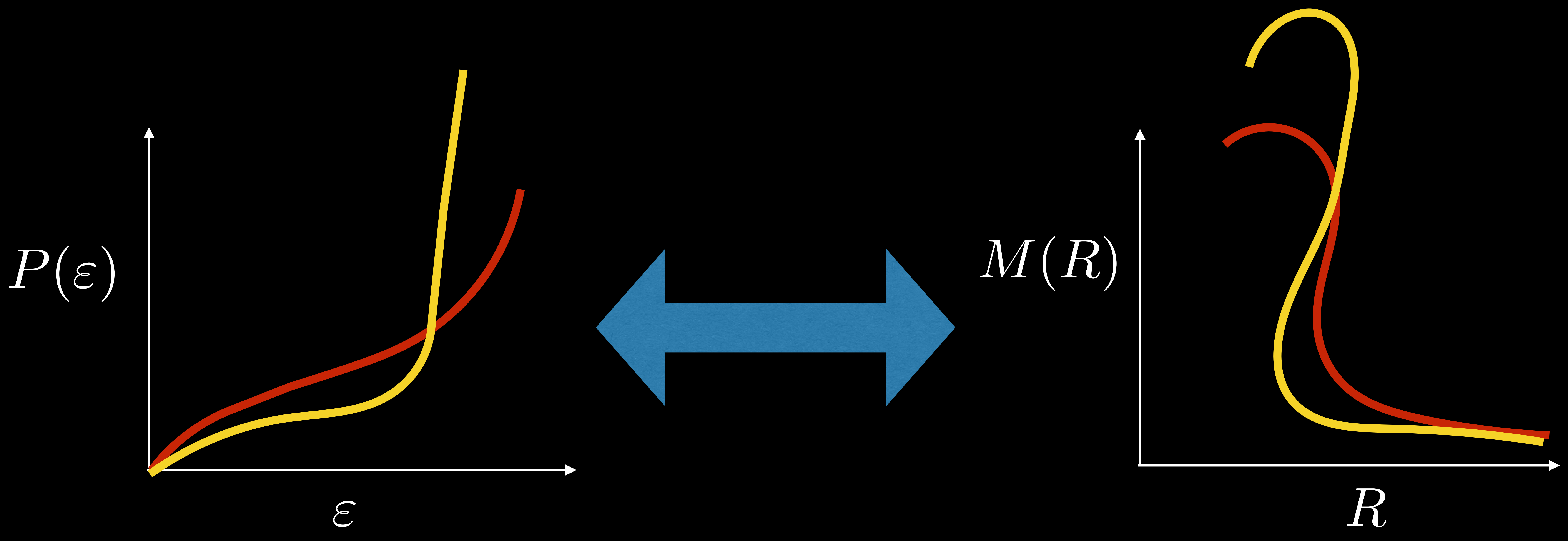

$$P(\varepsilon) + \mathrm{Gen.Rel.} = M(R)$$

Equation of State and Neutron Star Structure

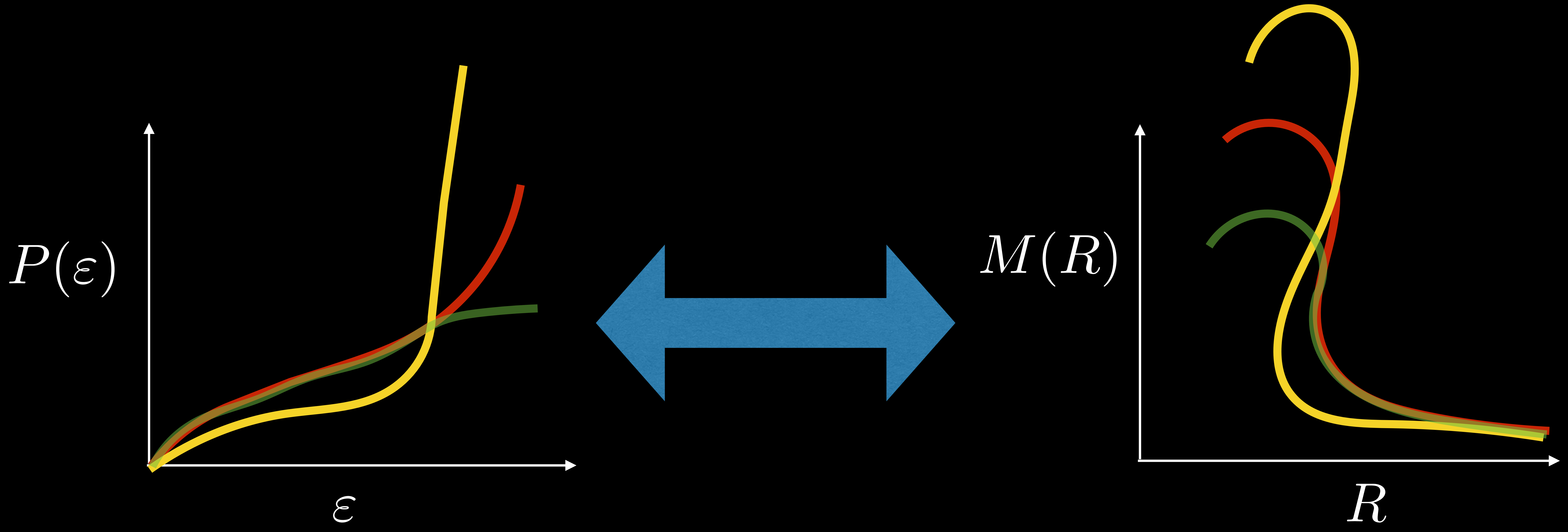

$$P(\varepsilon) + \mathrm{Gen.Rel.} = M(R)$$

Equation of State and Neutron Star Structure

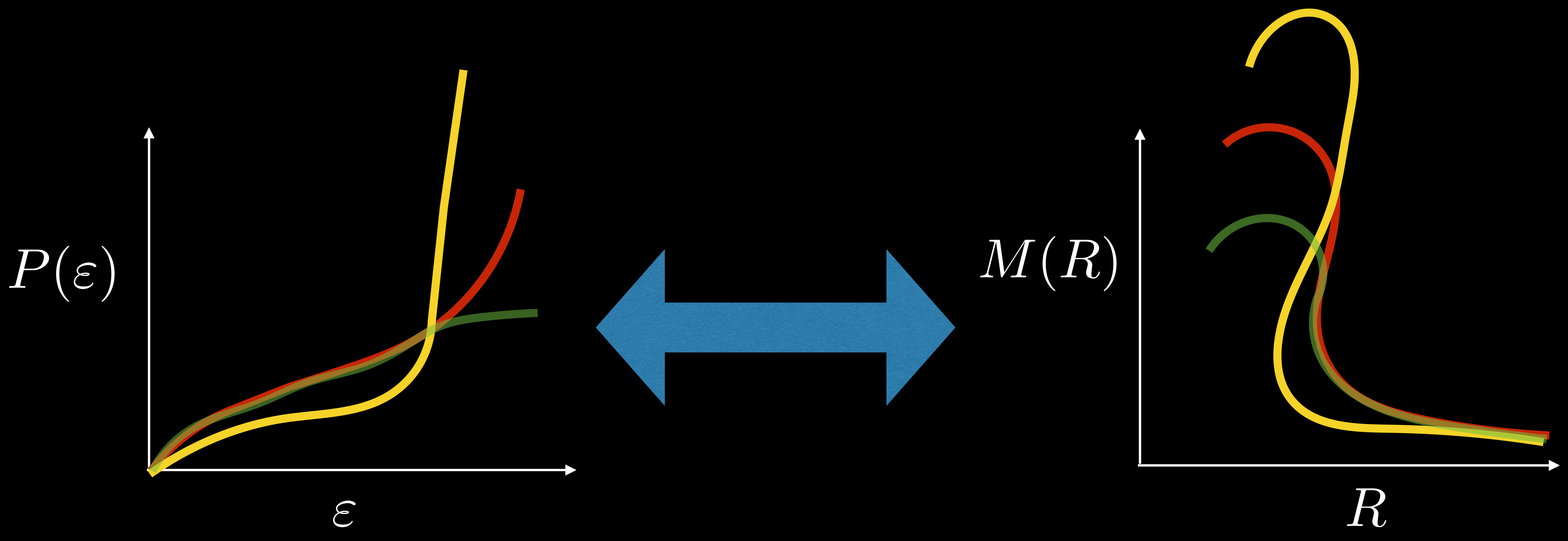

$$P(\varepsilon) + \mathrm{Gen.Rel.} = M(R)$$

A small radius and large maximum mass implies a rapid transition from low pressure to high pressure with density.

Constraints on the Equation of State

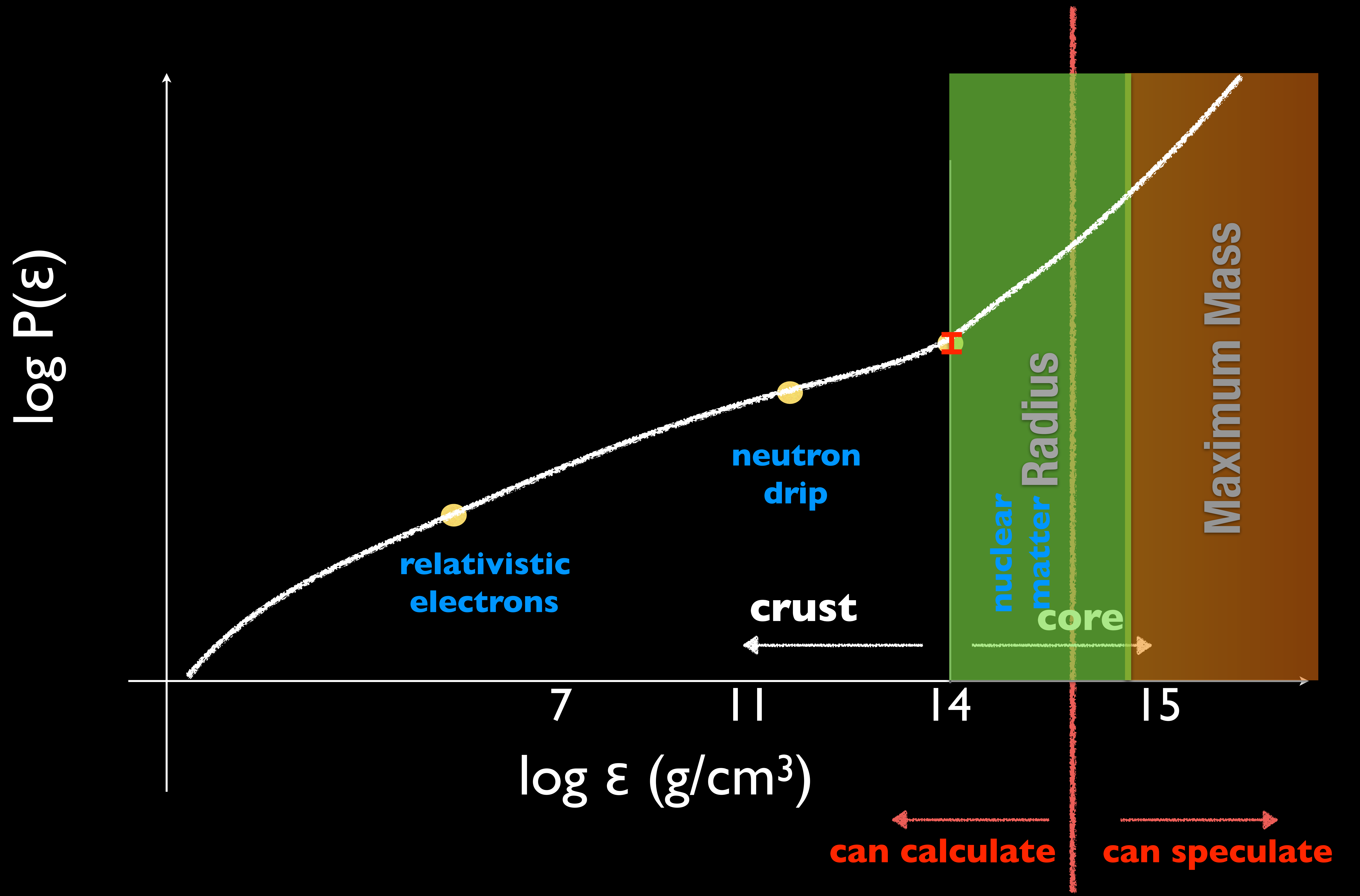

Constraints on the Equation of State

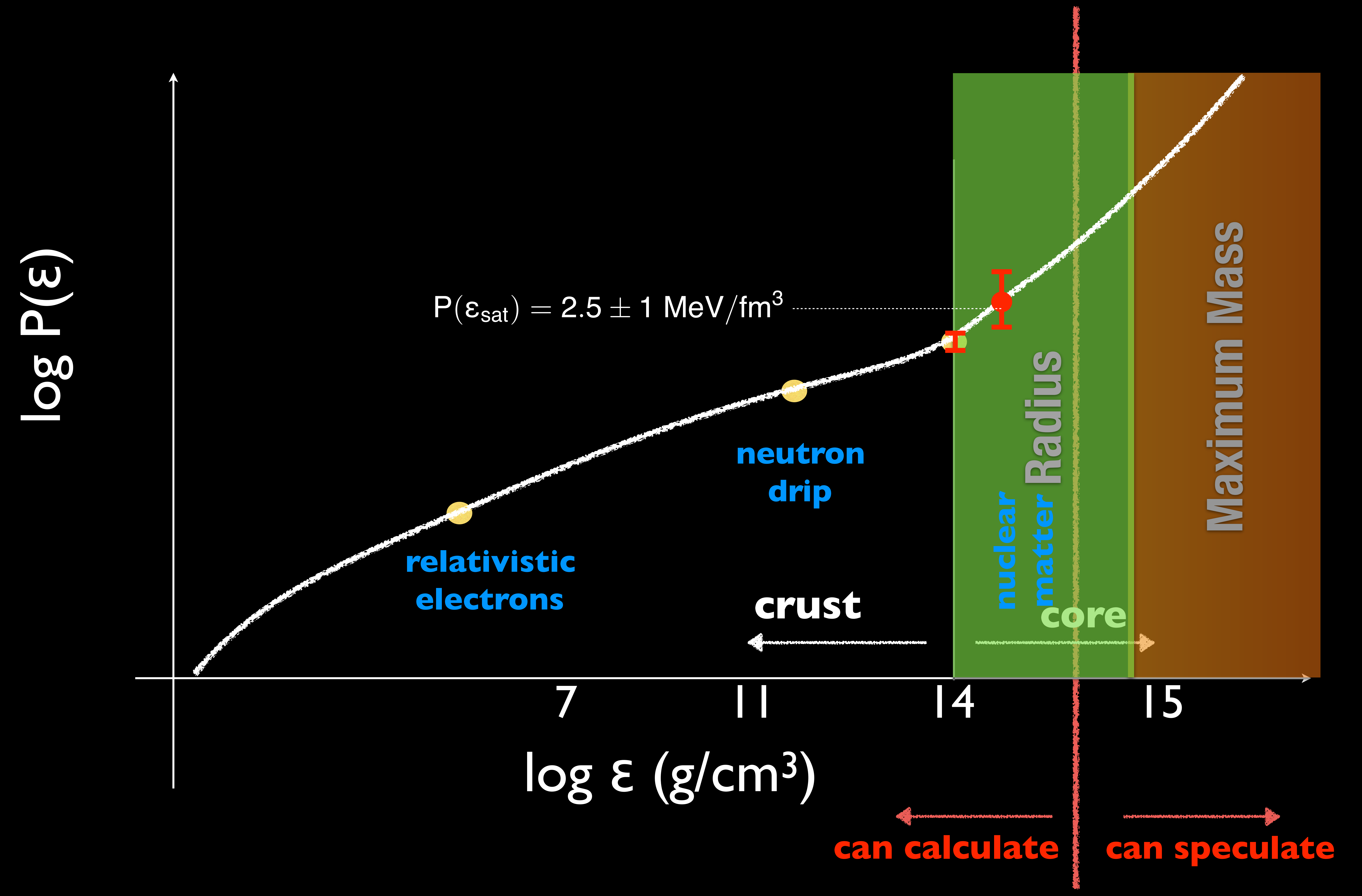

Constraints on the Equation of State

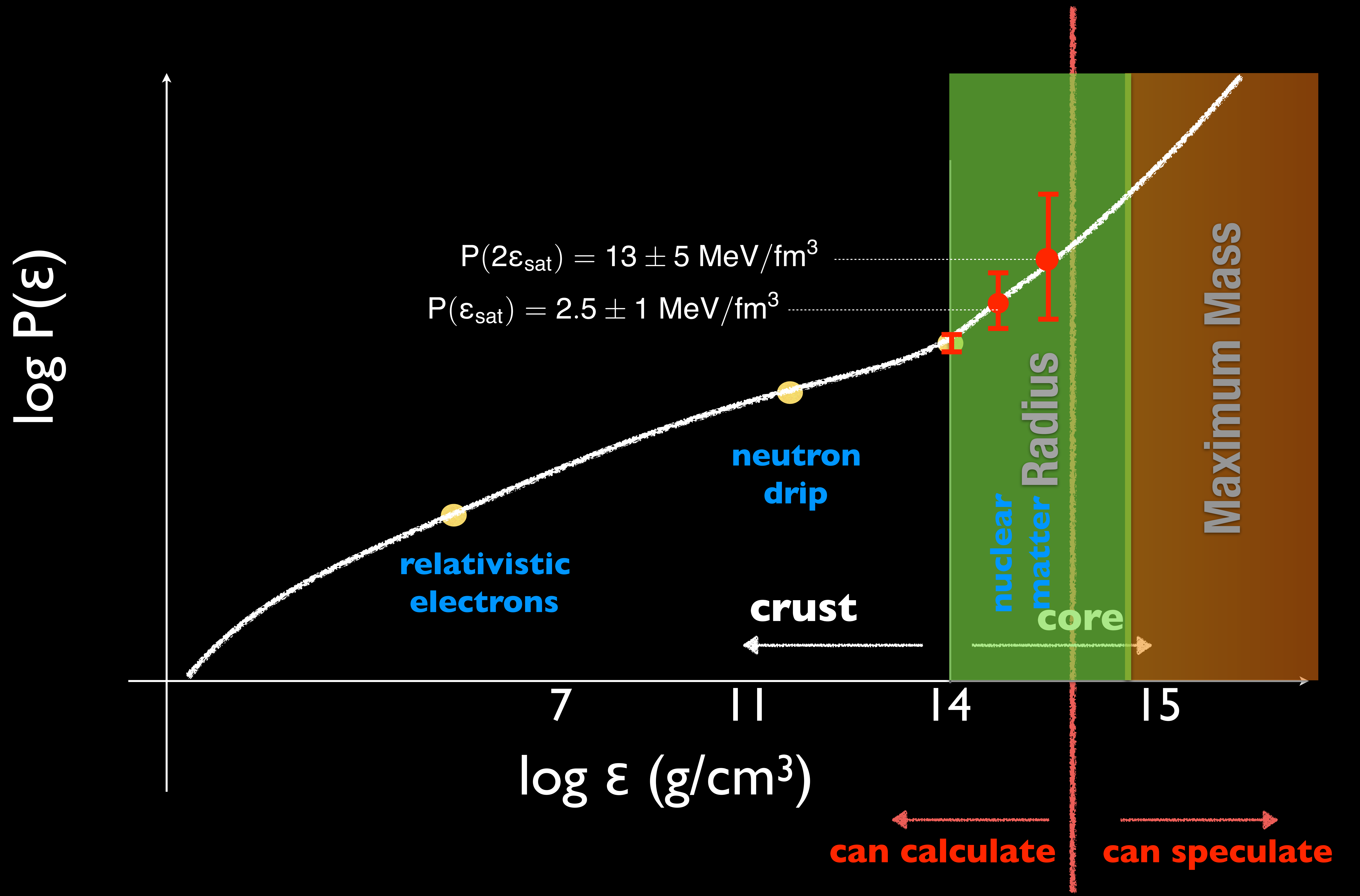

Constraints on the Equation of State

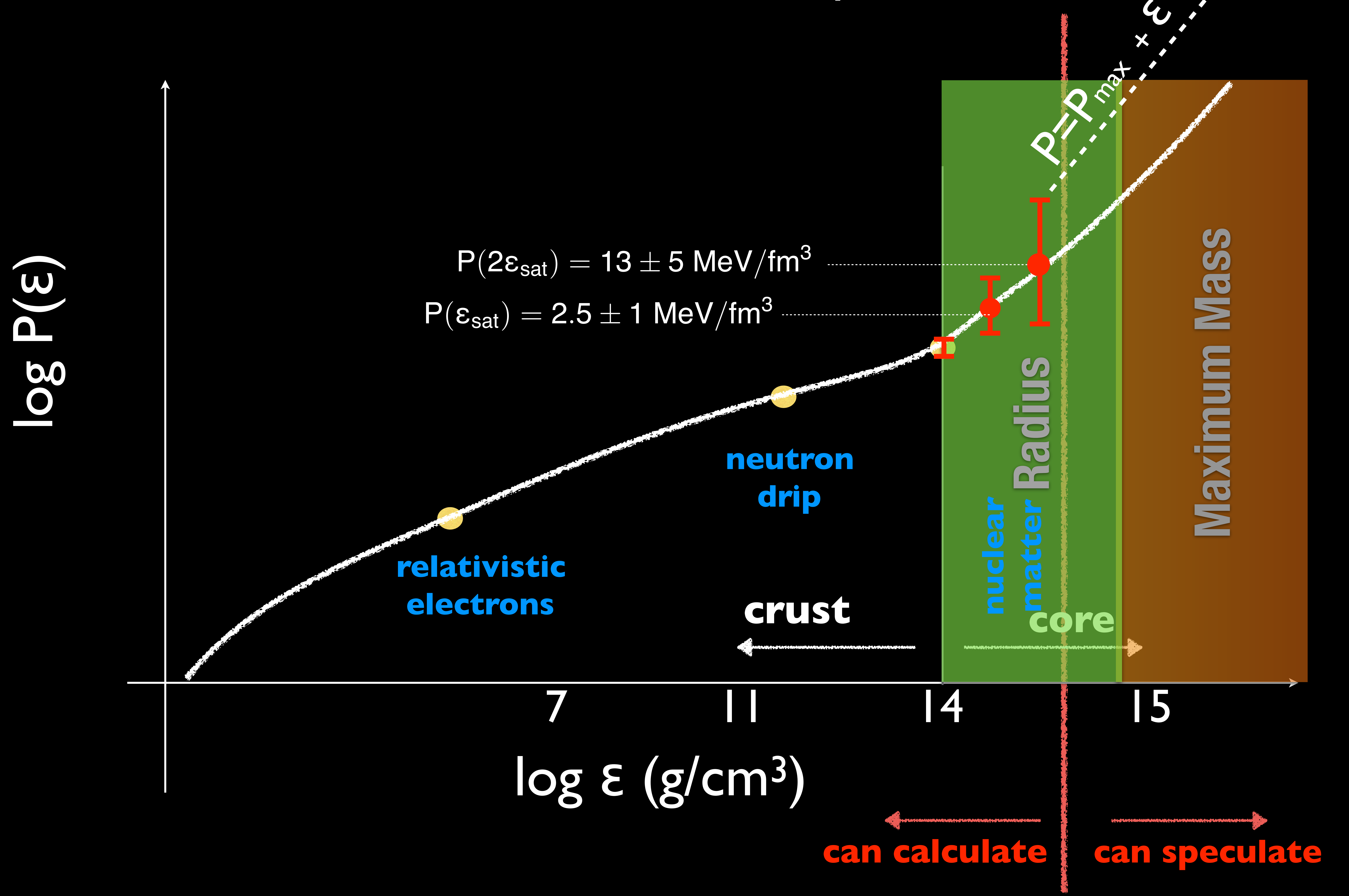

Constraints on the Equation of State

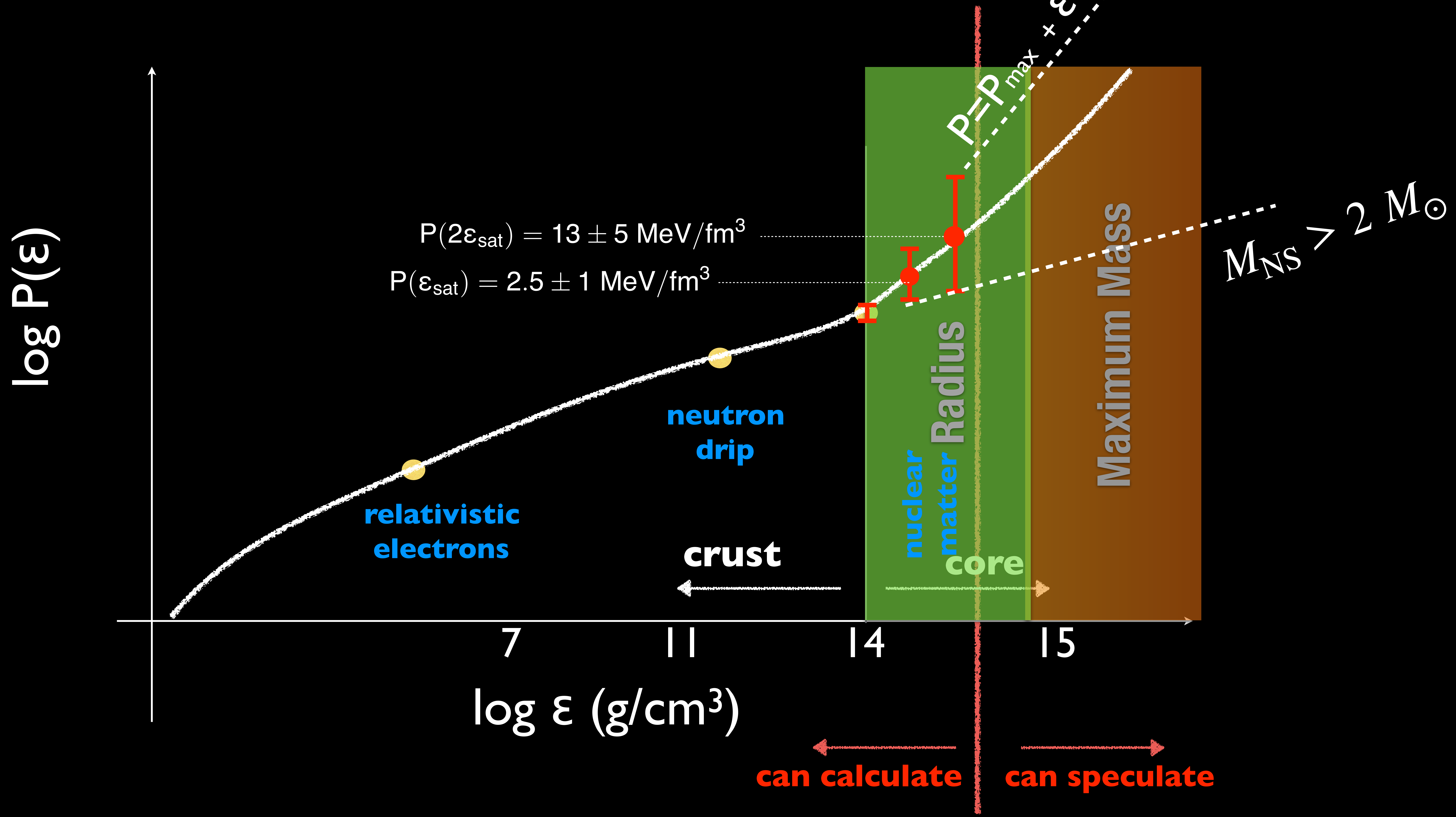

Dense matter EOS and NS structure

Neutron matter calculations and a sound speed at higher density constrained by 2 solar mass NS and causality provide useful constraints on the NS properties.

$R_{1.4} = 9.5 - 12.5$ km

$M_{max} = 2.0 - 2.5\ M_{solar}$

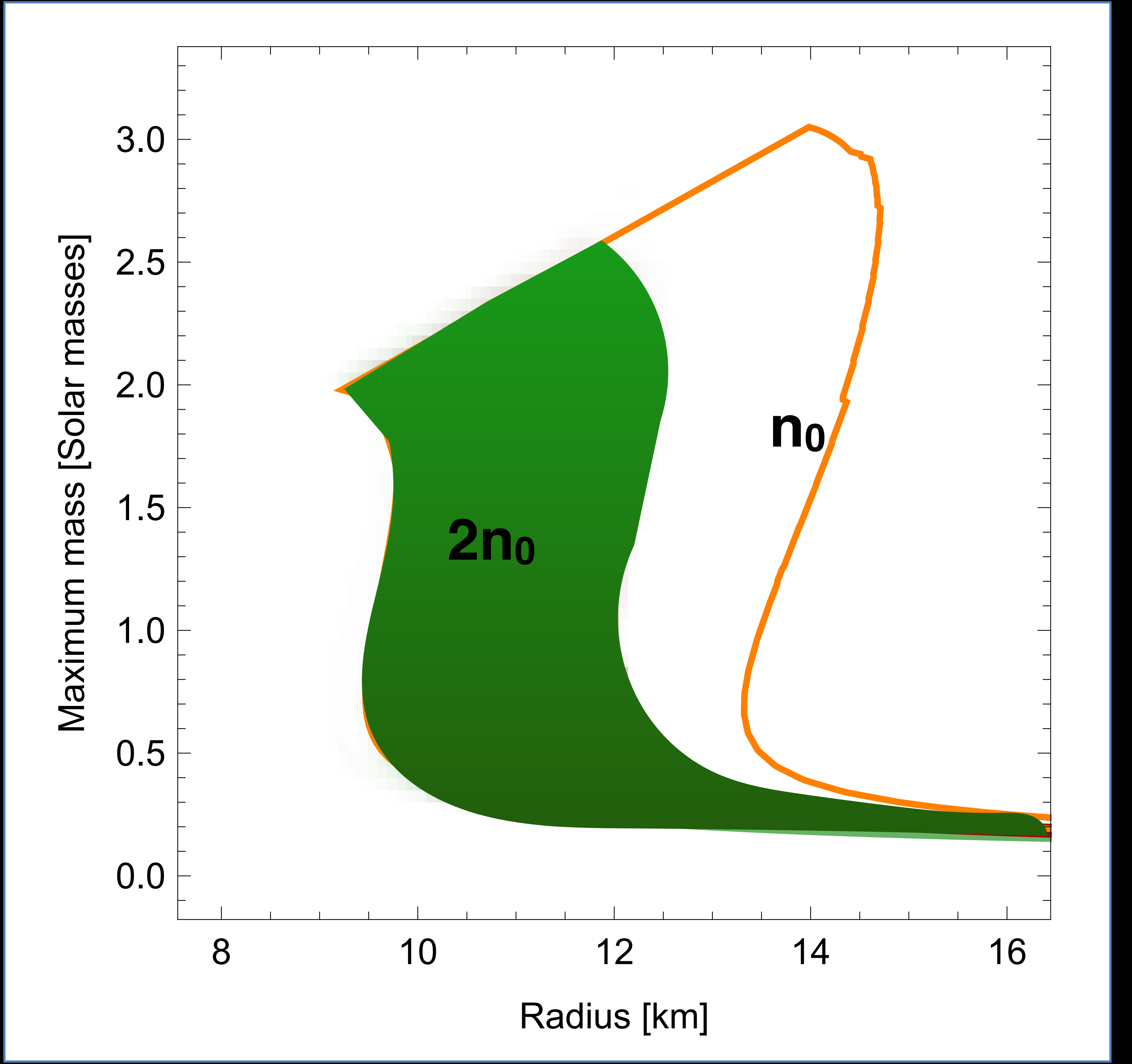

Tews, Gandolfi, Carlson, Reddy (2018), Tews, Margueron, Reddy (2018)
Hebeler, Schwenk, Lattimer and Pethick (2010,2013) and Carlson, Gandolfi, Reddy (2012)

Neutron Star Structure: Observations

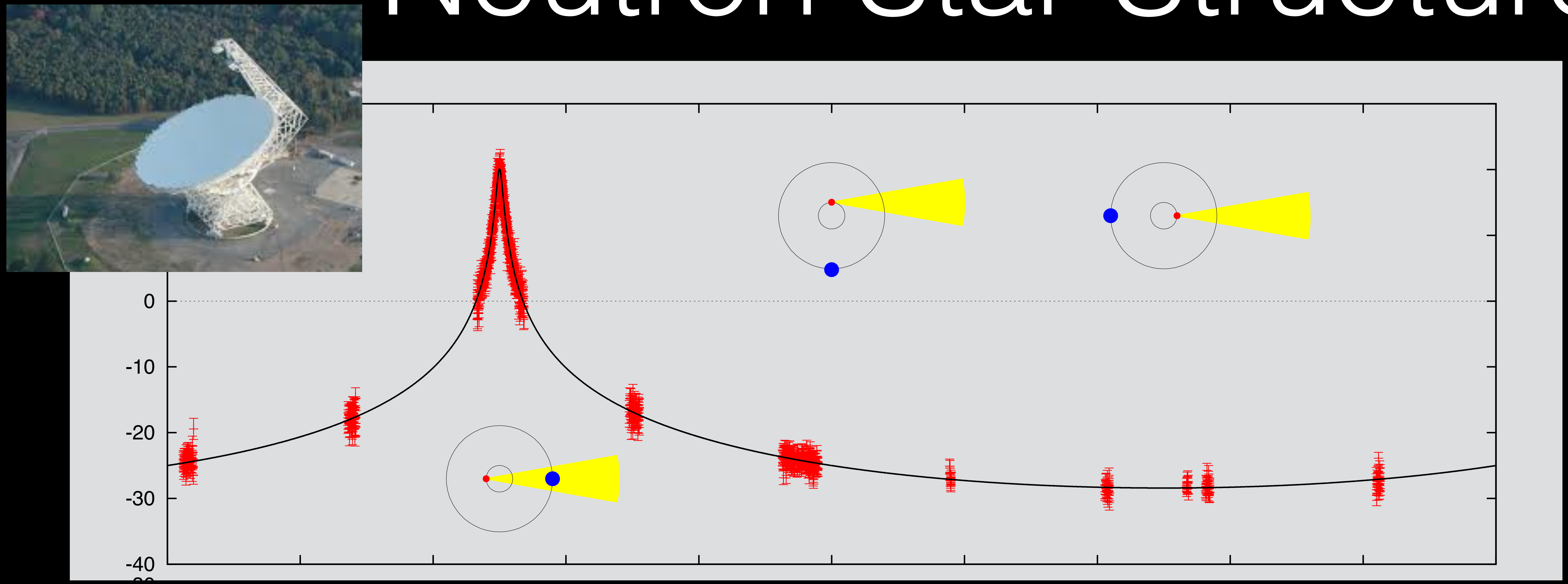

2 $M_\odot$ neutron stars exist.

PSR J1614-2230: M=1.93(2)

Demorest et al. (2010)

PSR J0348+0432: M=2.01(4) $M_\odot$

Anthoniadis et al. (2013)

MSP J0740+6620: M=2.17(10) $M_\odot$

Cromartie et al. (2019)

Neutron Star Structure: Observations

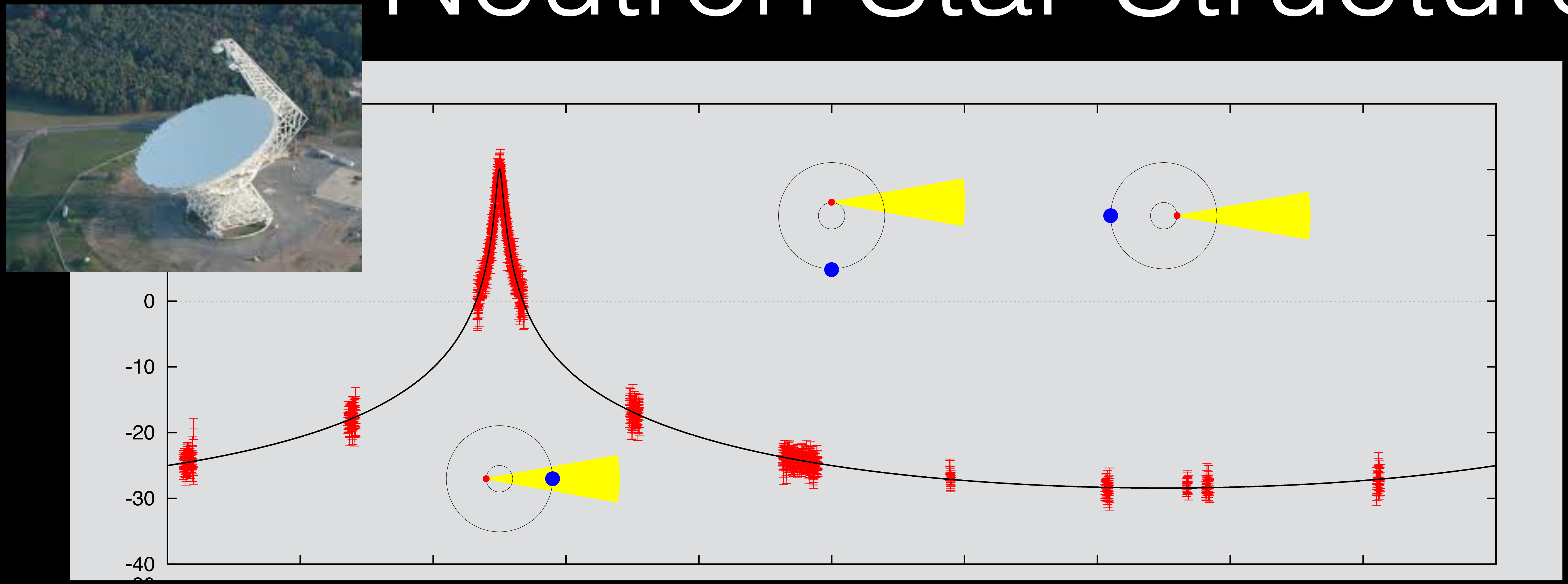

2 $M_\odot$ neutron stars exist.

PSR J1614-2230: M=1.93(2)

Demorest et al. (2010)

PSR J0348+0432: M=2.01(4) $M_\odot$

Anthoniadis et al. (2013)

MSP J0740+6620: M=2.17(10) $M_\odot$

Cromartie et al. (2019)

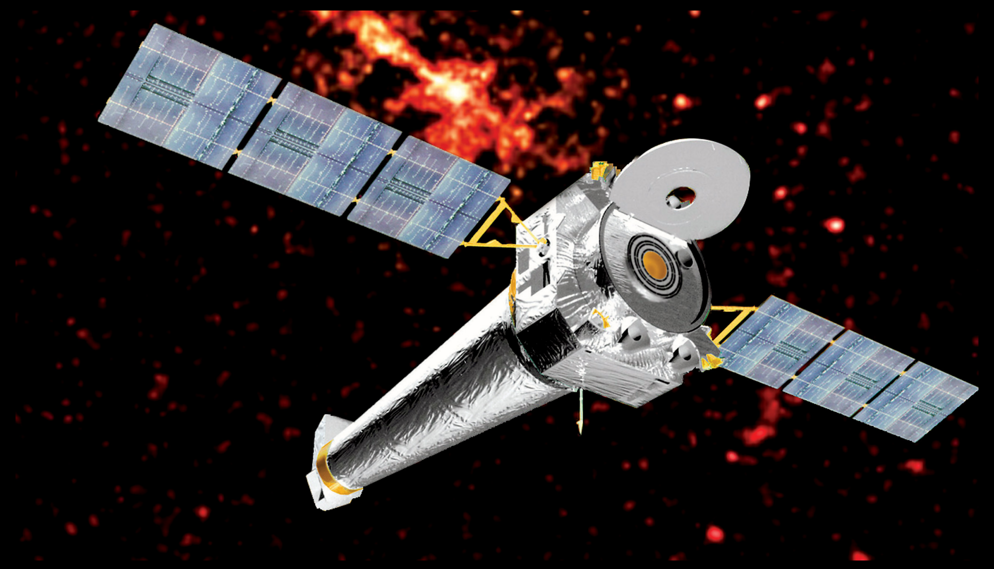

Inferred NS radii are small.

Despite poorly understood systematic errors, x-ray observations suggest R ~ 9-13 km. Perhaps even preferring a smaller range R~ 10-12 km.

Ozel & Freire (2016)

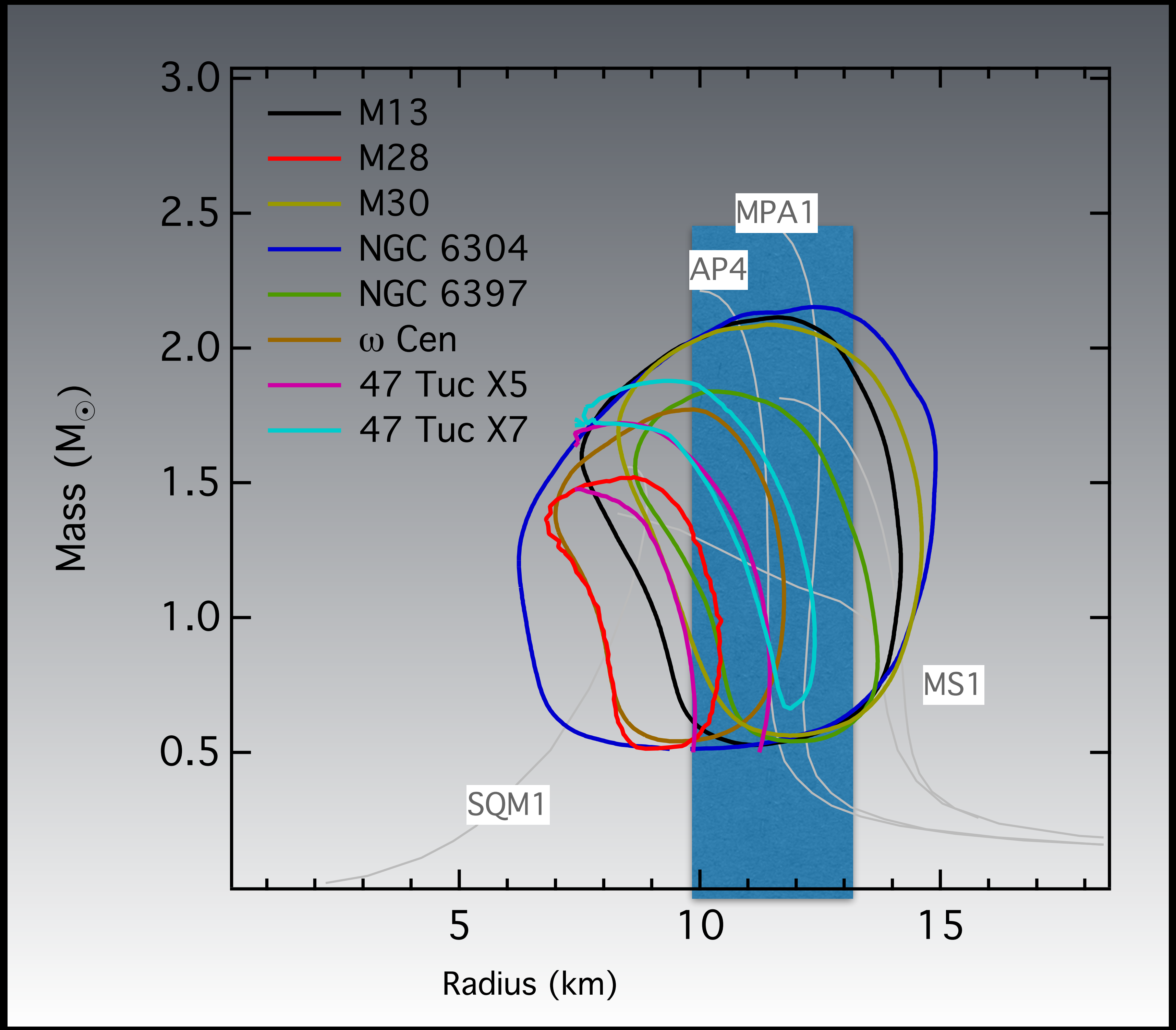

Binary Inspiral and Gravitational Waves

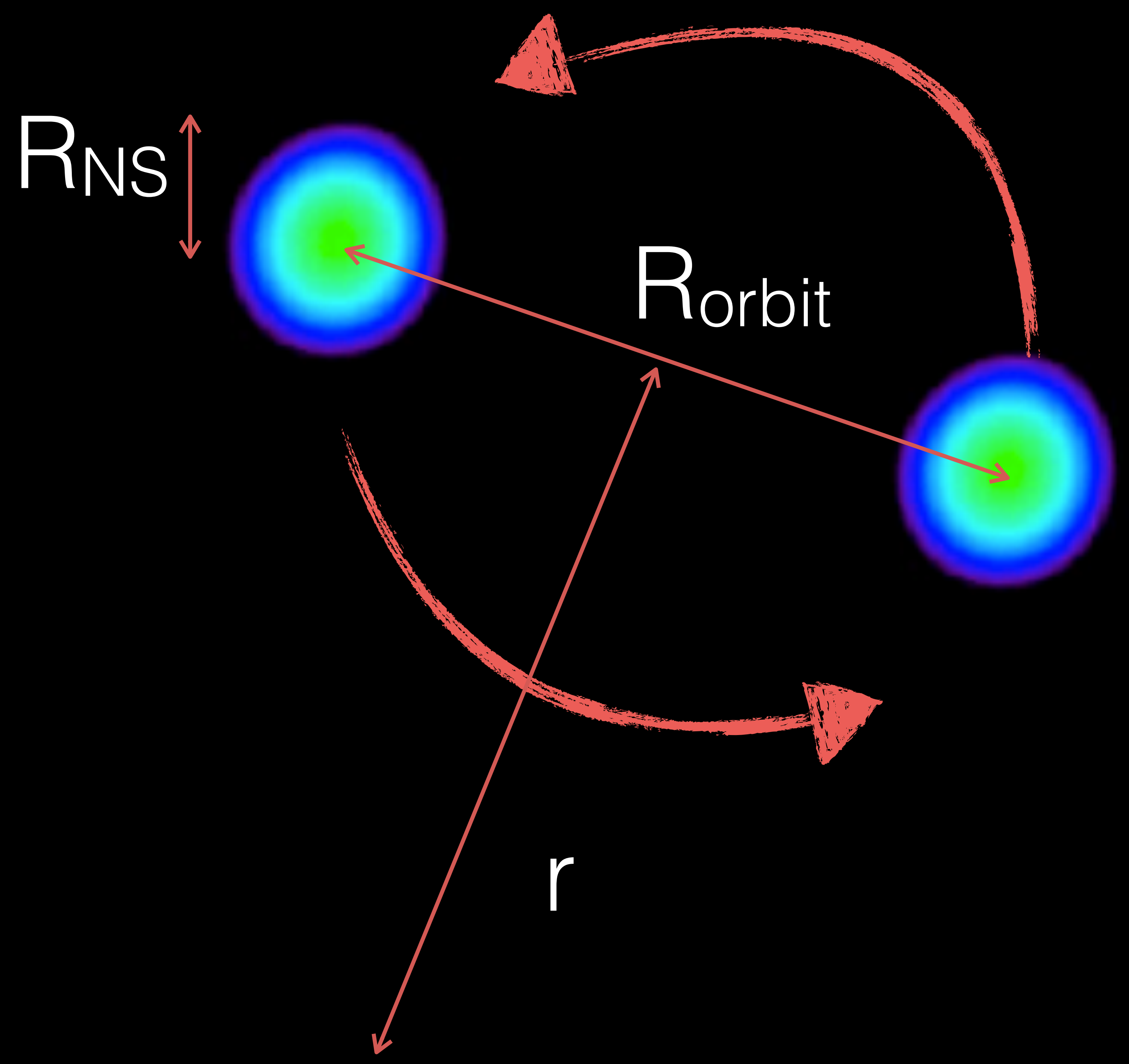

GWs are produced by fluctuating quadrupoles.

$$h_{\mu\nu}(r,t) = \frac{2G}{r}\,\ddot{I}_{ij}(t_R)$$

$$\ddot{I}_{ij}(t) \approx M\,R_{orbit}^2\,f^2 \approx M^{5/3}\,f^{2/3}$$

$$h \approx 10^{-23}\left(\frac{M_{NS}}{M_\odot}\right)^{5/3}\left(\frac{f}{200\ \mathrm{Hz}}\right)^{2/3}\left(\frac{100\ \mathrm{Mpc}}{r}\right)$$

- Advanced LIGO can detect GWs from binary neutron stars out to about 200 Mpc at design sensitivity. Detection rate ~ 1- 50 per year.

GW170817: Gravitational Waves from Neutron Stars!

Selected for a Viewpoint in *Physics*
PRL **119,** 161101 (2017) PHYSICAL REVIEW LETTERS week ending 20 OCTOBER 2017

GW170817: Observation of Gravitational Waves from a Binary Neutron Star Inspiral

B. P. Abbott *et al.*[*]
(LIGO Scientific Collaboration and Virgo Collaboration)

(Received 26 September 2017; revised manuscript received 2 October 2017; published 16 October 2017)

Component masses: $m_1 = 1.47 \pm 0.13\ M_\odot$

$m_2 = 1.17 \pm 0.09\ M_\odot$

Chirp Mass: $\mathscr{M} = \dfrac{(m_1 m_2)^{3/5}}{(m_1 + m_s)^{1/5}} = 1.188^{+0.004}_{-0.002}\ M_\odot$

Total Mass: $M = m_1 + m_2 = 2.74^{+0.04}_{-0.01}\ M_\odot$

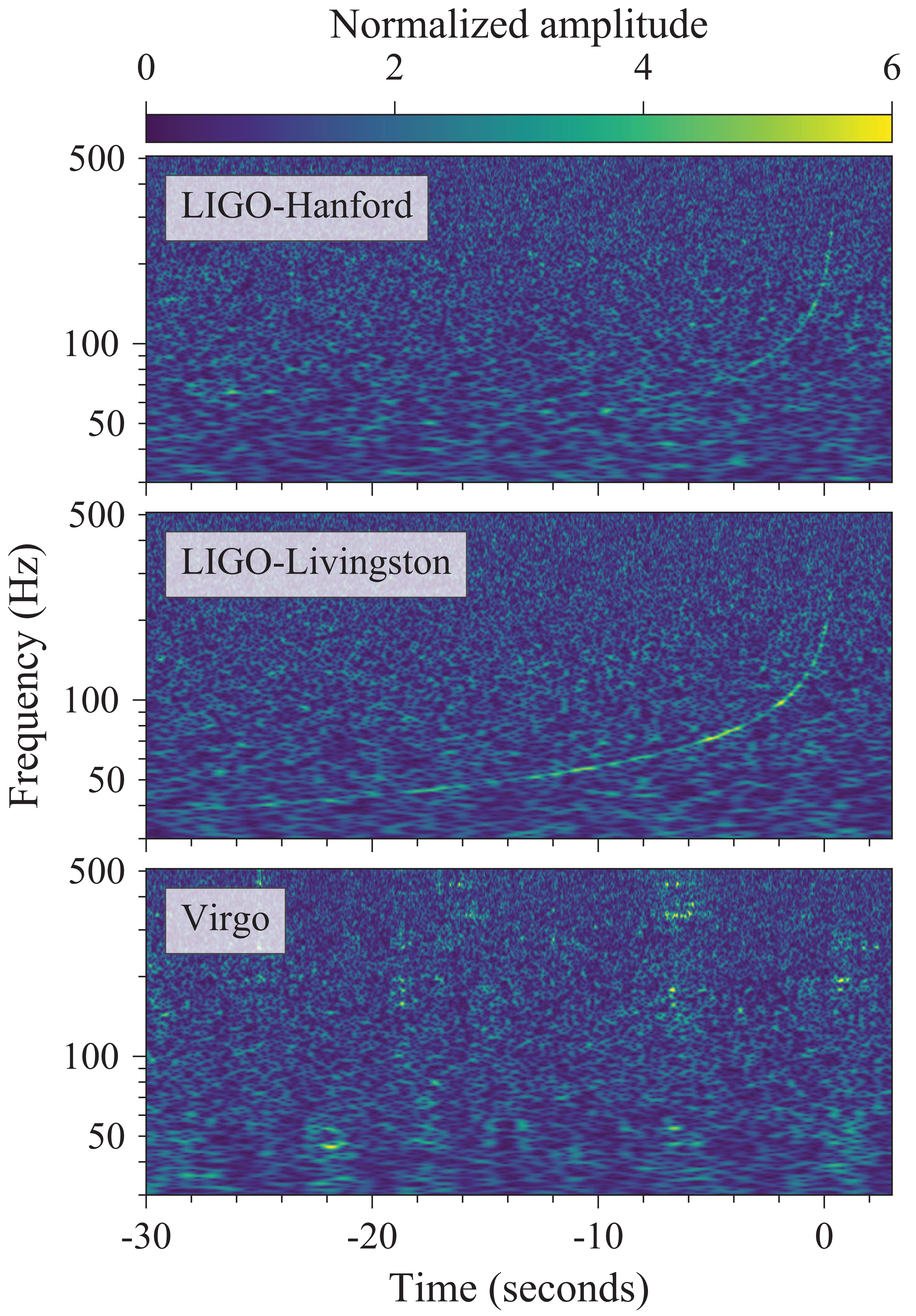

Tidal Deformation: Measuring the Neutron Star Radius

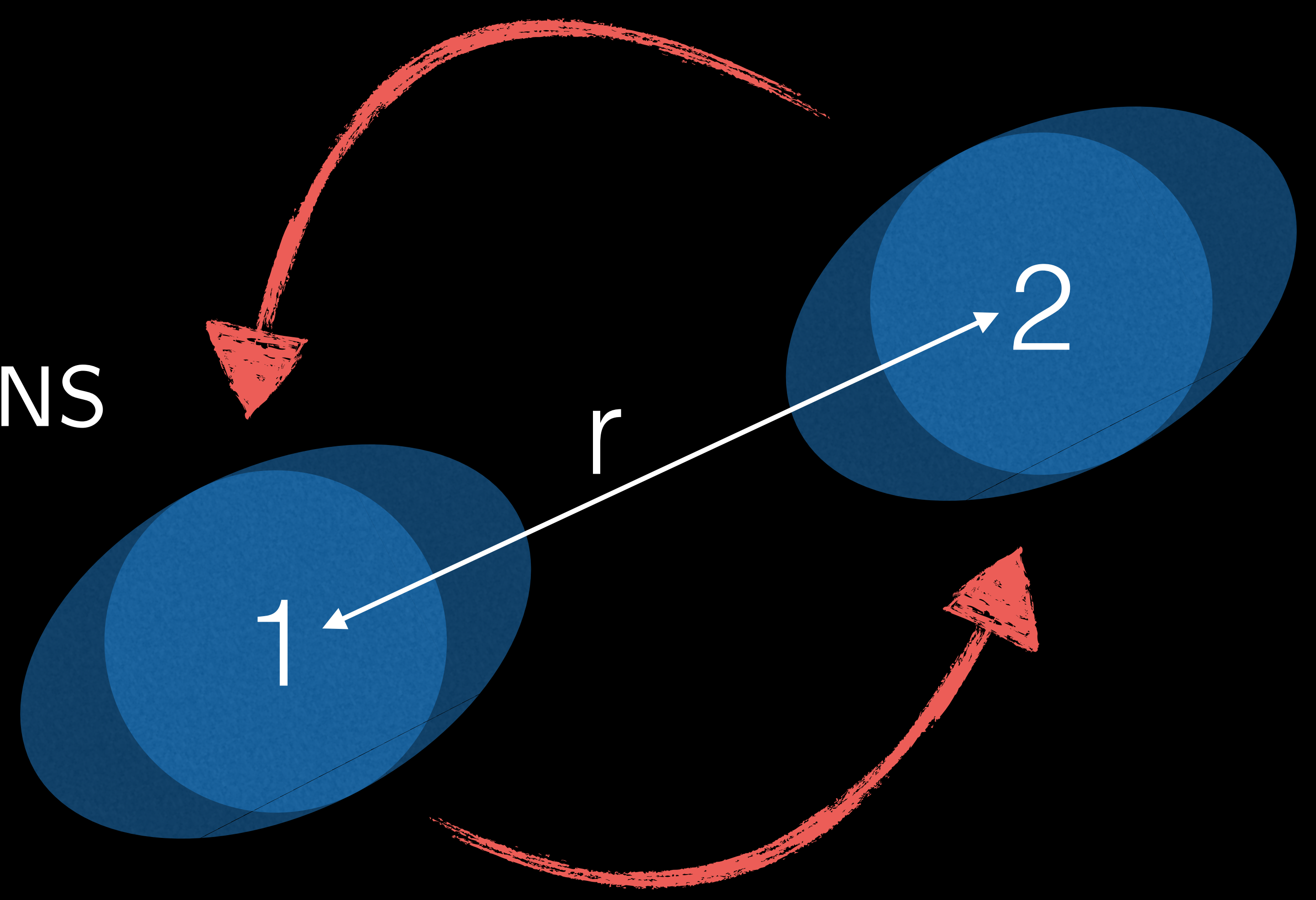

Tidal forces deform neutron stars.
Induces a quadrupole moment.

$$Q_{xy} = \lambda\ E_{xy} \qquad E_{xy} = -\frac{\partial^2 V_G}{\partial x \partial y}$$

tidal deformability

external field

Tidal Deformation: Measuring the Neutron Star Radius

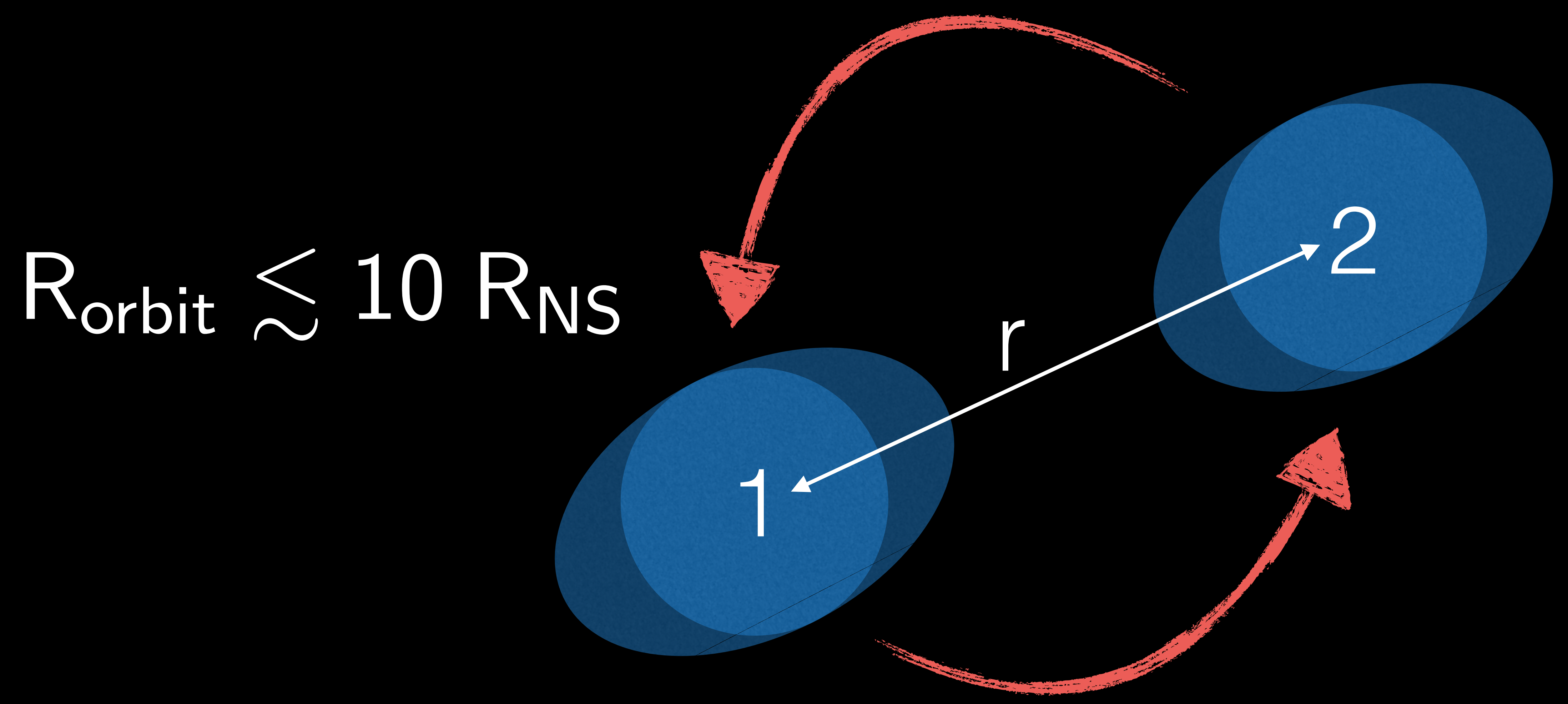

Tidal forces deform neutron stars.
Induces a quadrupole moment.

$$Q_{xy} = \lambda\ E_{xy} \qquad E_{xy} = -\frac{\partial^2 V_G}{\partial x \partial y}$$

tidal deformability   external field

Tidal interactions change the rotational phase: $\delta\Phi = -\frac{117}{256}\, v^5\, \frac{M}{\mu}\, \tilde{\Lambda}$

Tidal Deformation: Measuring the Neutron Star Radius

$R_{orbit} \lesssim 10\, R_{NS}$

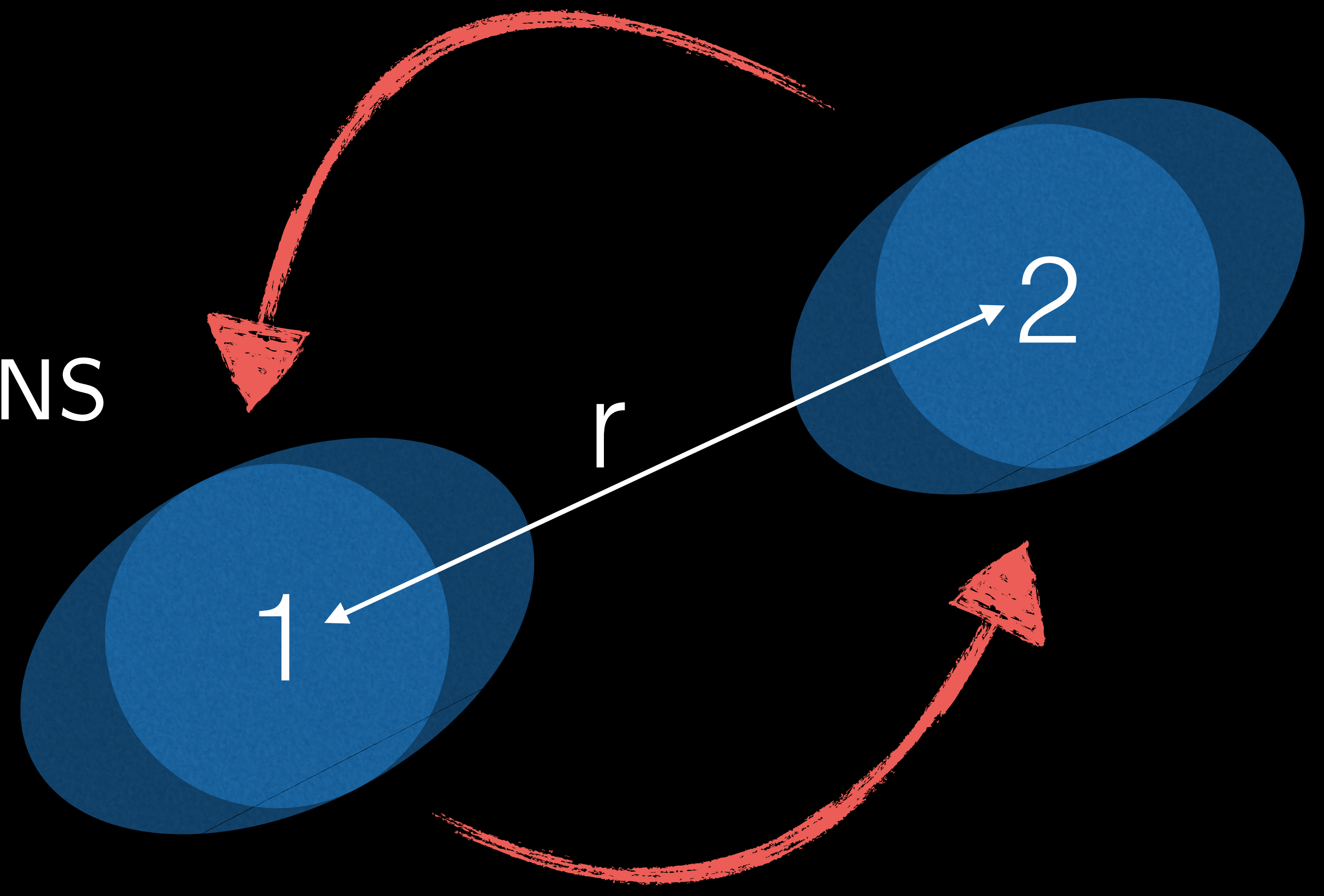

Tidal forces deform neutron stars.
Induces a quadrupole moment.

$$Q_{xy} = \lambda\, E_{xy} \qquad E_{xy} = -\frac{\partial^2 V_G}{\partial x \partial y}$$

tidal deformability

external field

Tidal interactions change the rotational phase: $\delta\Phi = -\frac{117}{256}\, v^5\, \frac{M}{\mu}\, \tilde{\Lambda}$

Dimensionless binary tidal deformability: $\tilde{\Lambda} = \frac{16}{13}\left(\left(\frac{M_1}{M}\right)^5 \left(1 + \frac{M_2}{M_1}\right) \Lambda_1 + 1 \leftrightarrow 2\right)$

Tidal Deformation: Measuring the Neutron Star Radius

$R_{orbit} \lesssim 10\, R_{NS}$

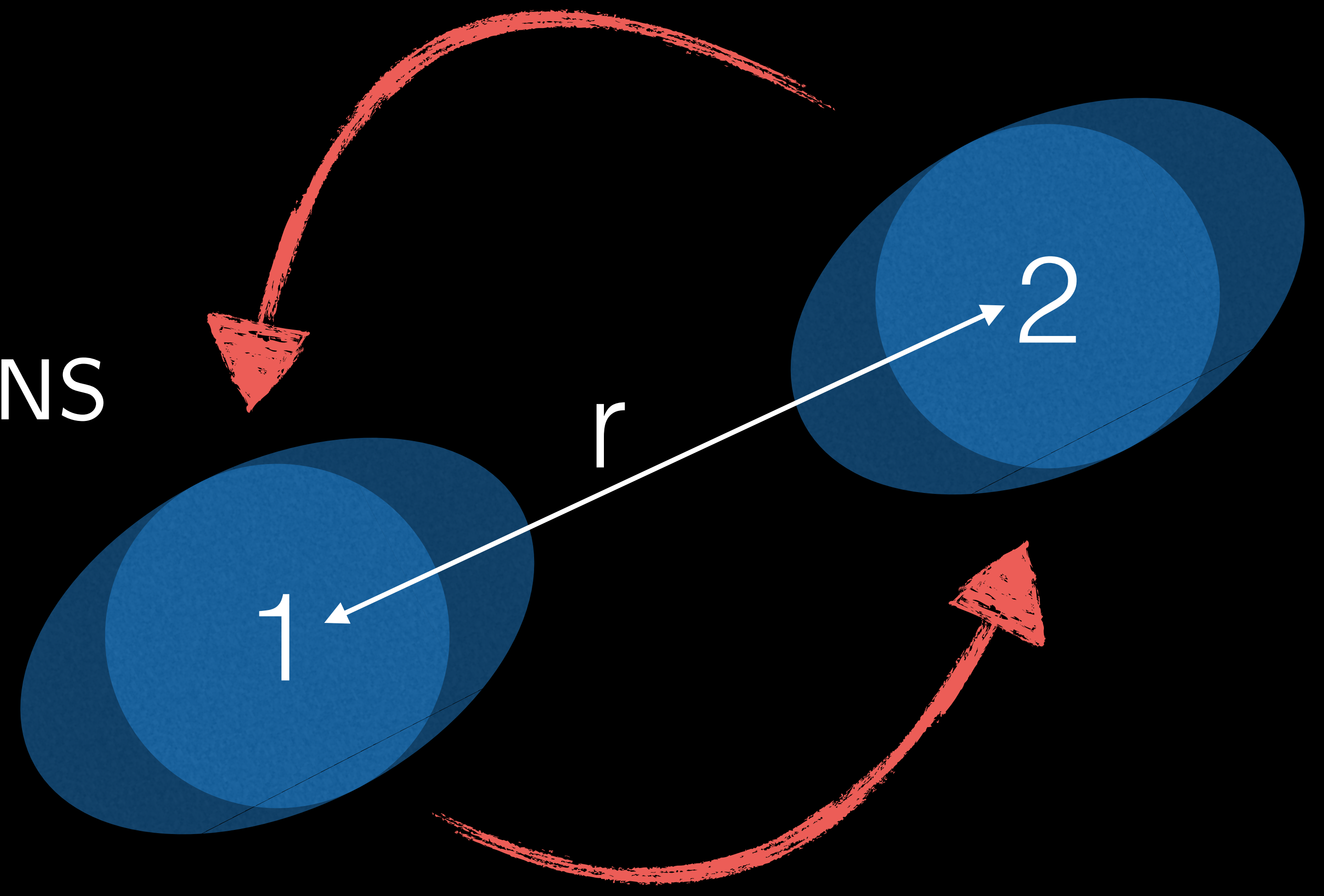

Tidal forces deform neutron stars.
Induces a quadrupole moment.

$$Q_{xy} = \lambda \; E_{xy} \qquad E_{xy} = -\frac{\partial^2 V_G}{\partial x \partial y}$$

tidal deformability — external field

Tidal interactions change the rotational phase: $\delta\Phi = -\frac{117}{256} v^5 \frac{M}{\mu} \tilde{\Lambda}$

Dimensionless binary tidal deformability: $\tilde{\Lambda} = \frac{16}{13}\left(\left(\frac{M_1}{M}\right)^5 \left(1 + \frac{M_2}{M_1}\right) \Lambda_1 + 1 \leftrightarrow 2\right)$

Tidal deformations are large for a large NS: $\Lambda_i = \frac{\lambda_i}{M_i^5} = k_2 \frac{R_i^5}{M_i^5}$

Tidal Effects at Late Times

B. Lackey, L. Wade. PRD 91, 043002 (2015)

Neutron Stars are Small

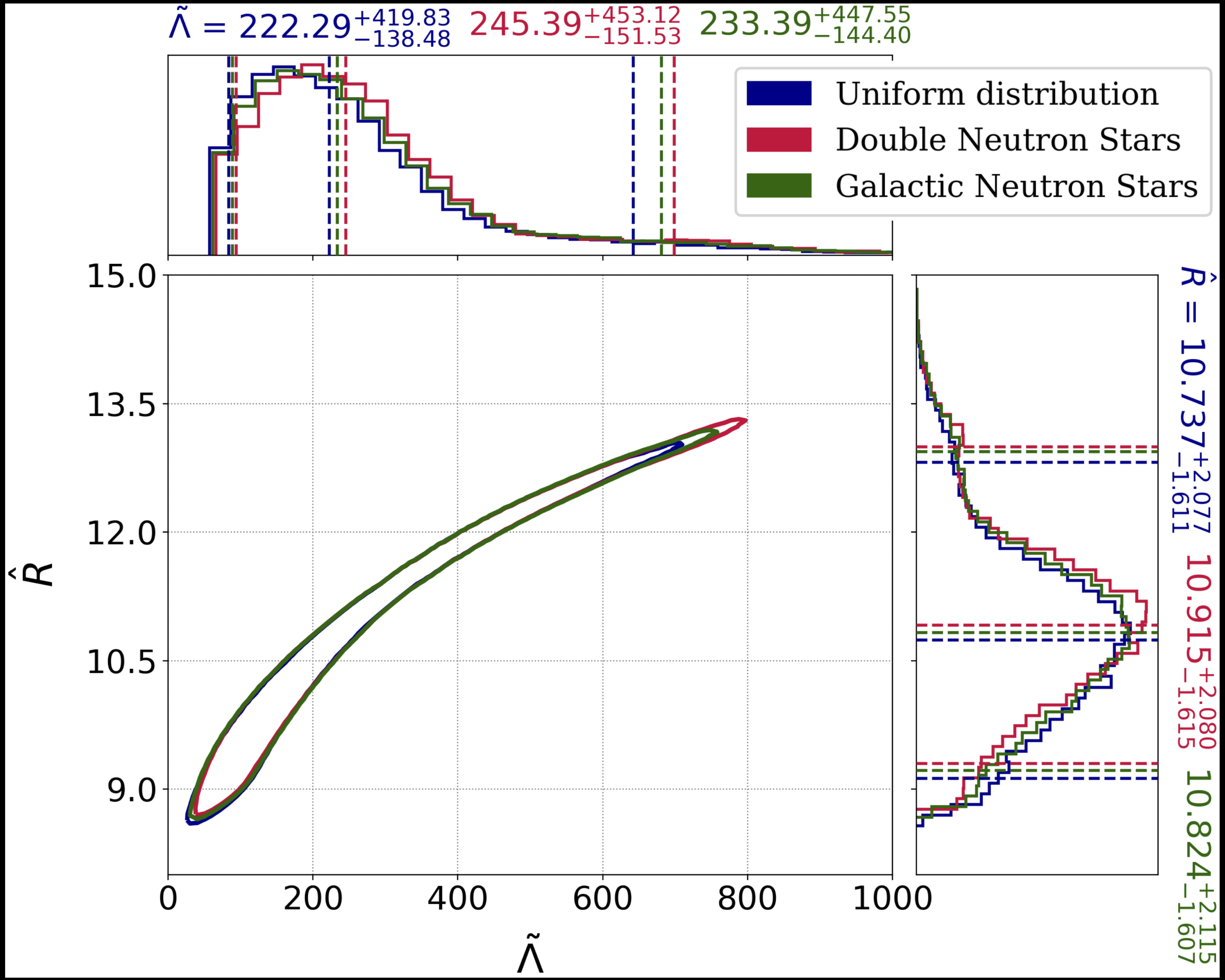

Tidal deformations observed in GW170817 are small and suggests that the NS radius:

R < 13 km

Requiring a maximum mass greater than 2 M_{sun} **implies:**

R > 9 km

De et al. PRL (2018)
See also LIGO and Virgo Scientific Collaboration arXiV:1805.11581v1

Speed of Sound in Dense Matter

Large observed maximum mass combined with small radius and neutron matter calculations suggests a rapid increase in pressure in the neutron star core. Implies a large and non-monotonic sound speed in dense QCD matter.

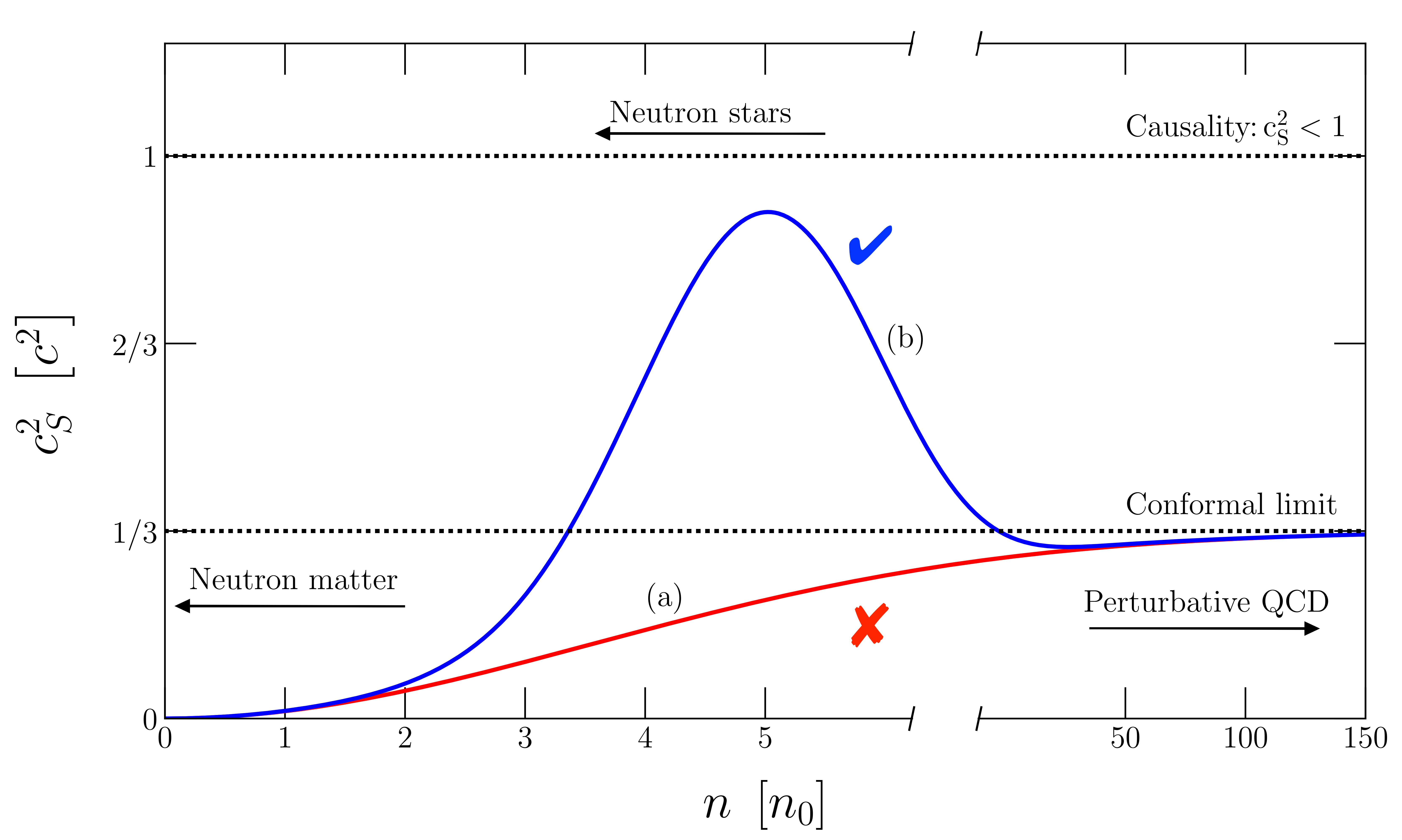

Tews, Carlson, Gandolfi and Reddy (2018), Steiner & Bedaque (2016)

Break

Neutron Star Dynamics

Measurements of neutron star masses and radii can constrain the equation of state.

The thermal evolution of neutron stars is sensitive to the thermal and transport properties of dense matter.

The spectrum of fluctuations at low energy is in turn very sensitive to the phase structure of degenerate matter.

- Proto-neutron star evolution and neutrinos from a galactic supernova.
- Cooling of isolated neutron stars
- Cooling of accreting neutron stars

Core-collapse Supernova

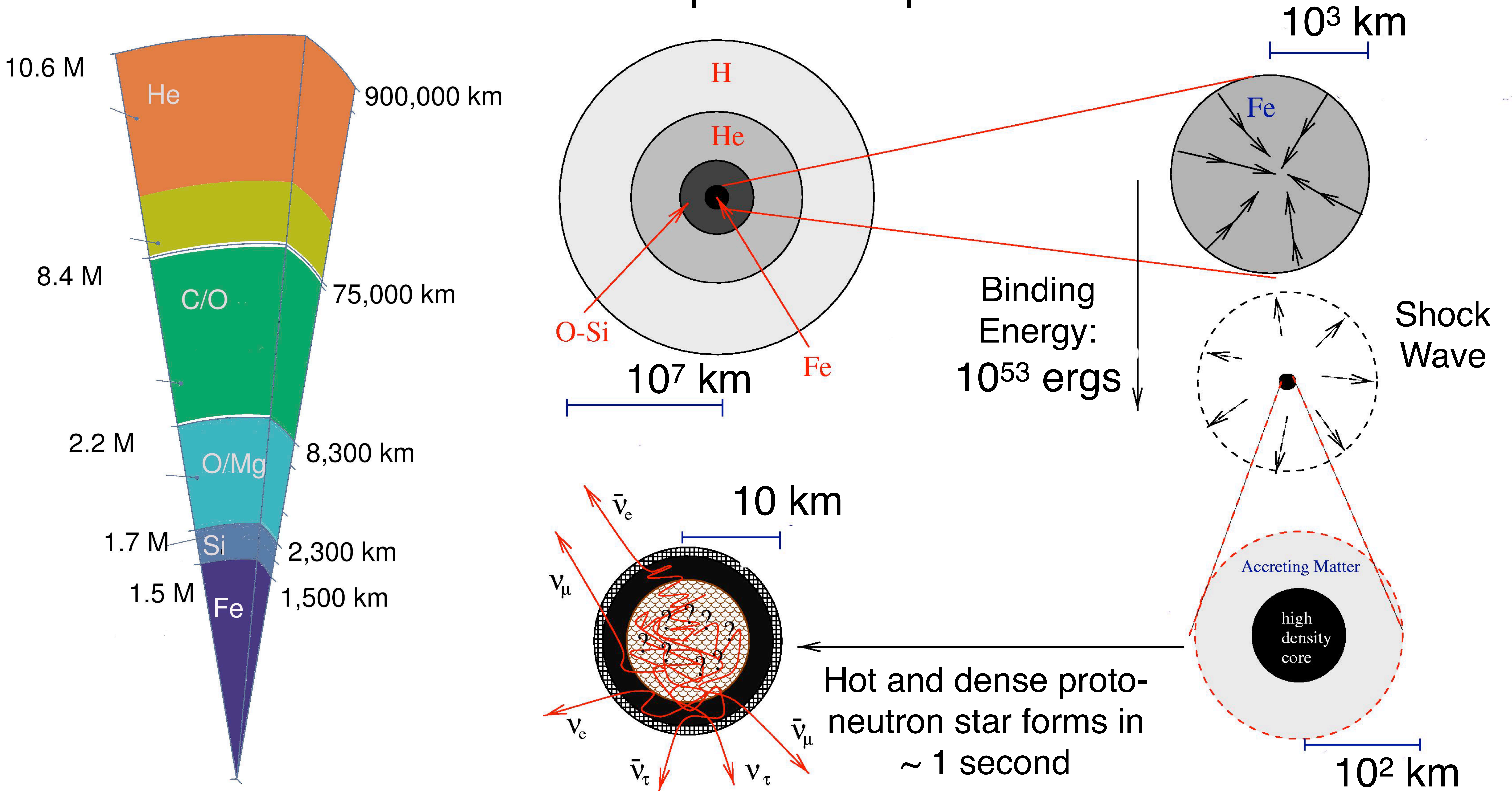

Thermal evolution of an isolated neutron star from birth to old age.

Direct detection of neutrinos is only possible during the first minute or so from a galactic supernova.

X-ray observations from the surface of a population of neutron stars informs us about late time thermal evolution.

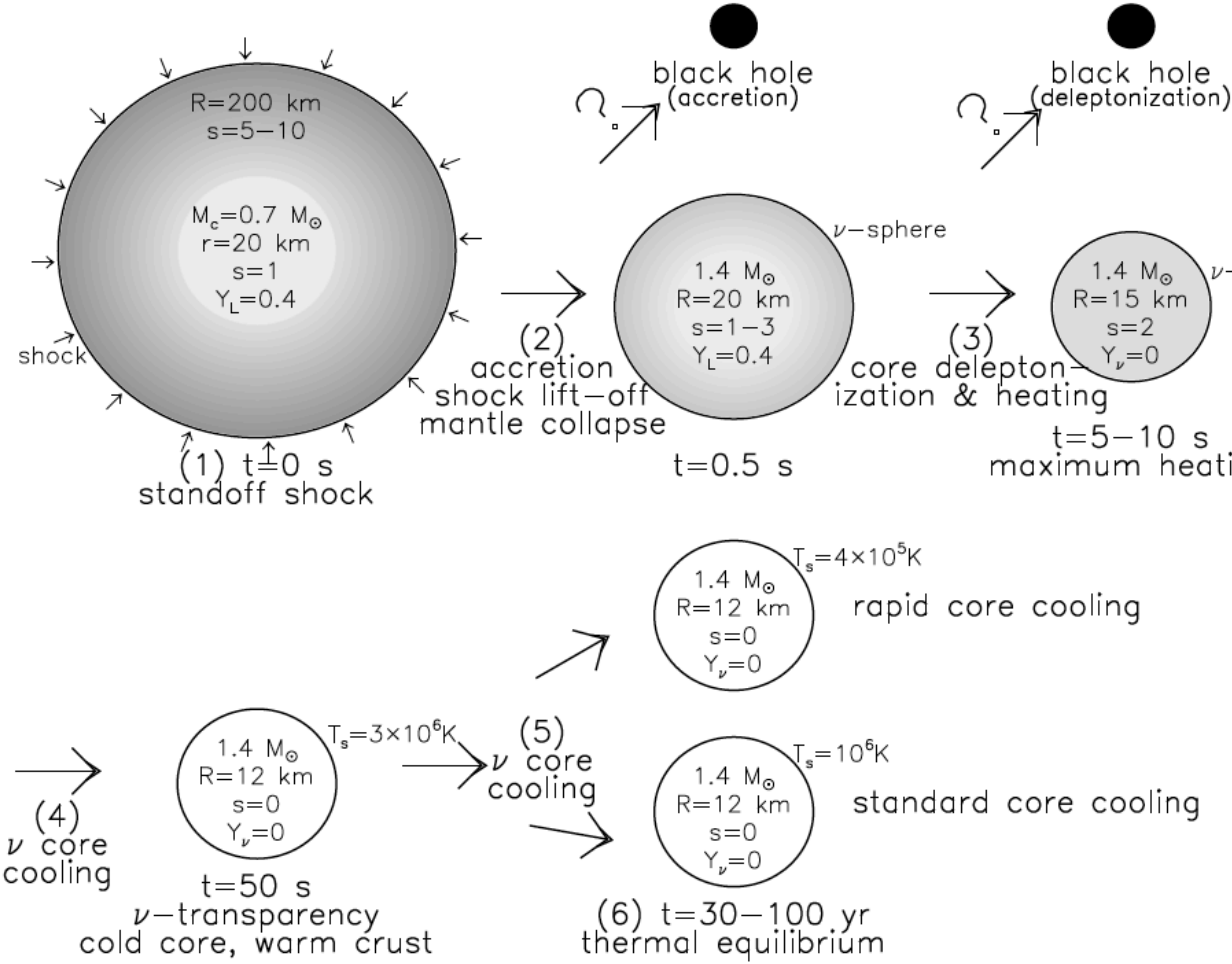

Proto-Neutron Star Evolution

The proto-neutron star contains a large fraction of the gravitational binding energy - trapped in the form of neutrinos.

Lepton number is also trapped. The electron fraction is high - implies a large proton fraction.

The entropy of the core is modest.

The shock heated layers at R>10 kms has higher entropy.

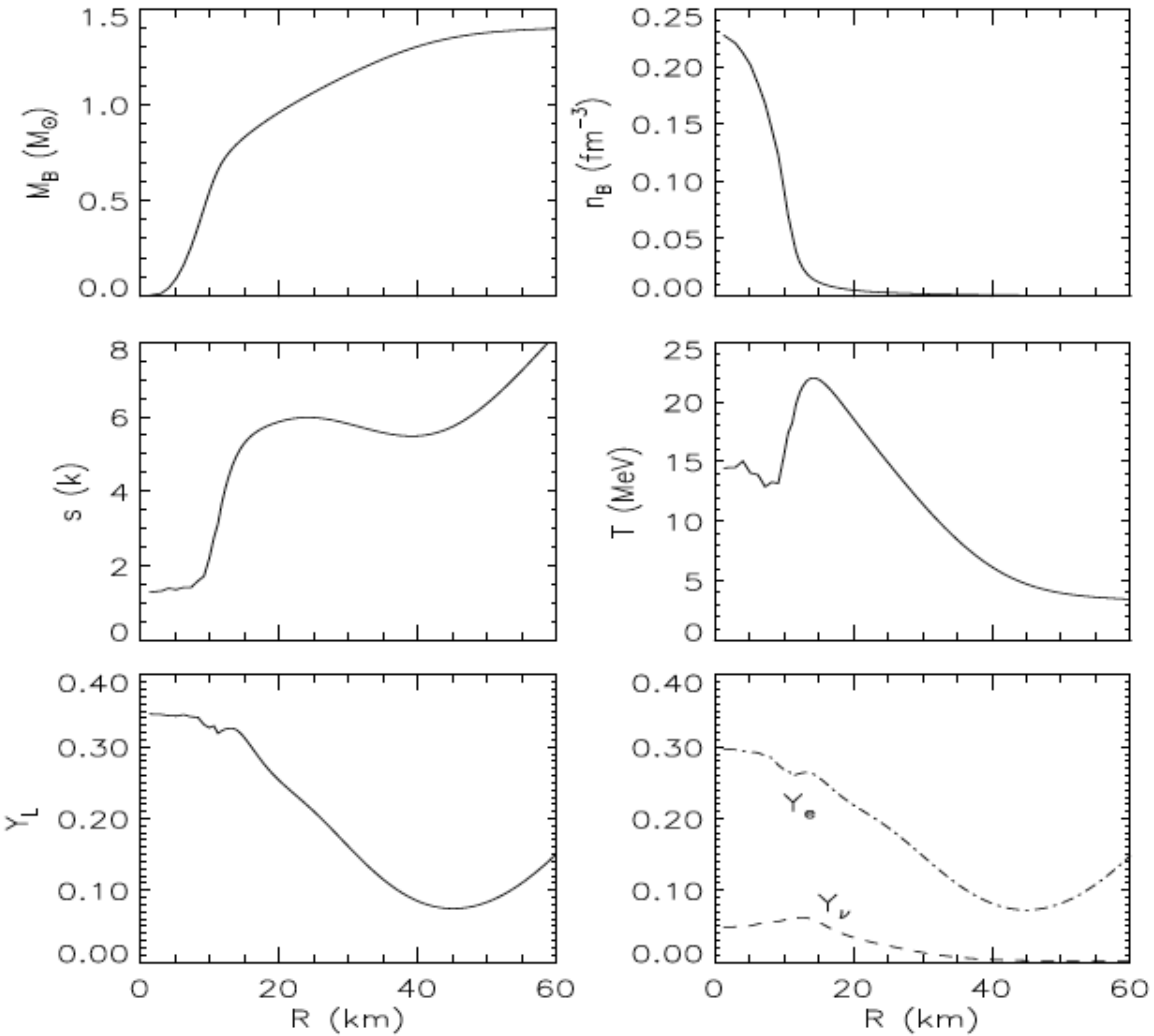

Pons, Reddy, Lattimer, Prakash 1998

Proto-Neutron Star Evolution

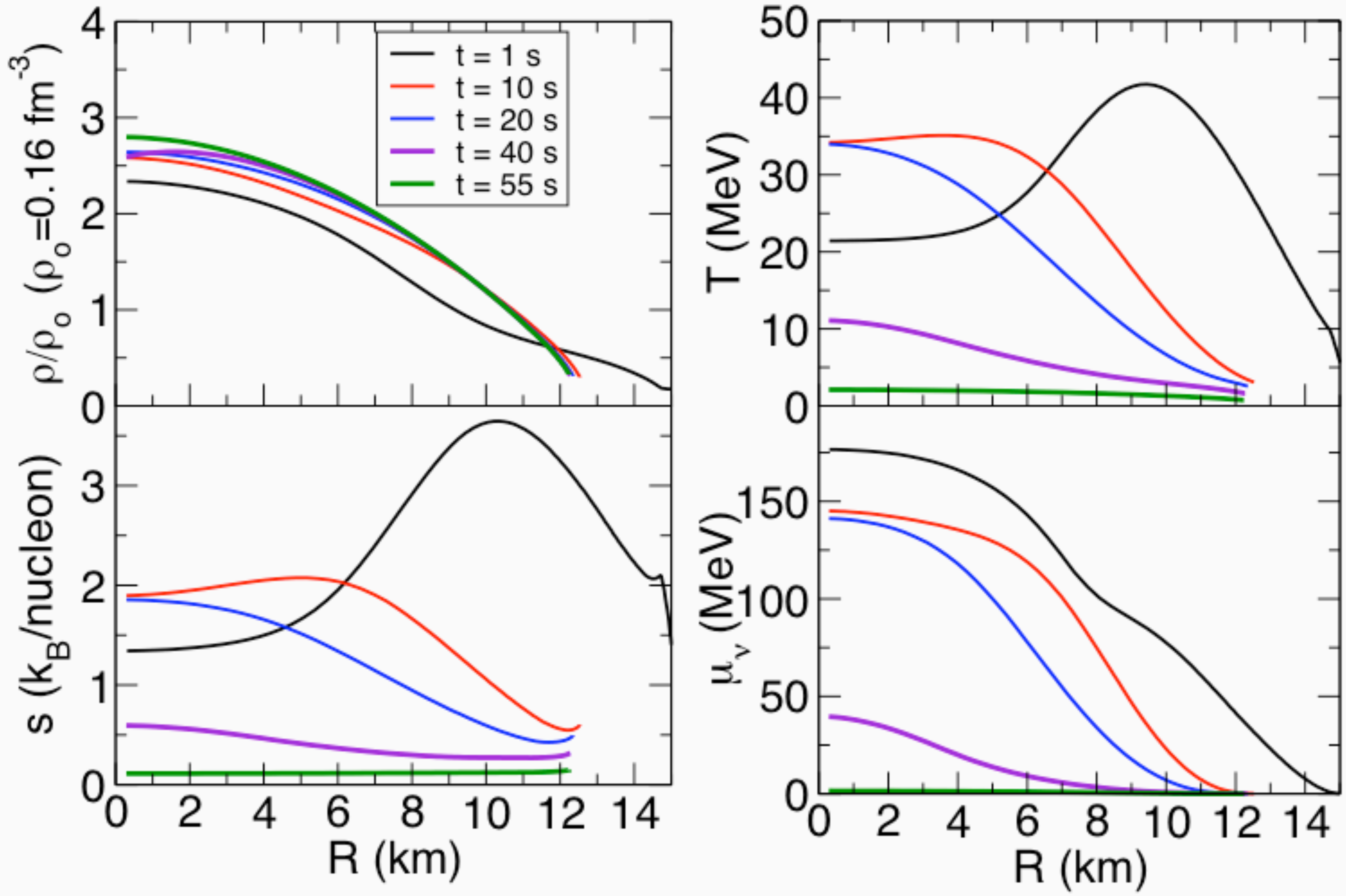

$$T(t) \approx T(0)\left(1-\frac{t}{\tau_c}\right)$$

$$\tau_C \simeq \frac{C_V\ R^2}{c\langle\lambda_{\nu_X}\rangle}$$

$$Y_\nu(t) \approx Y_\nu(0)\ \exp\left(-\frac{t}{\tau_D}\right)$$

$$\tau_D \simeq \frac{3}{\pi^2}\ \frac{\partial Y_L}{\partial Y_\nu}\frac{R^2}{c\langle\lambda_{\nu_e}\rangle}$$

Pons, Reddy, Lattimer, Prakash 1998

Supernova Neutrinos

SN 1987a: ~ 20 neutrinos ..in support of supernova theory

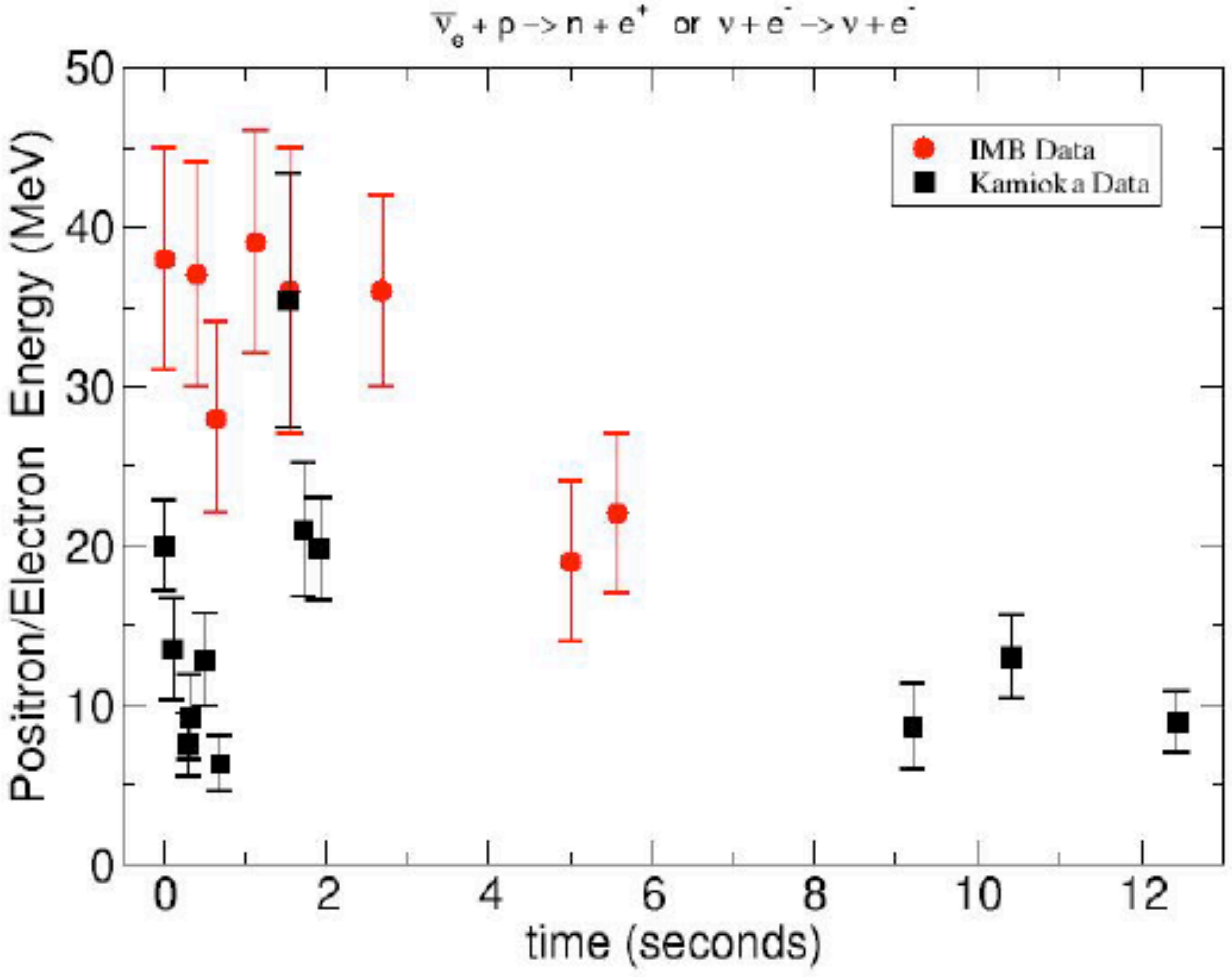

> 10,000 events expected from a future galactic supernovae.

Temporal structure set by neutrino diffusion + convection + fall-back.

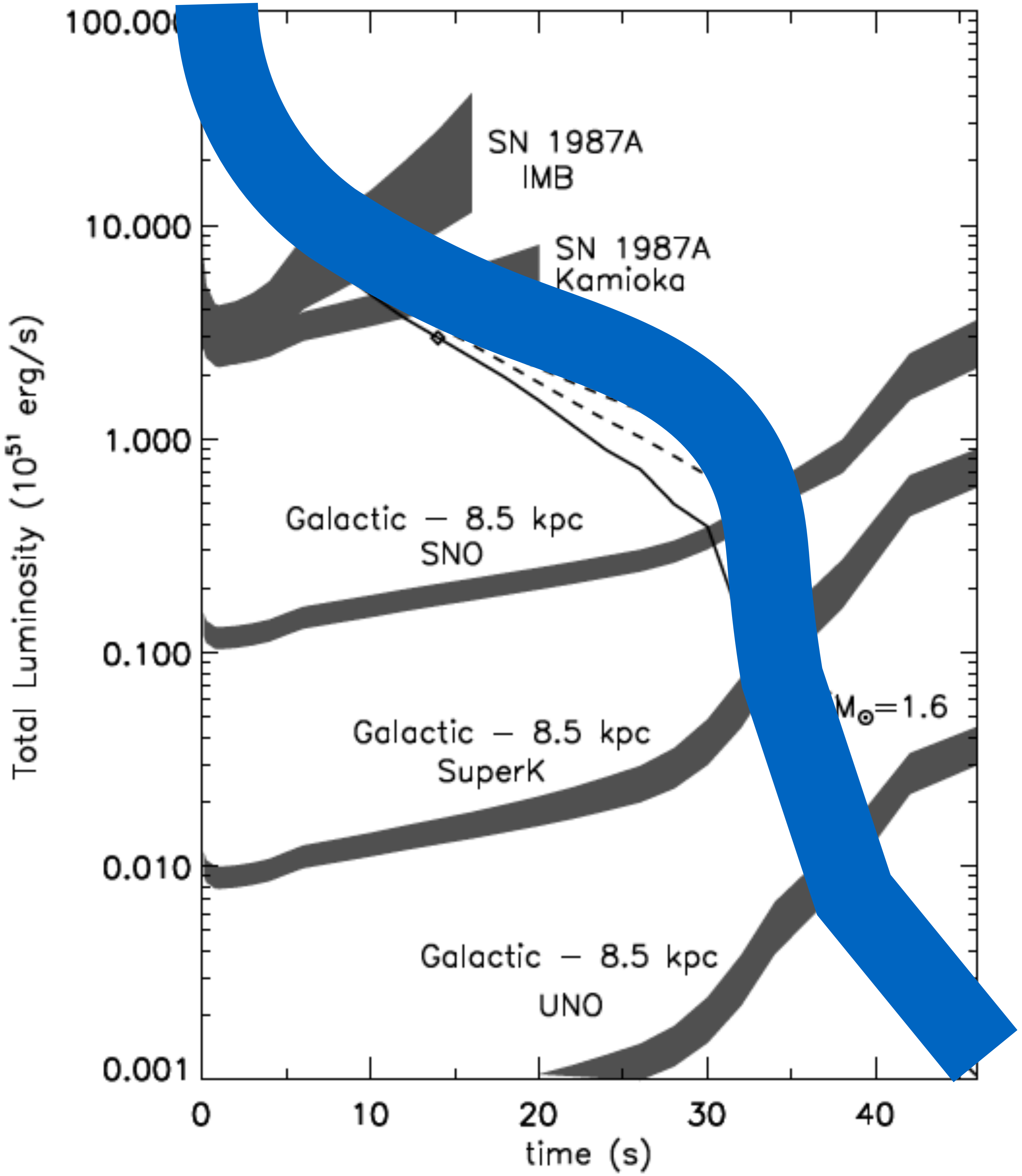

Supernova Neutrinos

SN 1987a: ~ 20 neutrinos ..in support of supernova theory

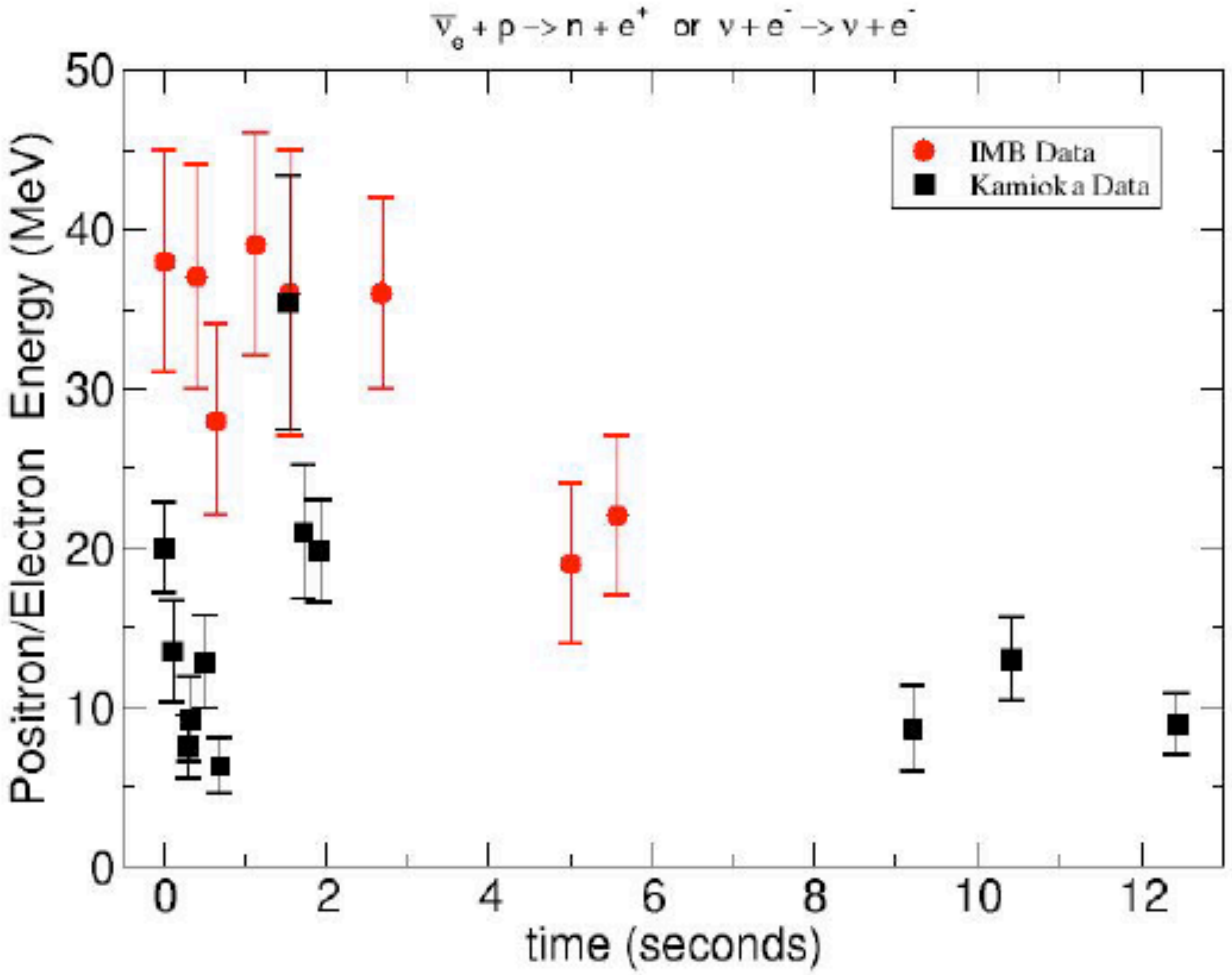

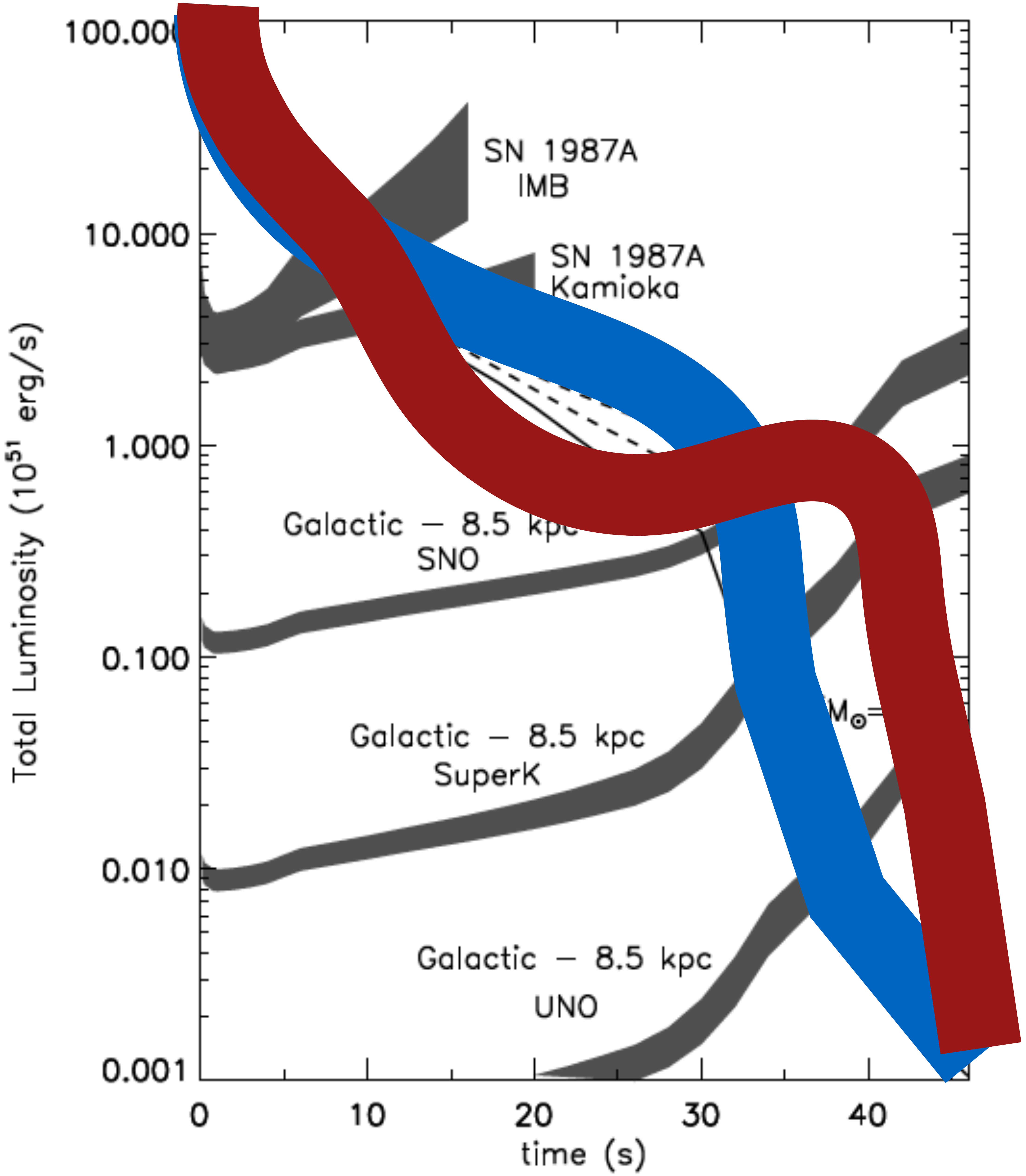

> 10,000 events expected from a future galactic supernovae.

Temporal structure set by neutrino diffusion + convection + fall-back.

Neutrino Mean Free Paths in Dense Matter

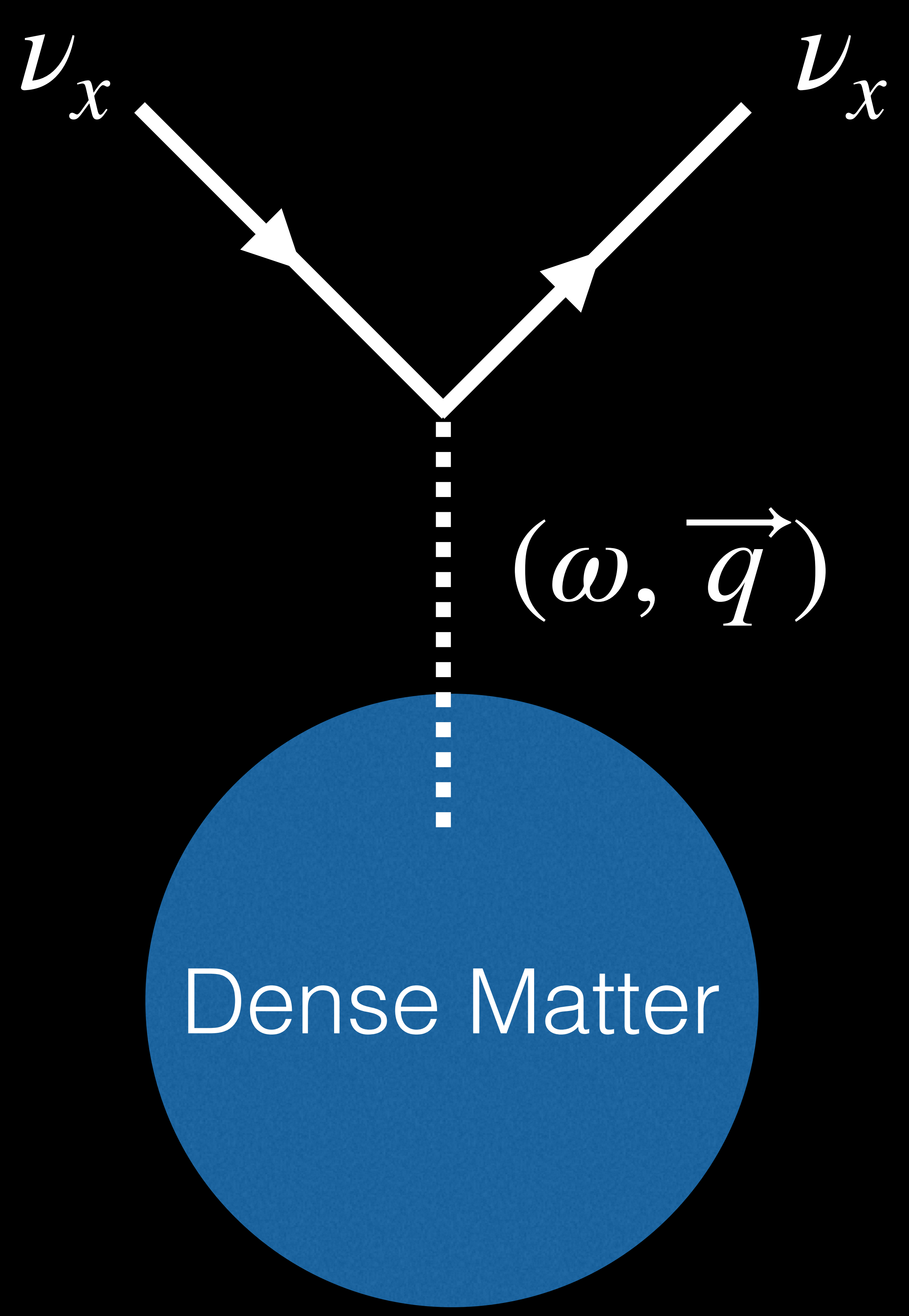

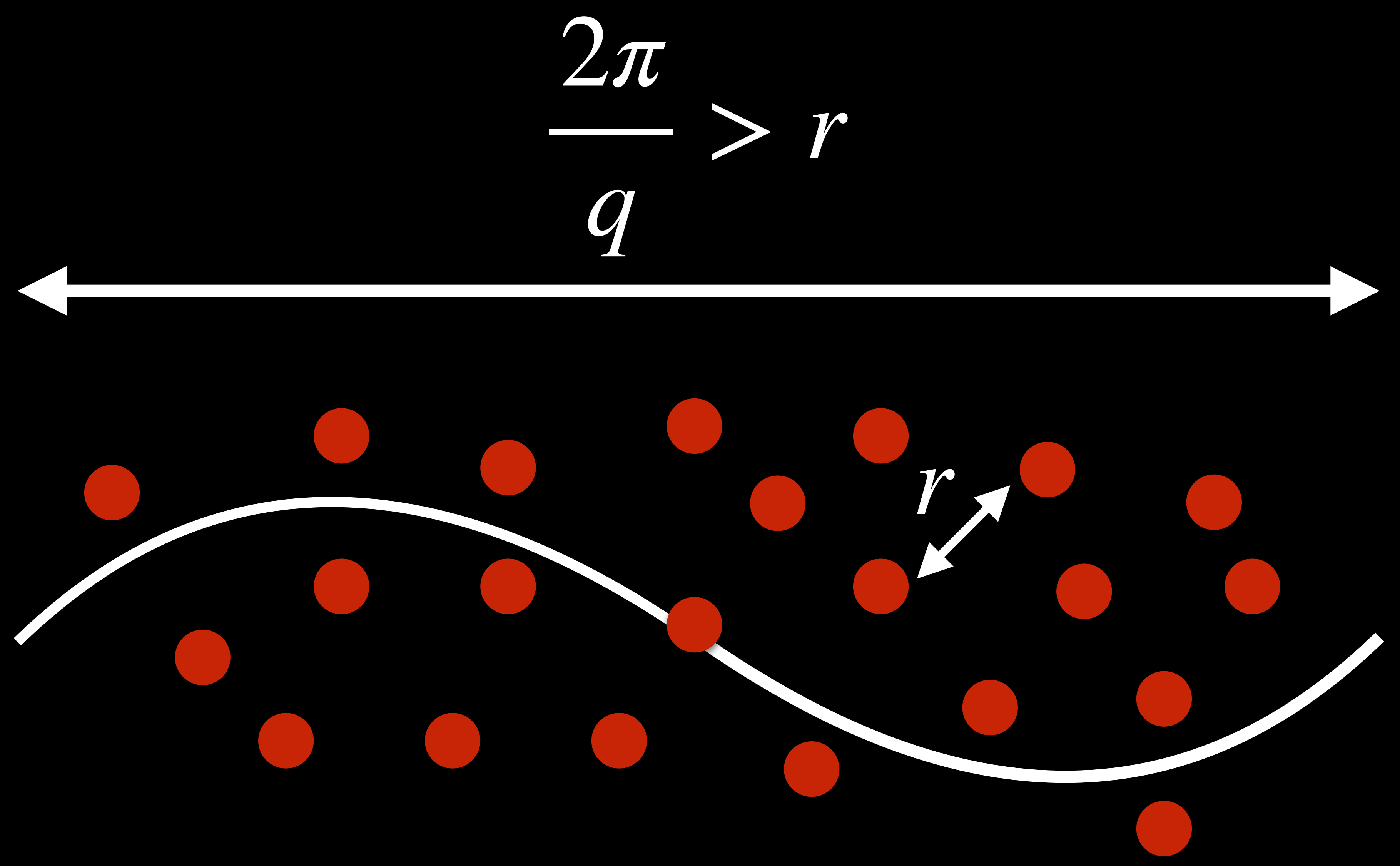

Scattering from different target particles in the medium interfere. Correlations between particles important in determining the neutrino scattering rates.

Correlation functions of dense matter at low energy is strongly influenced by interactions between target particles and the phased structure of matter.

Linear Response

Perturbation:

$$\mathcal{H}_{int} = \int d^3x \; \mathcal{O}(x) \; \phi_{ext}(x,t)$$

Response:

$$\delta\rho(\vec{q},\omega) = \Pi^R(\vec{q},\omega) \; \phi_{ext}(\vec{q},\omega)$$

Response function:
Polarization function
or Generalized Susceptibility

$$\Pi^R(\vec{q},\omega) = \frac{-i}{\hbar} \int dt \; e^{i\omega t} \; \theta(t) \; \langle [\mathcal{O}(-\vec{q},t), \mathcal{O}(\vec{q},0)] \rangle$$

Response to static and uniform perturbations is related to thermodynamic derivatives.

$$\phi_{ext}(\vec{q} \to 0, \omega = 0) = \delta\mu$$

Linear Response

Perturbation:

$$\mathcal{H}_{int} = \int d^3x \; \mathcal{O}(x) \; \phi_{ext}(x,t)$$

Response:

$$\delta\rho(\vec{q},\omega) = \Pi^R(\vec{q},\omega) \; \phi_{ext}(\vec{q},\omega)$$

Response function:
Polarization function
or Generalized Susceptibility

$$\Pi^R(\vec{q},\omega) = \frac{-i}{\hbar} \int dt \; e^{i\omega t} \; \theta(t) \; \langle [\mathcal{O}(-\vec{q},t), \mathcal{O}(\vec{q},0)] \rangle$$

Response to static and uniform perturbations is related to thermodynamic derivatives.

$$\phi_{ext}(\vec{q} \to 0, \omega = 0) = \delta\mu$$

perturbation can be viewed as a change in the chemical potential

Linear Response

Perturbation:

$$\mathcal{H}_{int} = \int d^3x \; \mathcal{O}(x) \; \phi_{ext}(x,t)$$

Response:

$$\delta\rho(\vec{q},\omega) = \Pi^R(\vec{q},\omega) \; \phi_{ext}(\vec{q},\omega)$$

Response function:
Polarization function
or Generalized Susceptibility

$$\Pi^R(\vec{q},\omega) = \frac{-i}{\hbar}\int dt \; e^{i\omega t} \; \theta(t) \; \langle[\mathcal{O}(-\vec{q},t),\mathcal{O}(\vec{q},0)]\rangle$$

Response to static and uniform perturbations is related to thermodynamic derivatives.

$$\phi_{ext}(\vec{q}\to 0,\omega=0) = \delta\mu$$

perturbation can be viewed as a change in the chemical potential

Compressibility sum-rule:

$\Pi^R(0,0) = \left(\frac{\partial n}{\partial \mu}\right)_T$ where $n = \langle\mathcal{O}(0,0)\rangle$ is the associated density.

Dynamic Structure Factor

A simpler correlation function $$\mathcal{S}(\vec{q},\omega) = \int dt\ e^{i\omega t}\ \langle \mathcal{O}(-\vec{q},t)\mathcal{O}(\vec{q},0)\rangle$$

$$= 2\pi\hbar \sum_{m,n} \frac{e^{\beta K_n}}{\mathcal{Z}}\ |\langle n|\mathcal{O}_q|m\rangle|^2\ \delta(K_n - K_m - \hbar\omega)$$

where K_n are eigenvalues of $K = \mathcal{H} - \mu\ N$ (grand canonical Hamiltonian)

Fluctuation-dissipation theorem: $$\mathcal{S}(\vec{q},\omega) = \frac{-2\hbar\ \mathrm{Im}\ \Pi^R(\vec{q},\omega)}{1 - e^{-\beta\hbar\omega}}$$

The dynamic structure factor incorporates all of the many-body effects into the neutrino scattering and absorption rates.

Sum Rules

Static structure factor: $$\mathcal{S}_q = \int_{-\infty}^{\infty} \frac{d\omega'}{2\pi}\, \mathcal{S}(q,\omega')$$

F-sum rule: $$\boxed{\int_{-\infty}^{\infty} d\omega'\ \omega'\ \mathrm{Im}\ \Pi^R(q,\omega') = \langle[[\mathcal{H},\mathcal{O}_q],\mathcal{O}_q]\rangle}$$

Compressibility sum-rule: $$\boxed{-\int_{-\infty}^{\infty} \frac{d\omega'}{\pi}\ \frac{\mathrm{Im}\ \Pi^R(0,\omega')}{\omega'} = \mathrm{Re}\ \Pi^R(0,0) = \left(\frac{\partial n}{\partial \mu}\right)_T}$$

At T=0:

$$\int_{-\infty}^{\infty} \frac{d\omega'}{2\pi}\ \frac{(1-e^{-\beta\hbar\omega'})\mathcal{S}(q\to 0,\omega')}{\hbar\omega'} = \boxed{\int_{0}^{\infty} \frac{d\omega'}{2\pi}\ \frac{\mathcal{S}(q\to 0,\omega')}{\hbar\omega'} = \left(\frac{\partial n}{\partial \mu}\right)_{T=0}}$$

At high temperature: $(1-e^{-\beta\hbar\omega'}) \simeq \beta\hbar\omega'$

$$\boxed{\mathcal{S}_{q=0} = \mathrm{lt}_{q\to 0}\int_{-\infty}^{\infty} d\omega'\ \mathcal{S}(q,\omega) = T\ \left(\frac{\partial n}{\partial \mu}\right)_T}$$

General Structure of the Dynamic Response

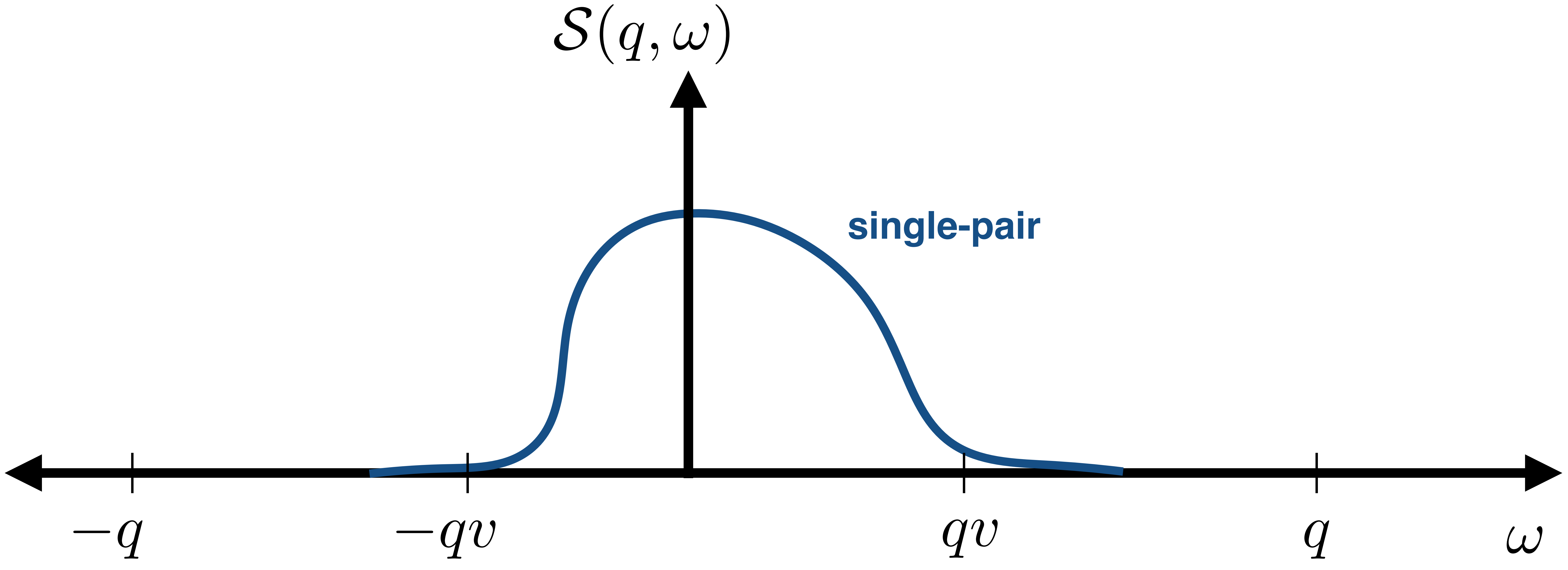

General Structure of the Dynamic Response

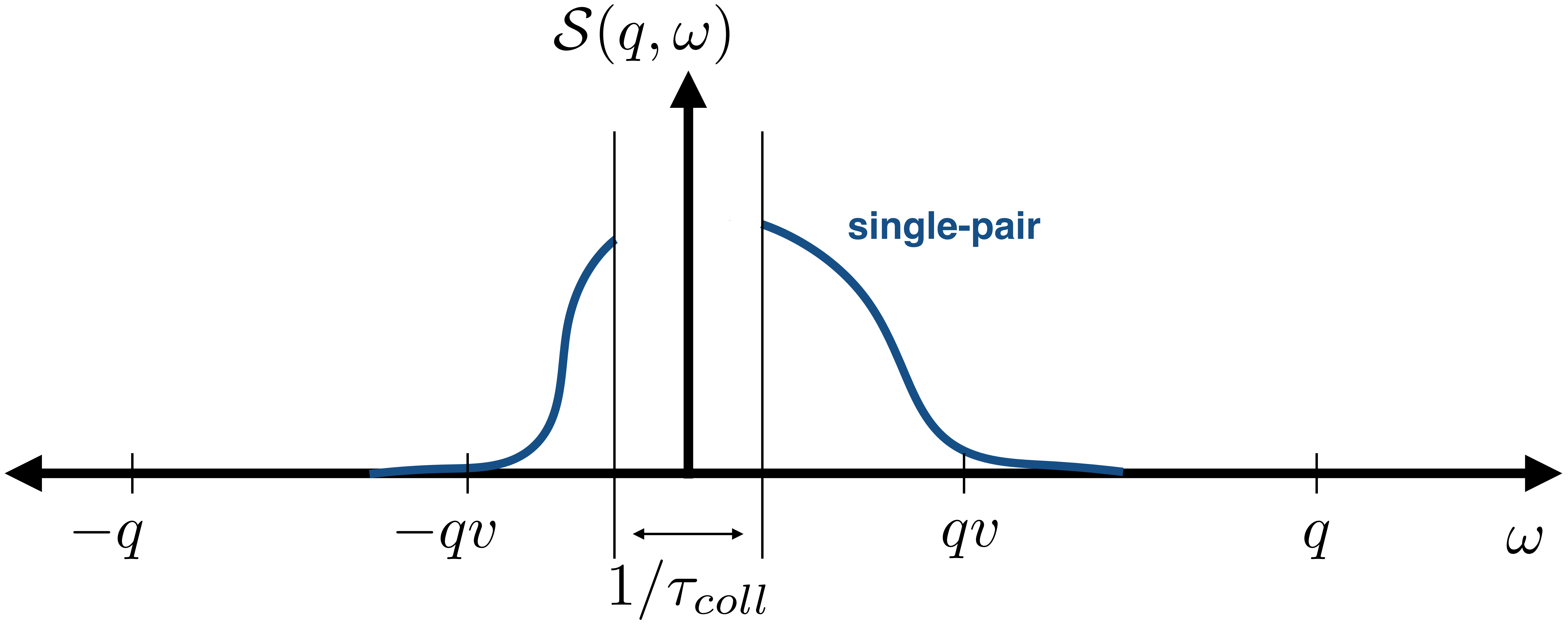

General Structure of the Dynamic Response

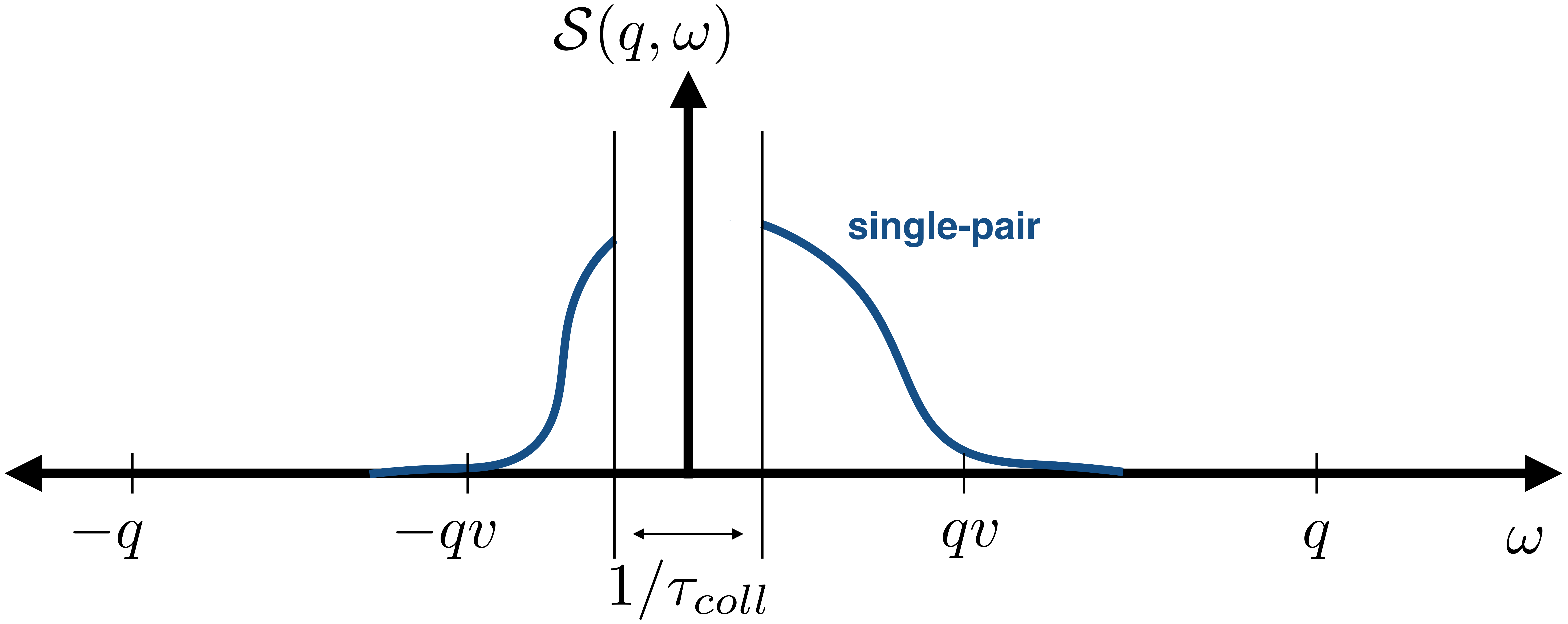

- At small ω response is governed by hydrodynamics.

General Structure of the Dynamic Response

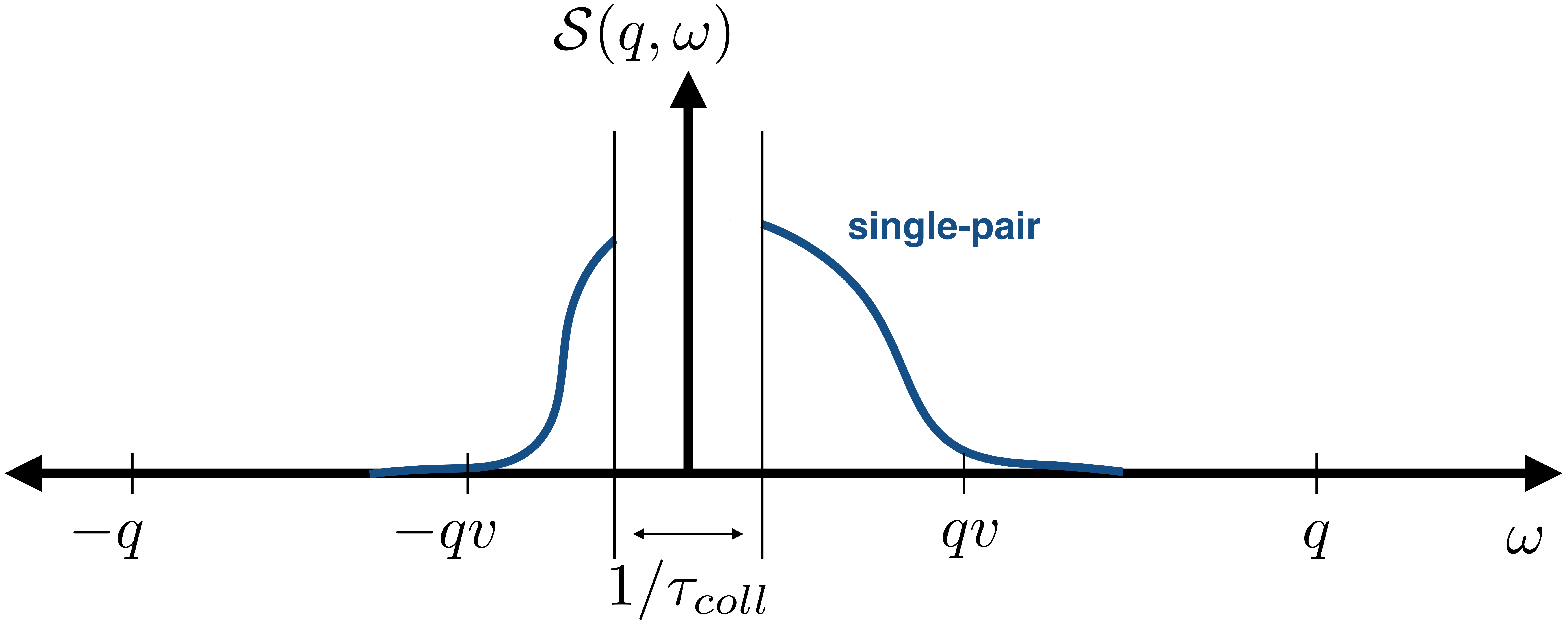

- At small ω response is governed by hydrodynamics.
- Single-pair response dominates for $|\omega\tau_{coll}| > 1$ and $|\omega| < qv$.

General Structure of the Dynamic Response

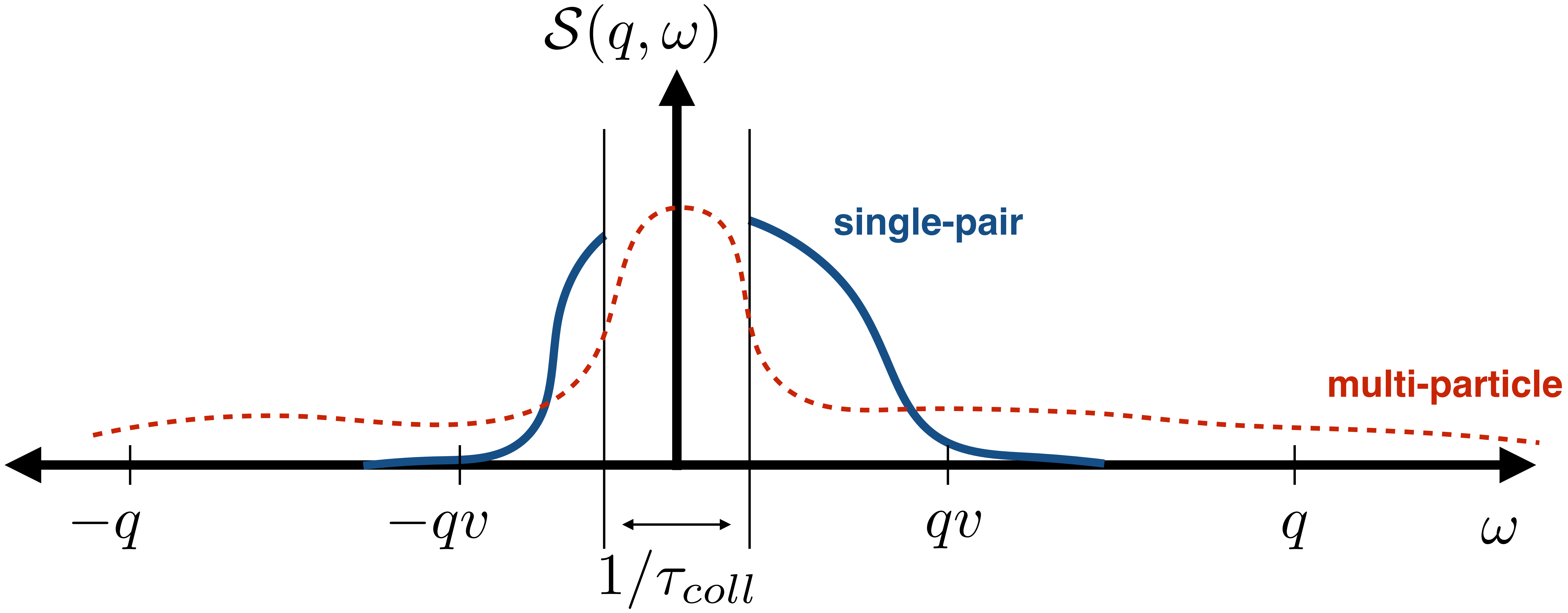

- At small ω response is governed by hydrodynamics.
- Single-pair response dominates for $|\omega\tau_{coll}| > 1$ and $|\omega| < qv$.

General Structure of the Dynamic Response

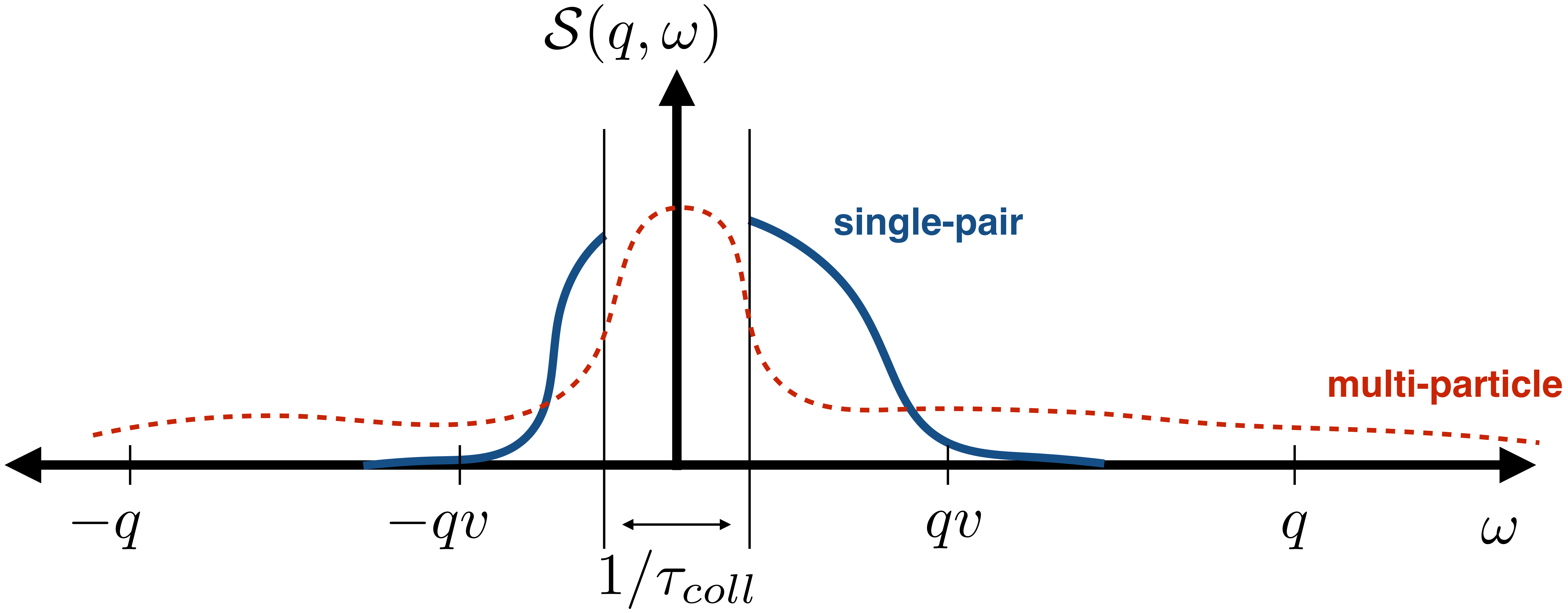

- At small ω response is governed by hydrodynamics.
- Single-pair response dominates for $|\omega\tau_{coll}| > 1$ and $|\omega| < qv$.
- Multi-particle response dominates for $|\omega| > qv$.

General Structure of the Dynamic Response

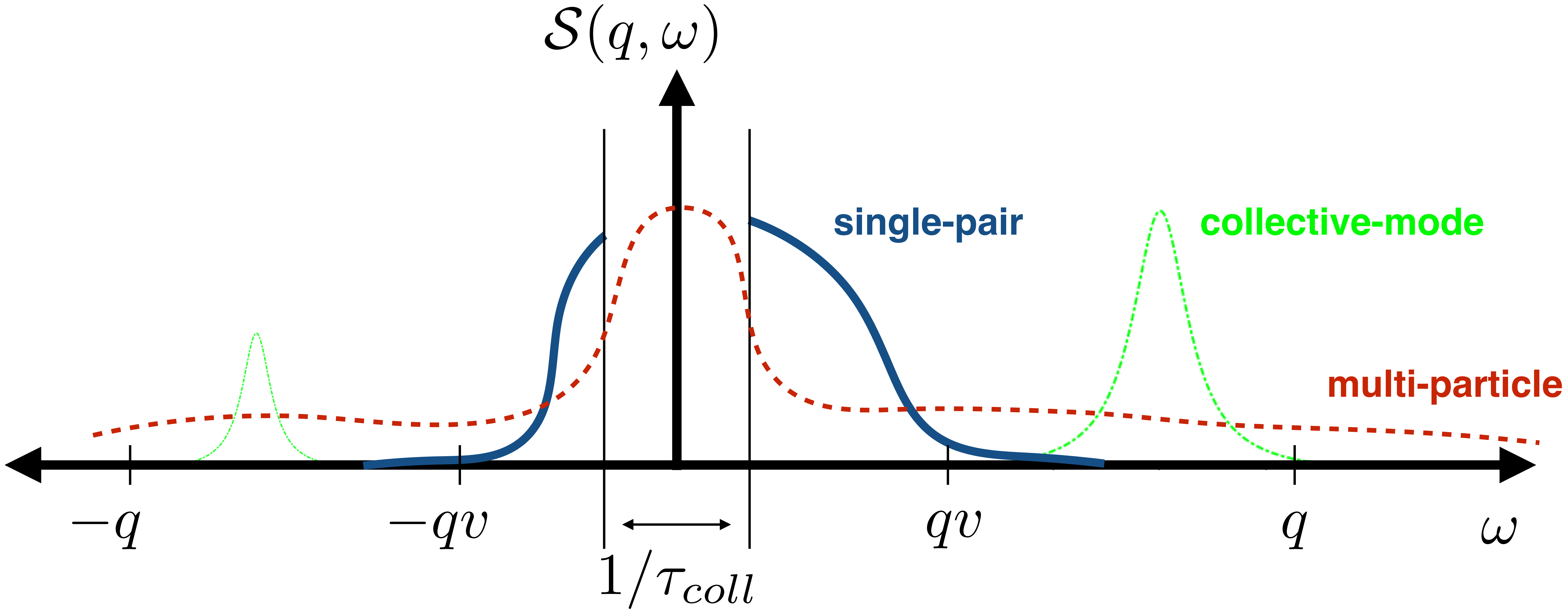

- At small ω response is governed by hydrodynamics.
- Single-pair response dominates for $|\omega\tau_{coll}| > 1$ and $|\omega| < qv$.
- Multi-particle response dominates for $|\omega| > qv$.

General Structure of the Dynamic Response

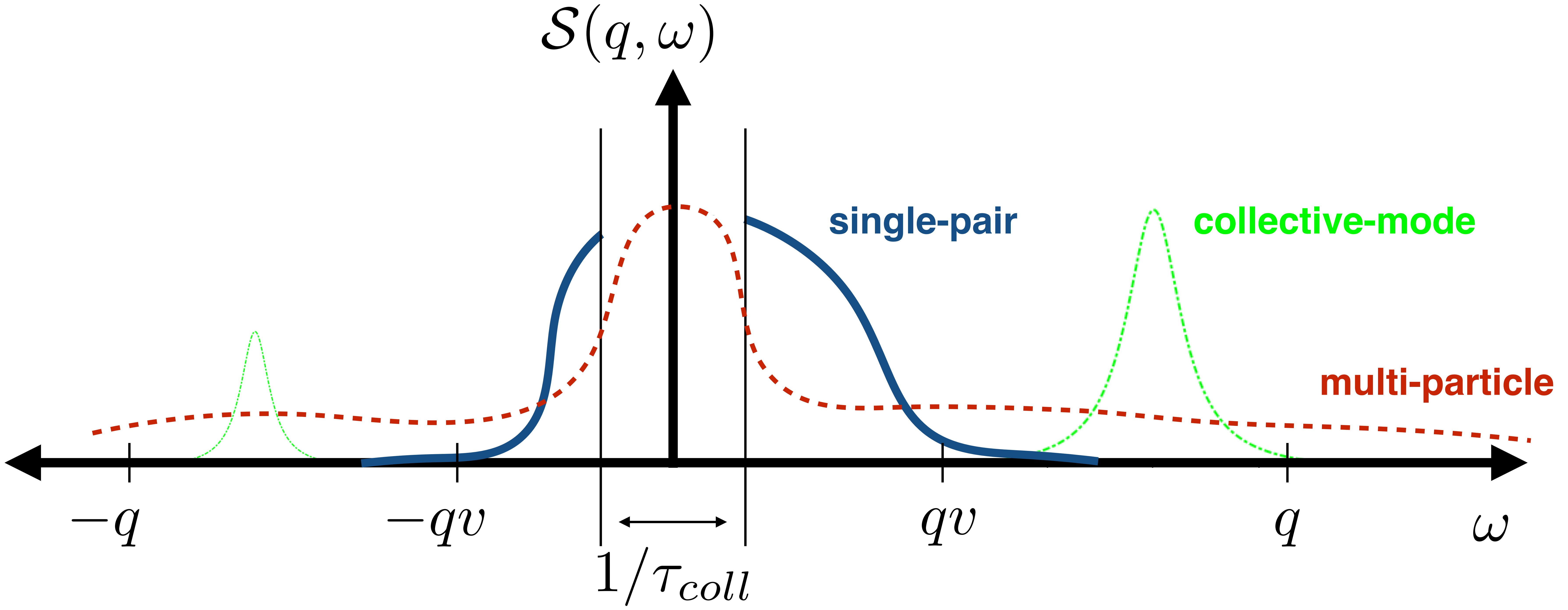

- At small ω response is governed by hydrodynamics.
- Single-pair response dominates for $|\omega\tau_{\text{coll}}| > 1$ and $|\omega| < qv$.
- Multi-particle response dominates for $|\omega| > qv$.
- Collective modes arise due to repulsive interactions.

General Structure of the Dynamic Response

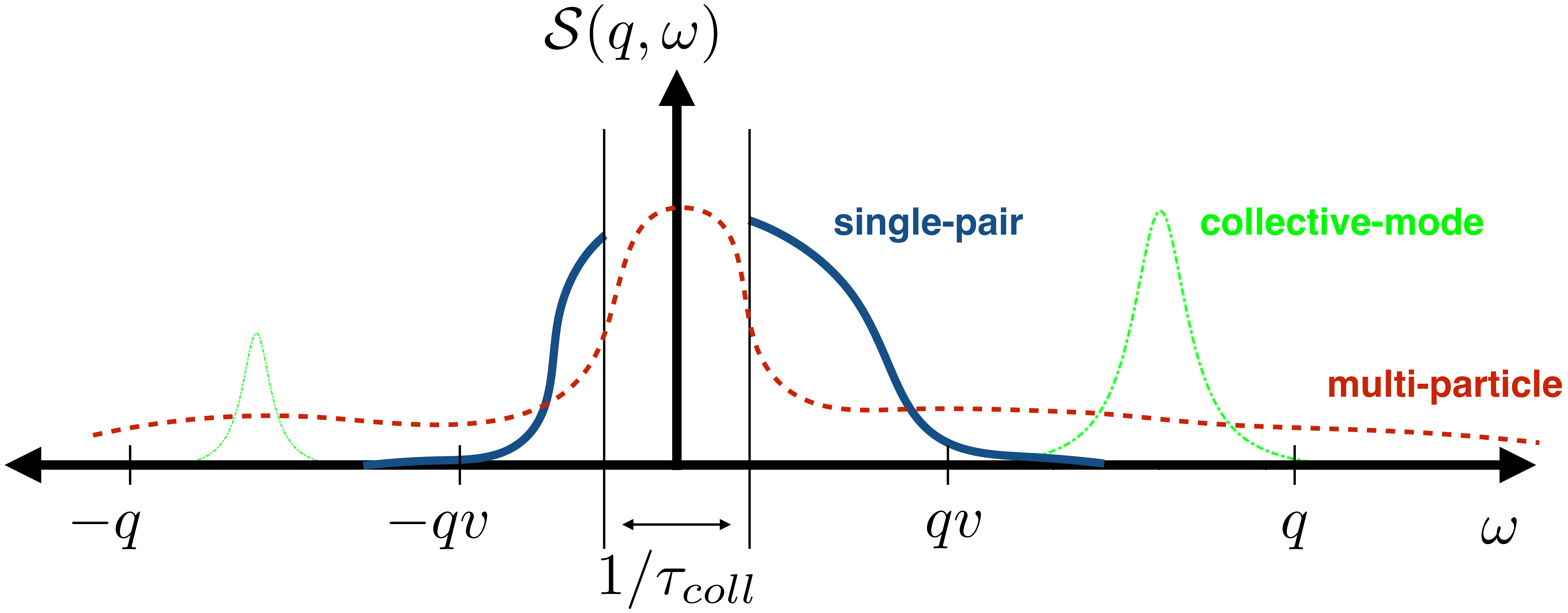

- At small ω response is governed by hydrodynamics.
- Single-pair response dominates for $|\omega\tau_{coll}| > 1$ and $|\omega| < qv$.
- Multi-particle response dominates for $|\omega| >$ qv.
- Collective modes arise due to repulsive interactions.

In hot and dense nuclear matter single-pair, multi-particle and collective modes all contribute to low energy response.

Neutrino Interactions in Dense Matter

Low energy Lagrangian: $\mathcal{L} = \frac{G_F}{\sqrt{2}} \, l_\mu \, j^\mu$ $\qquad l_1 + N_2 \rightarrow l_3 + N_4$

Absorption:	$l_\mu^{cc} = \bar{l}\gamma_\mu(1-\gamma_5)\nu_l$	$j^\mu_{cc} = \bar{\Psi}_p \left(\gamma^\mu(g_V - g_A\gamma_5) + F_2 \frac{i\sigma^{\mu\alpha}q_\alpha}{2M}\right) \Psi_n$
Scattering:	$l_\mu^{nc} = \bar{\nu}\gamma_\mu(1-\gamma_5)\nu$	$j^\mu_{nc} = \bar{\Psi}_i \, (\gamma^\mu(C_V^i - C_A^i\gamma_5) + F_2^i \frac{i\sigma^{\mu\alpha}q_\alpha}{2M}) \, \Psi_i$

Rate: $$\frac{d\Gamma(E_1)}{dE_3 d\mu_{13}} = \frac{G_F^2}{32\pi^2}\frac{p_3}{E_1}(1-f_3(E_3))L_{\mu\nu} \, \mathcal{S}^{\mu\nu}(q_0,q)$$

Dynamic structure function: $$\mathcal{S}^{\mu\nu}(q_0,q) = \frac{-2 \, \mathrm{Im} \, \mathbf{\Pi}^{\mu\nu}(q_0,q)}{1-\exp\left(-(q_0+\Delta\mu)/T\right)}$$

Current-current correlations functions: $$\mathbf{\Pi}^{\mu\nu}(q_0,q) = -i\int dt \; d^3x \; \theta(t) \; e^{i(q_0 t - \vec{q}\cdot\vec{x})}\langle \; |[j_\mu \; (\vec{x},t), j_\nu(\vec{0},0)]| \; \rangle$$

difficult to calculate in general due to the non-perturbative nature of strong interactions.

Sawyer (1970s), Iwamoto & Pethick (1980s),
Burrows & Sawyer, Horowitz & Wehrberger, Raffelt et al., Reddy et al. (1990s),
Benhar, Carlson, Gandolfi, Horowitz, Lavato, Pethick, Reddy, Roberts, Schwenk, Shen, and others (2000s)

Neutrino Scattering off Non-Relativistic Targets

Current simplifies in the non-relativistic limit: $j^\mu_{nc} = \underbrace{\Psi^\dagger \Psi}_{\text{density}}\ \delta^\mu_0 + \underbrace{\Psi^\dagger \sigma_k \Psi}_{\text{spin-density}}\ \delta^\mu_k + \mathcal{O}[\frac{p}{M}]$

density

spin-density

dynamic response functions

$$\frac{d\Gamma(E_1)}{d\Omega dE_3} = \frac{G_F^2}{4\pi^2}\ E_3^2\ \left[C_V^2(1+\cos\theta_{13})S_\rho(\omega,q) + C_A^2(3-\cos\theta_{13})S_\sigma(\omega,q)\right]$$

S(q,ω) of a classical dense liquid

Density-density correlation function is:

$$\langle \rho(\mathbf{q},\mathbf{0})\rho(\mathbf{q},\mathbf{t})\rangle = \langle \mathbf{\Sigma_i}\ \mathbf{e}^{-\mathbf{iq.r_i}}\mathbf{\Sigma_j}\ \mathbf{e}^{-\mathbf{iq.r_j(t)}}\rangle$$

Ensemble average

Positions at t=0

Positions at t

Equation of motion for particles:

$$\mathbf{r}_j(\Delta t) = \mathbf{r}_j(0) + \mathbf{v}_j\ \Delta t + \frac{1}{2\ m}\Sigma_{i\neq j}\mathbf{F}_{ij}\ t^2$$

Carlson & Reddy (2004)

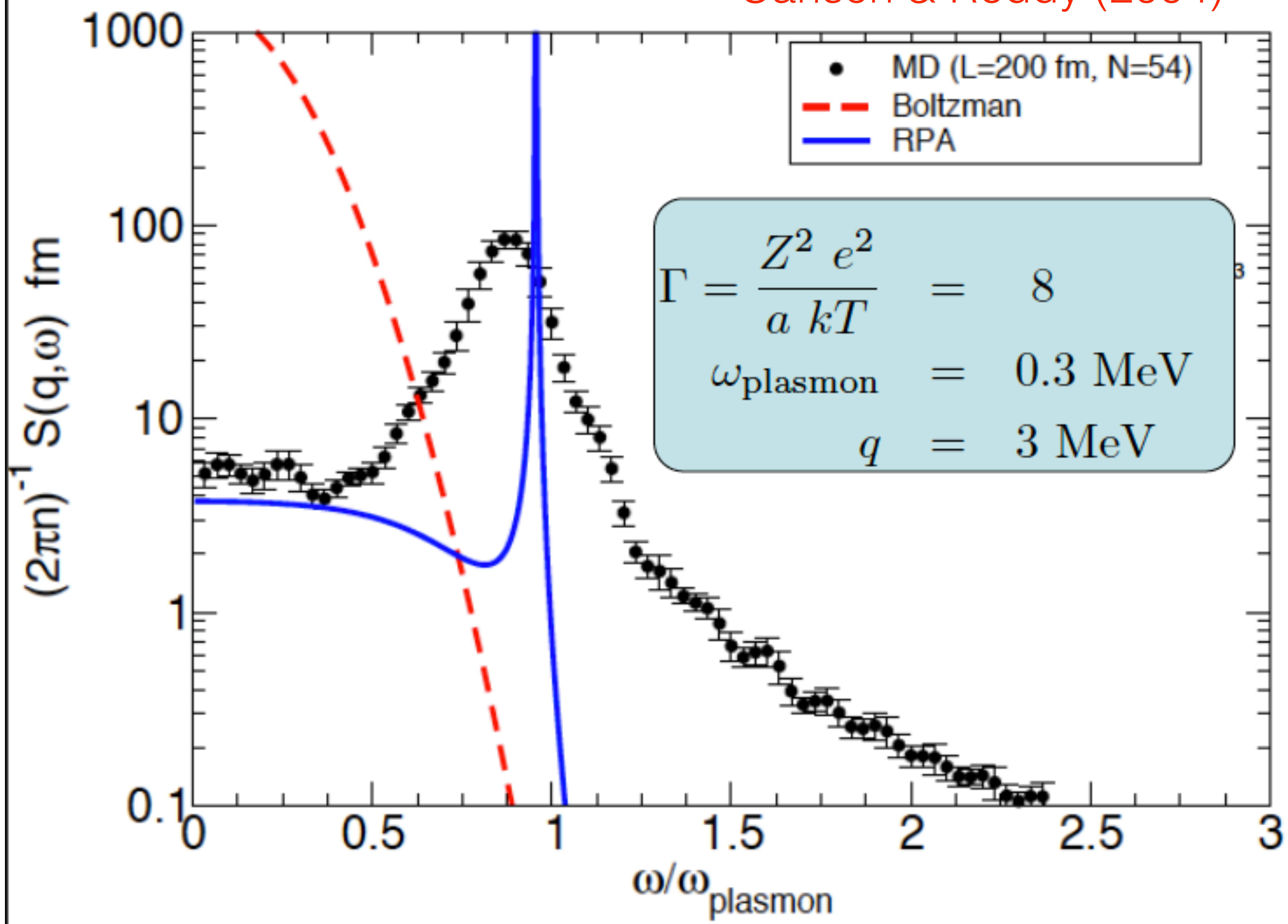

For a large number of classical particles the equations of motion are obtained through numerical simulations - Molecular Dynamics.
The response can also be calculated diagrammatic methods. Typically require approximations and re-summations. One such approximation is called the Random Phase Approximation or RPA.

Mean Field Theory & Random Phase Approximation

Particles interact with a space and time independent background density. The forward scattering changes its dispersion relation.

Coupling to external probes is screened. This screening is accounted for by RPA. The dressed vertex is calculated by summing a class of diagrams.

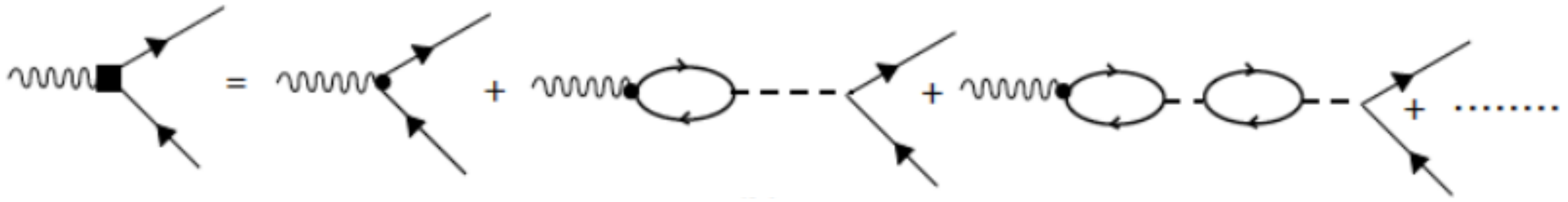

The correlation functions (response) are calculated using the dressed propagator and vertices.

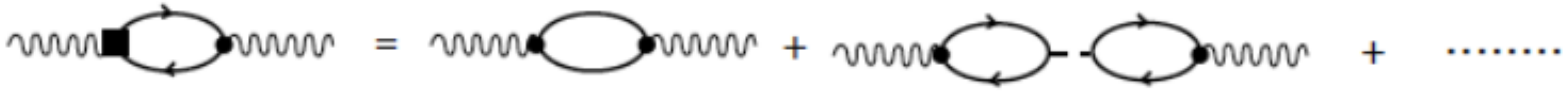

Neutrino Scattering in Nuclear Matter

$$\frac{d\Gamma(E_1)}{d\Omega dE_3} = \frac{G_F^2}{4\pi^2}\; E_3^2 \;\left[C_V^2(1+\cos\theta_{13})S_\rho(\omega,q) + C_A^2(3-\cos\theta_{13})S_\sigma(\omega,q)\right]$$

Neutrinos scatter off density and spin fluctuations. Coupling to spin is stronger.

- Nuclear interactions suppress spin fluctuations.
- Density fluctuations are suppressed at high density and enhanced at low density.

Net effect is to speed up diffusion.

$$D_\nu \propto \int dE_\nu\; f(E_\nu)E_\nu^2\; \lambda_\nu(E_\nu)$$

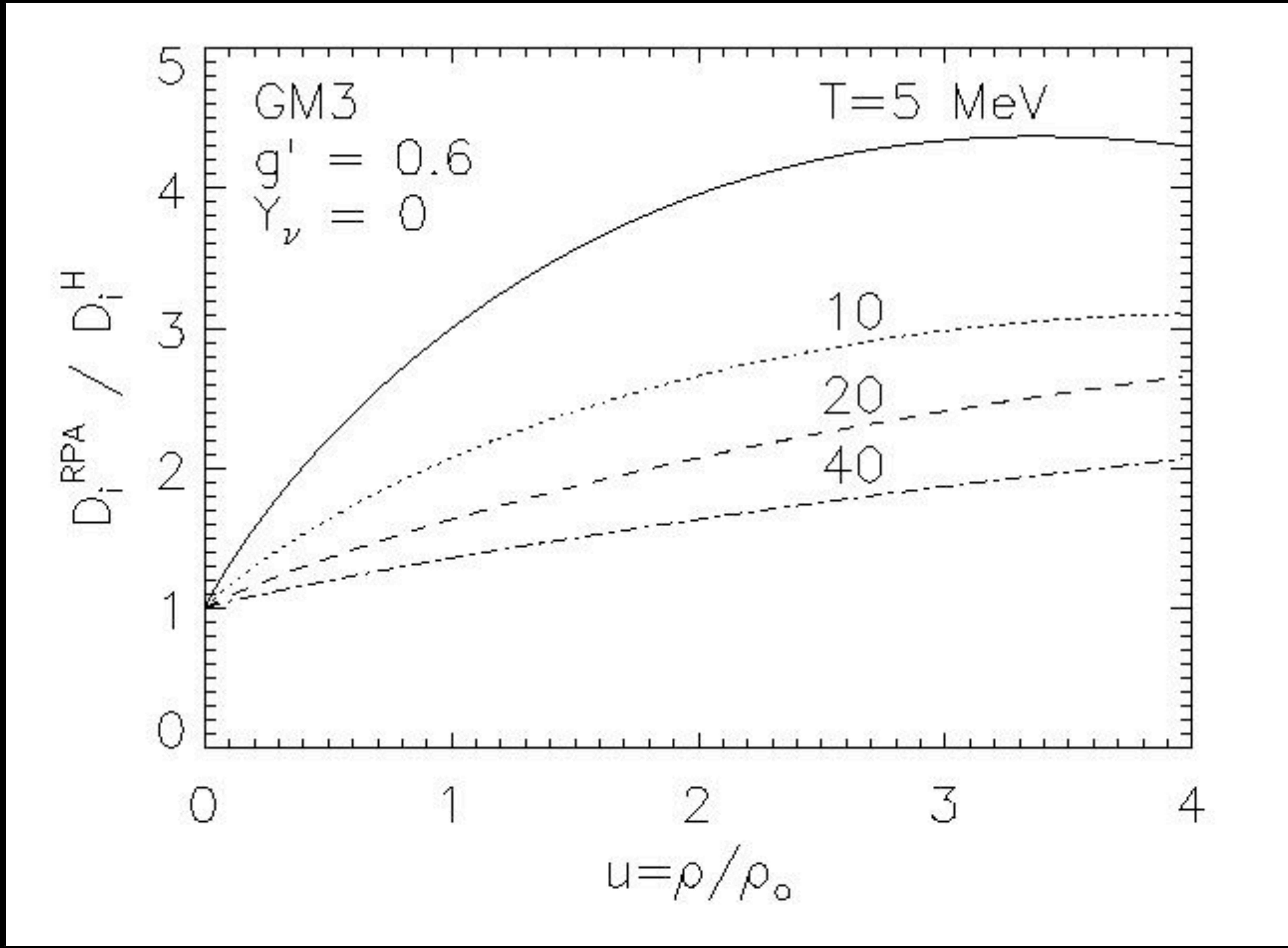

Charged Current Reactions in Neutron-Rich Matter

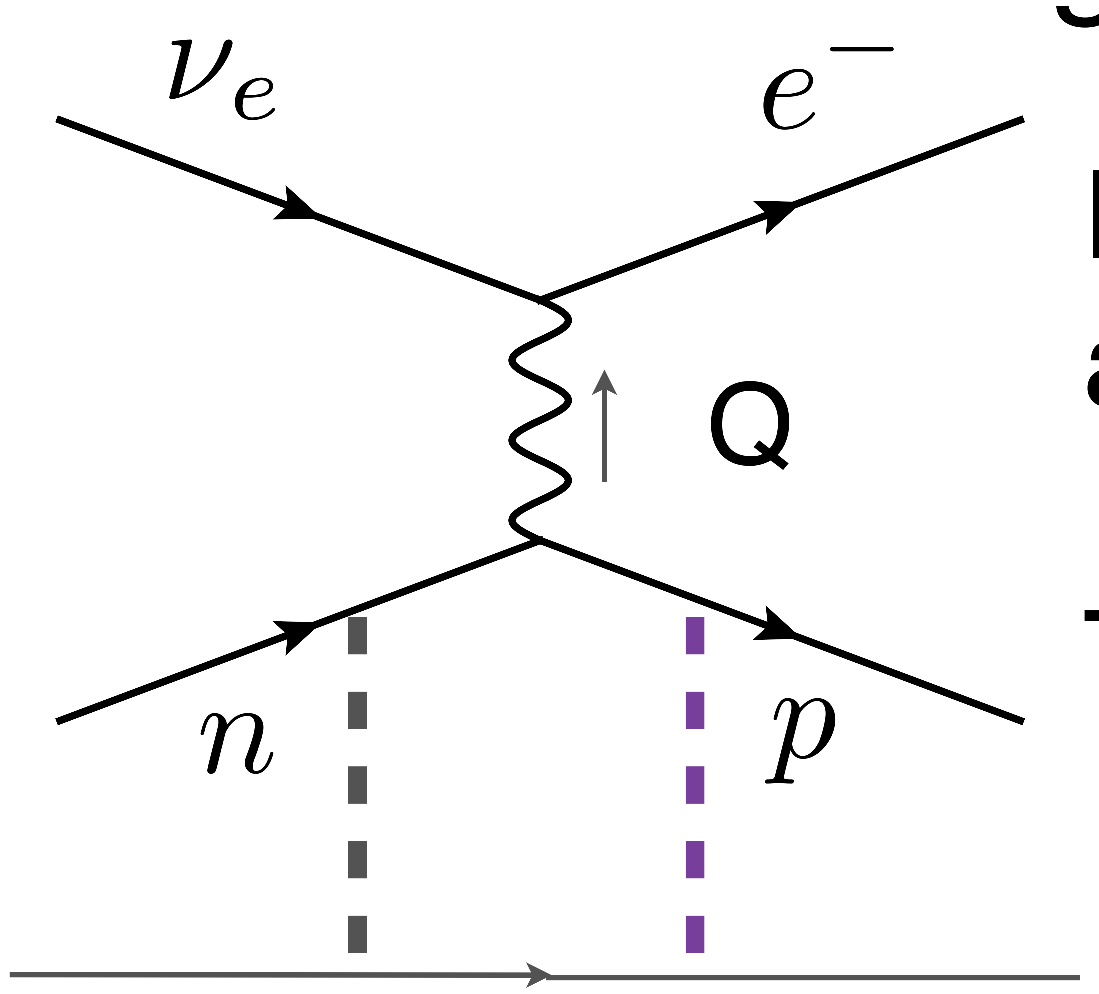

Dense Medium

Potential energy difference between neutrons and protons is large - and related to the low density symmetry energy.

The pseudo-potential is suitable to calculate the nucleon self-energy.

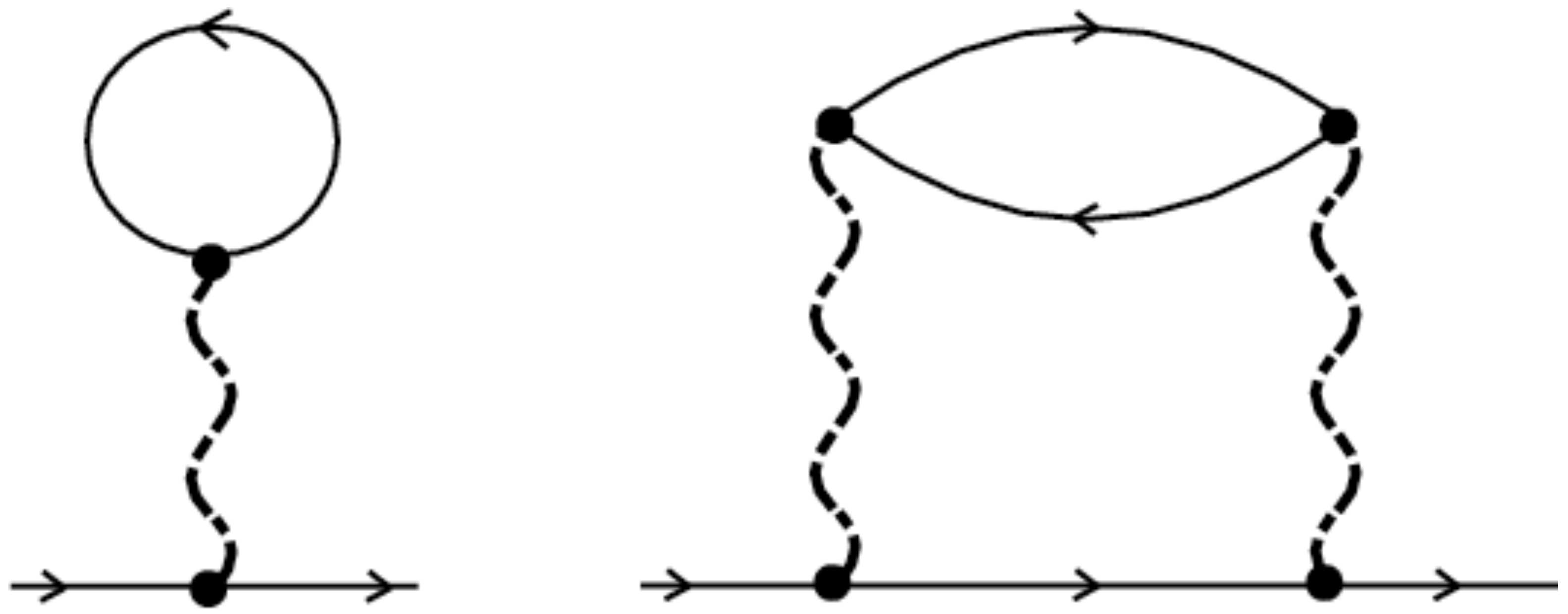

(a) (b)

$$E_n(p) \approx m_n + \frac{p^2}{2m_n^*} + U_n + i\,\Gamma_n$$

$$E_p(p+q) \approx m_p + \frac{(p+q)^2}{2m_n^*} + U_p + i\,\Gamma_p$$

$$\mathrm{Q} = \varepsilon_n(\vec{k}) - \varepsilon_p(\vec{k} - \vec{q})$$

$$= M_n - M_p + \Sigma_n(k) - \Sigma_n(k-q)$$

Reddy, Prakash & Lattimer (1998), Martinez-Pinedo et al. (2012), Roberts & Reddy (2012), Rrapaj, Bartl, Holt, Reddy, Schwenk (2015)

Charged Current Reactions in Neutron-Rich Matter

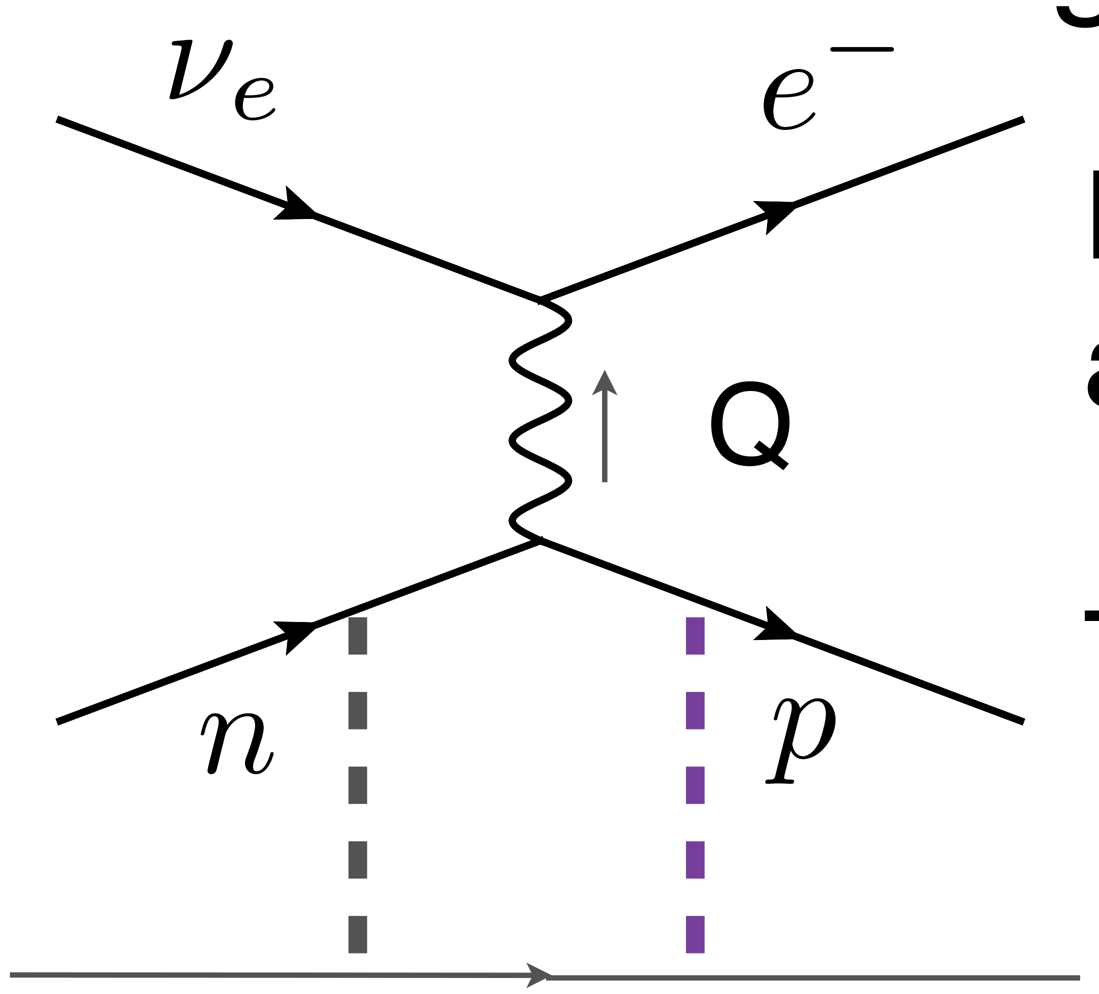

Dense Medium

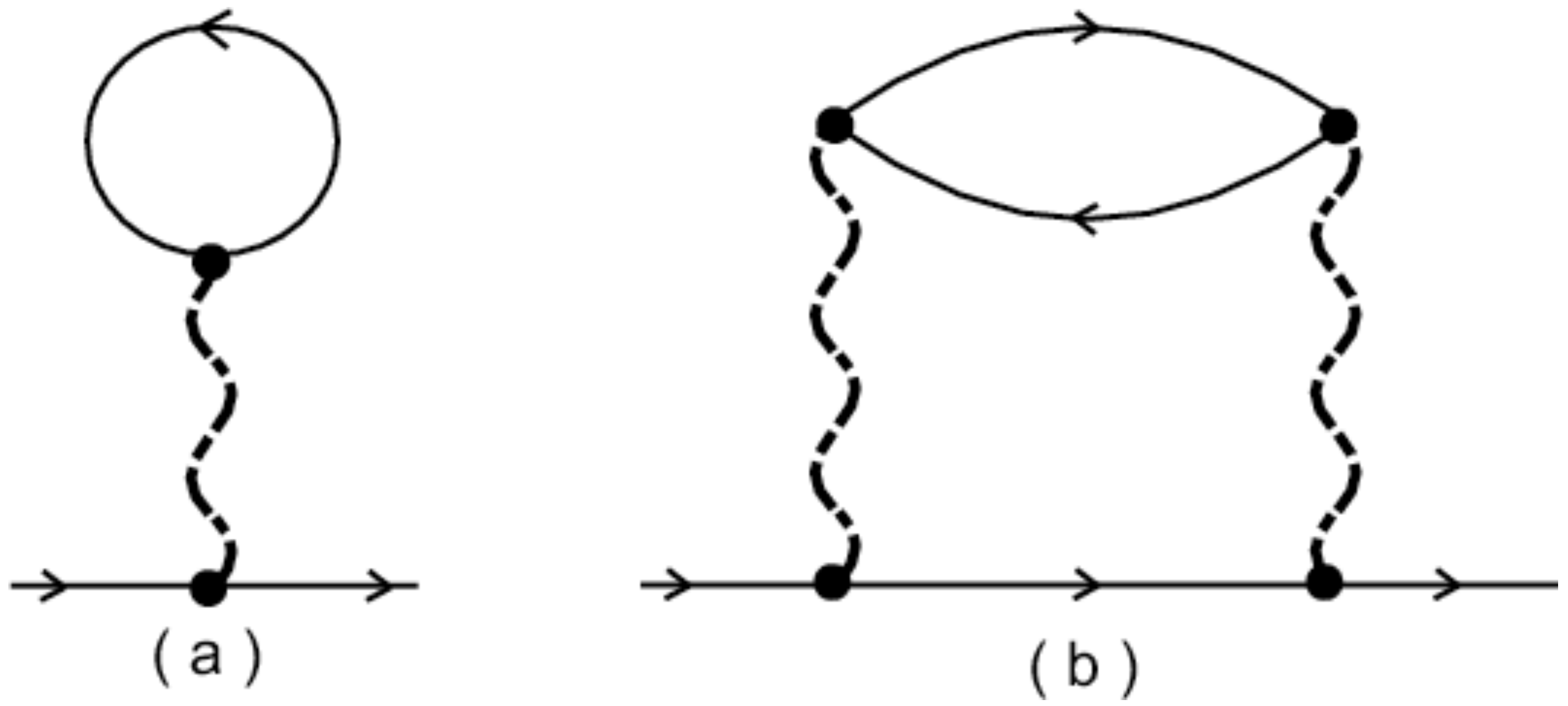

Potential energy difference between neutrons and protons is large - and related to the low density symmetry energy.

The pseudo-potential is suitable to calculate the nucleon self-energy.

$$\mathrm{Q} = \varepsilon_n(\vec{k}) - \varepsilon_p(\vec{k} - \vec{q})$$

$$= M_n - M_p + \Sigma_n(k) - \Sigma_n(k - q)$$

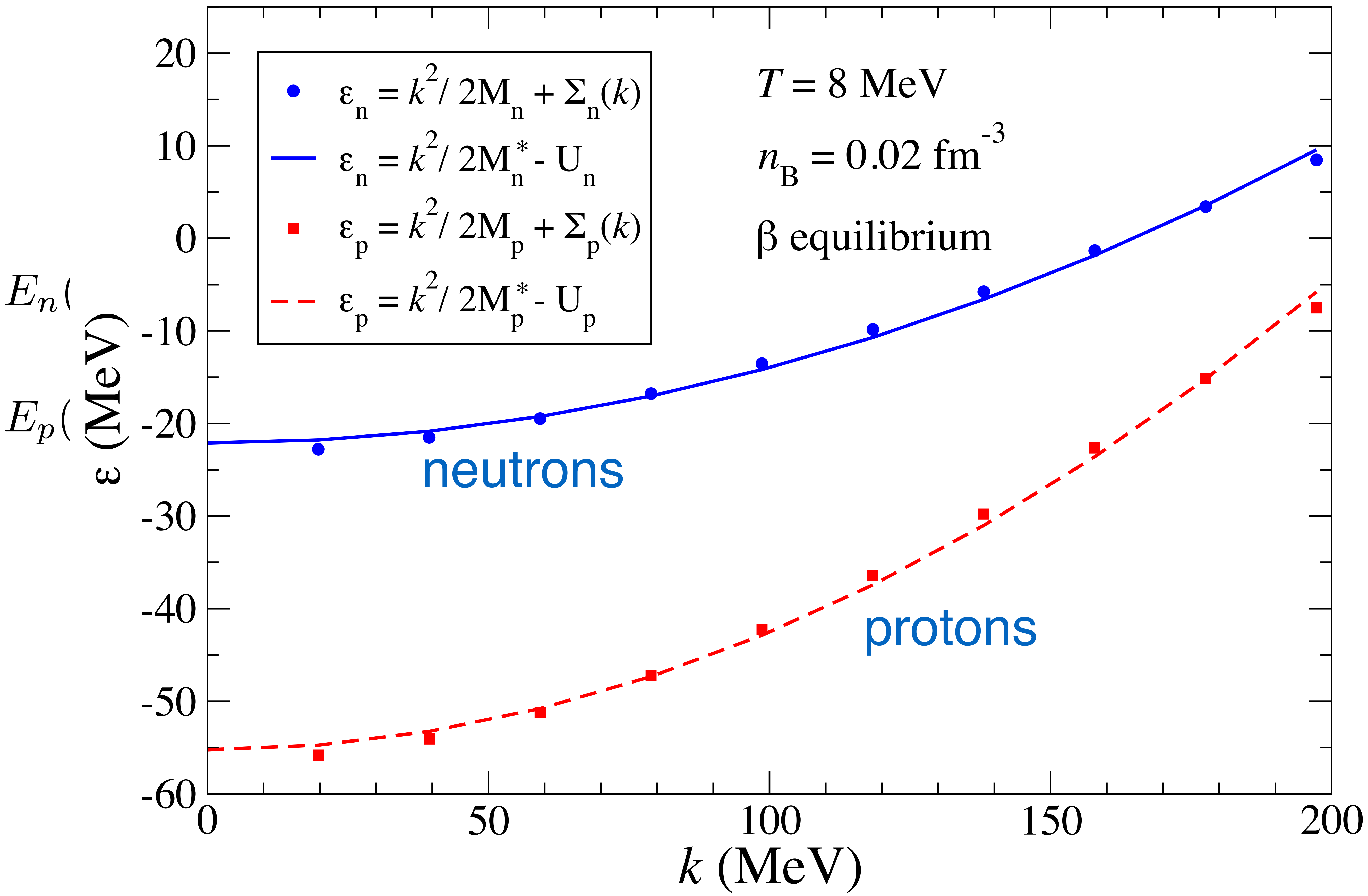

Reddy, Prakash & Lattimer (1998), Martinez-Pinedo et al. (2012), Roberts & Reddy (2012), Rrapaj, Bartl, Holt, Reddy, Schwenk (2015)

Charged Currents: Asymmetric Energy Shifts are Important

$$\frac{d\Gamma}{\cos\theta dE_e} = \frac{G_F^2}{2\pi} p_e \ E_e \left(1 - f_e(E_e)\right) \times \left[(1+\cos\theta) S_\tau(q_0, q) + g_A^2 (3 - \cos\theta) S_{\sigma\tau}(q_0, q)\right]$$

- Energy shift helps overcome electron final state blocking.
- Enhances ν_e absorption
- Larger energy needed to produce neutrons suppresses anti-ν_e absorption.

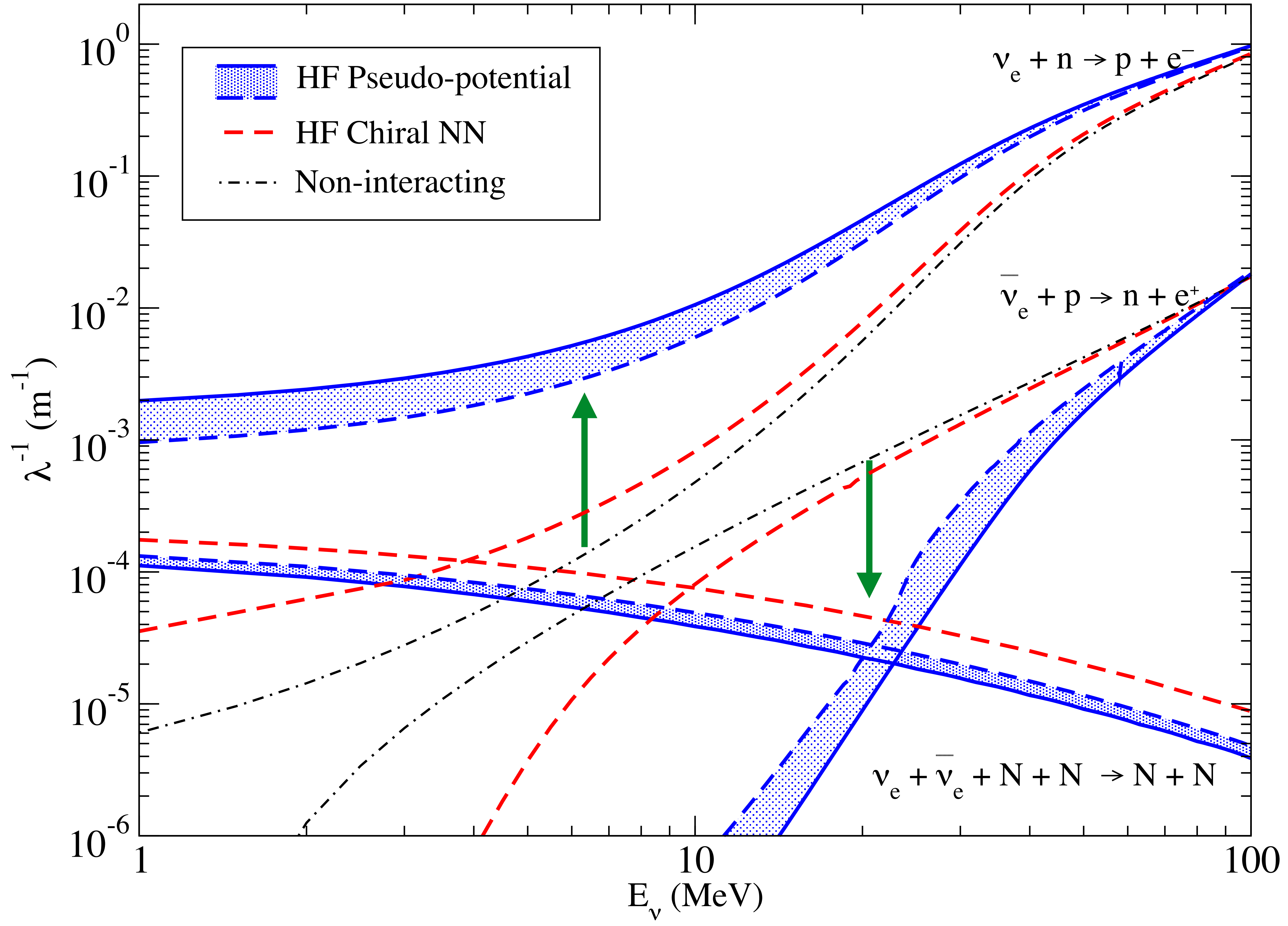

Roberts & Reddy (2012) Rrapaj, Holt, Bartl, Reddy & Schwenk (2015)

Neutrino Scattering in Novel High Density Phase in the Core

Two examples:

- Generic first-order transitions.
- Superconducting quark matter.

Mixed Phase are Generic to First-order Transitions

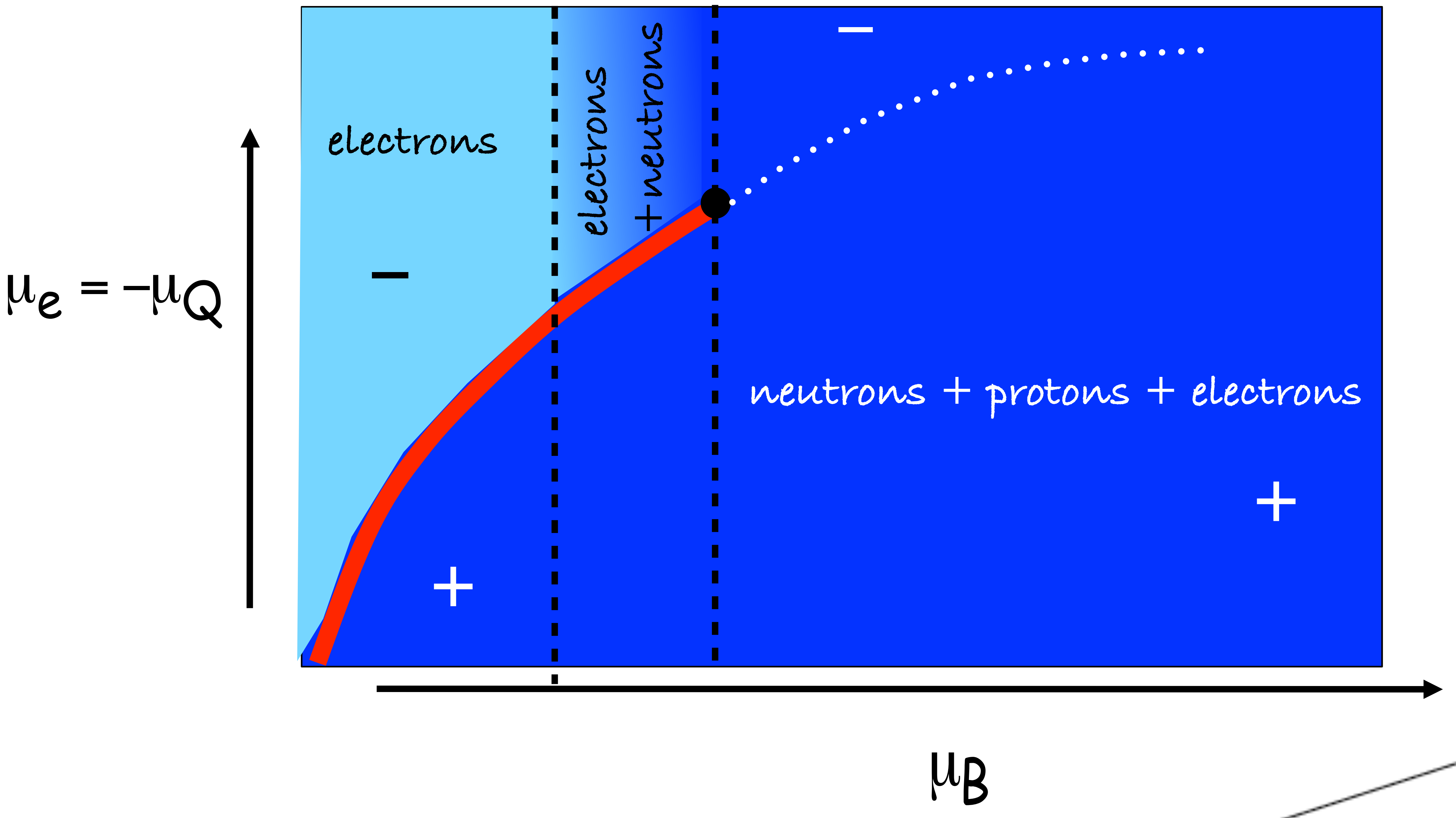

Nuclear Matter to Quark Matter

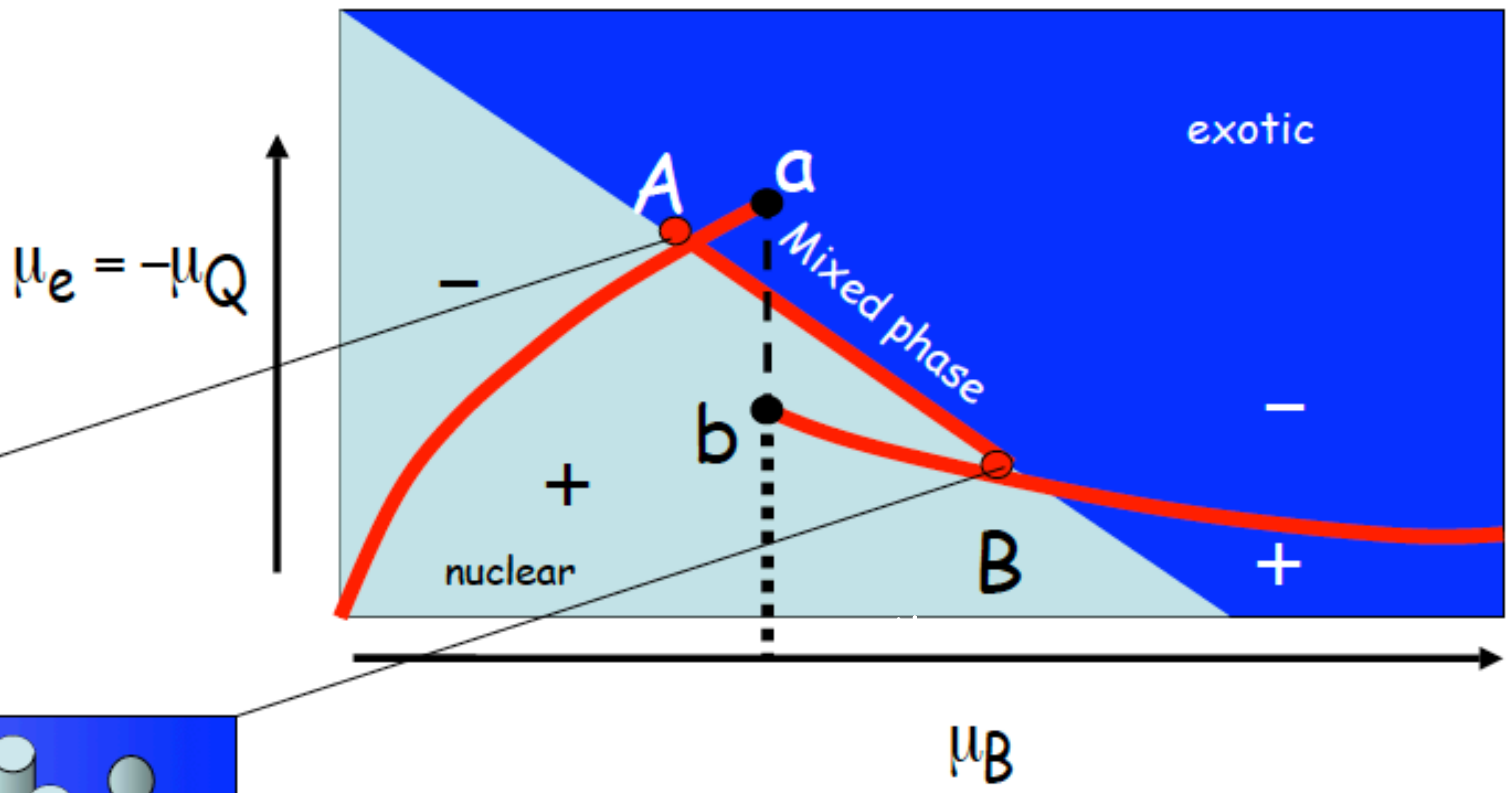

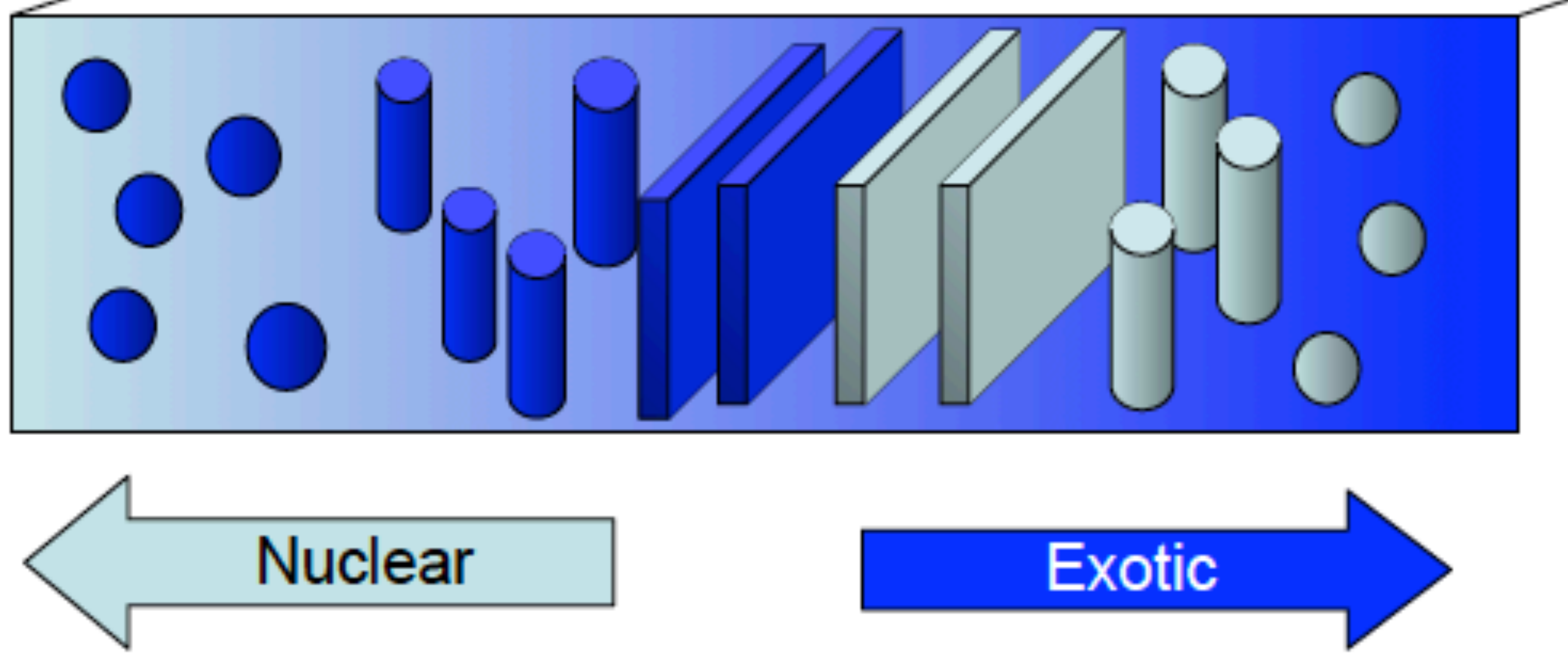

Mixed Phase:
Heterogeneous phase with structures of size 5-10 fm.

Neutrino Scattering in the Mixed Phase

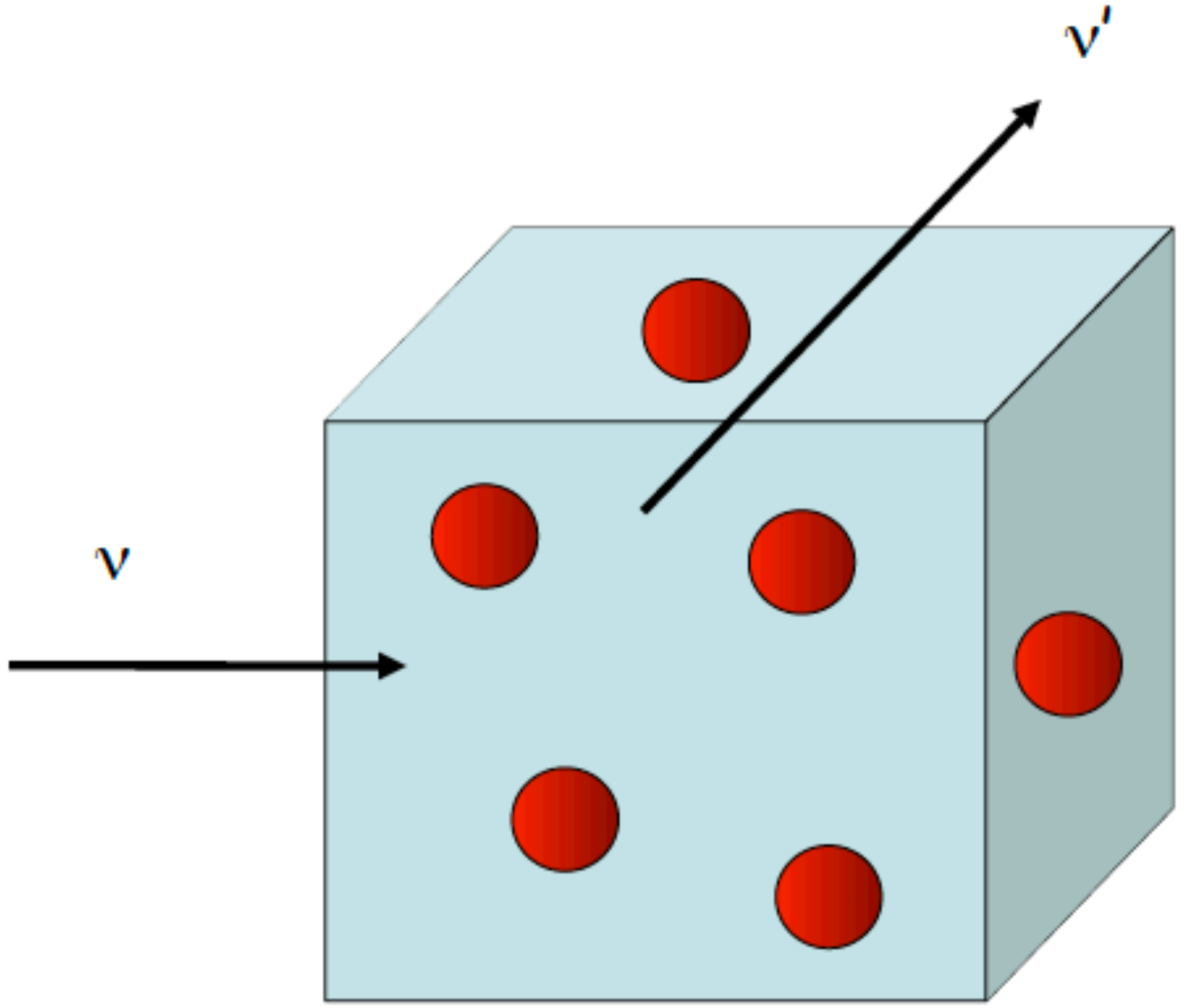

quark droplets in nuclear matter.

$$\frac{d\sigma}{d\cos(\theta)} = N_D \frac{G_F^2}{16\pi} S_q \, Q_W^2 E_\nu^2 (1 + \cos(\theta))$$

number density of droplets

weak charge of the droplet.

Neutrino Scattering in the Mixed Phase

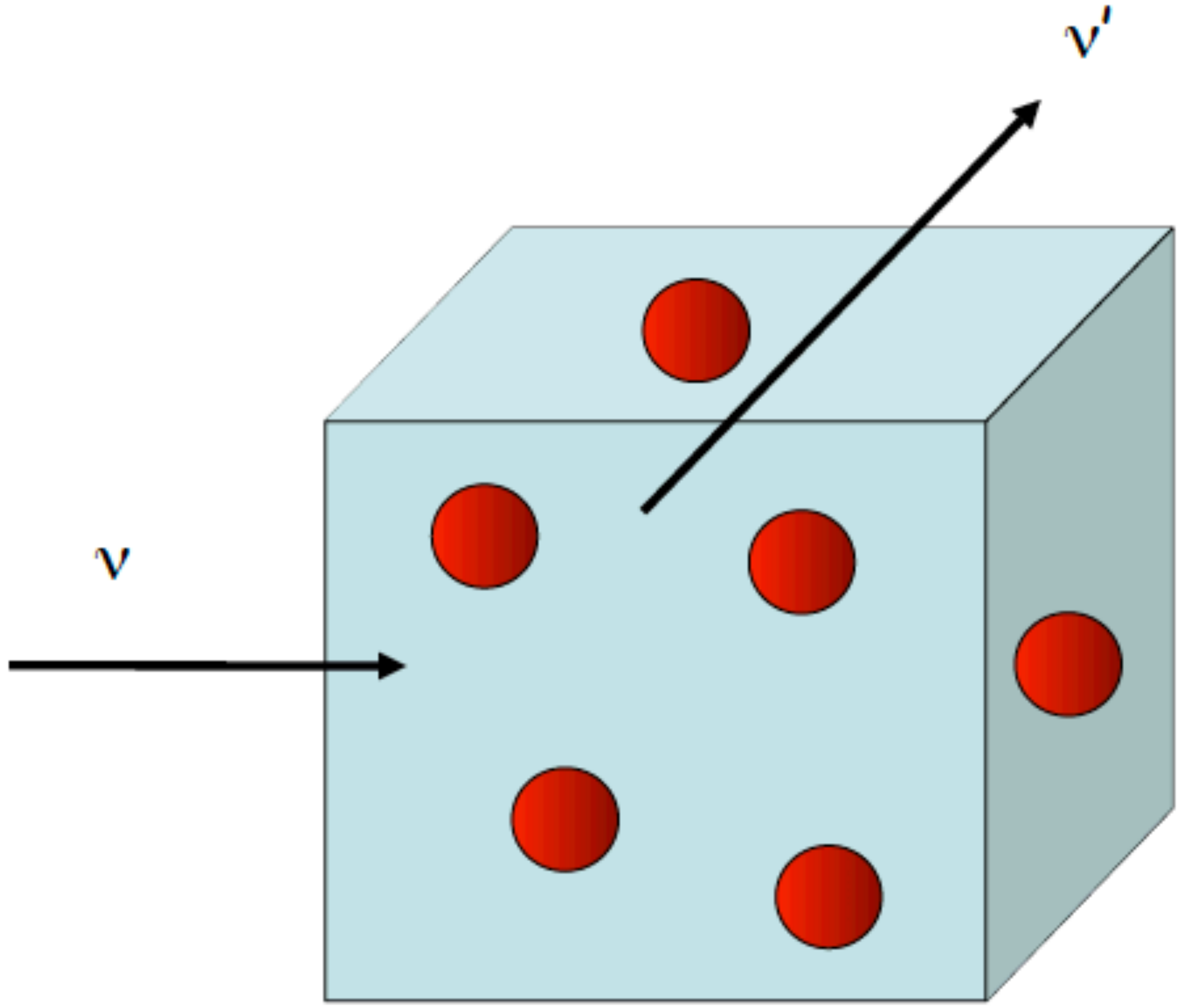

quark droplets in nuclear matter.

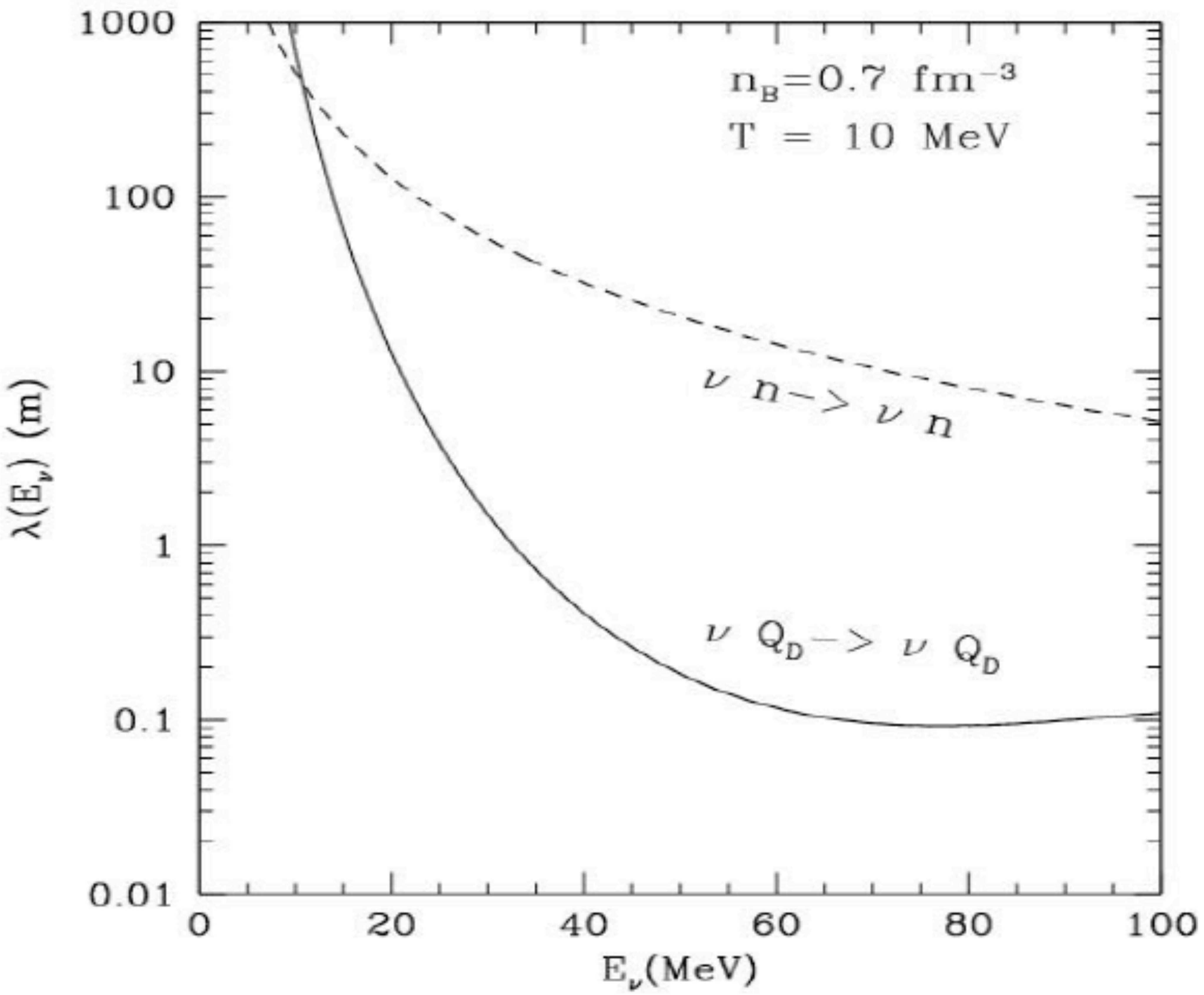

$$\frac{d\sigma}{d\cos(\theta)} = N_D \frac{G_F^2}{16\pi} S_q \, Q_W^2 E_\nu^2 (1 + \cos(\theta))$$

number density of droplets

weak charge of the droplet.

Neutrino Scattering in the Mixed Phase

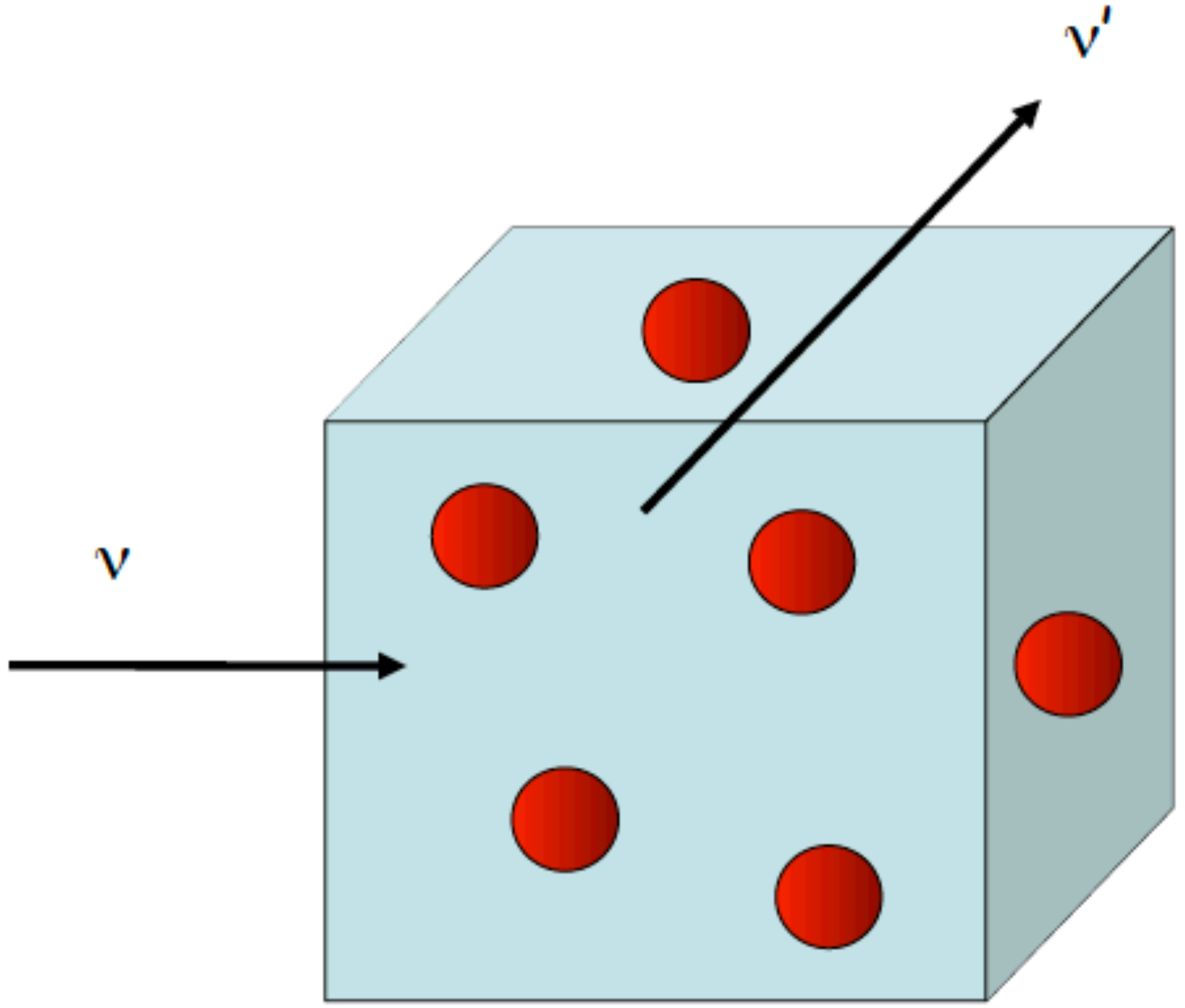

quark droplets in nuclear matter.

$$\frac{d\sigma}{d\cos(\theta)} = N_D \frac{G_F^2}{16\pi} S_q \, Q_W^2 E_\nu^2 (1+\cos(\theta))$$

number density of droplets

weak charge of the droplet.

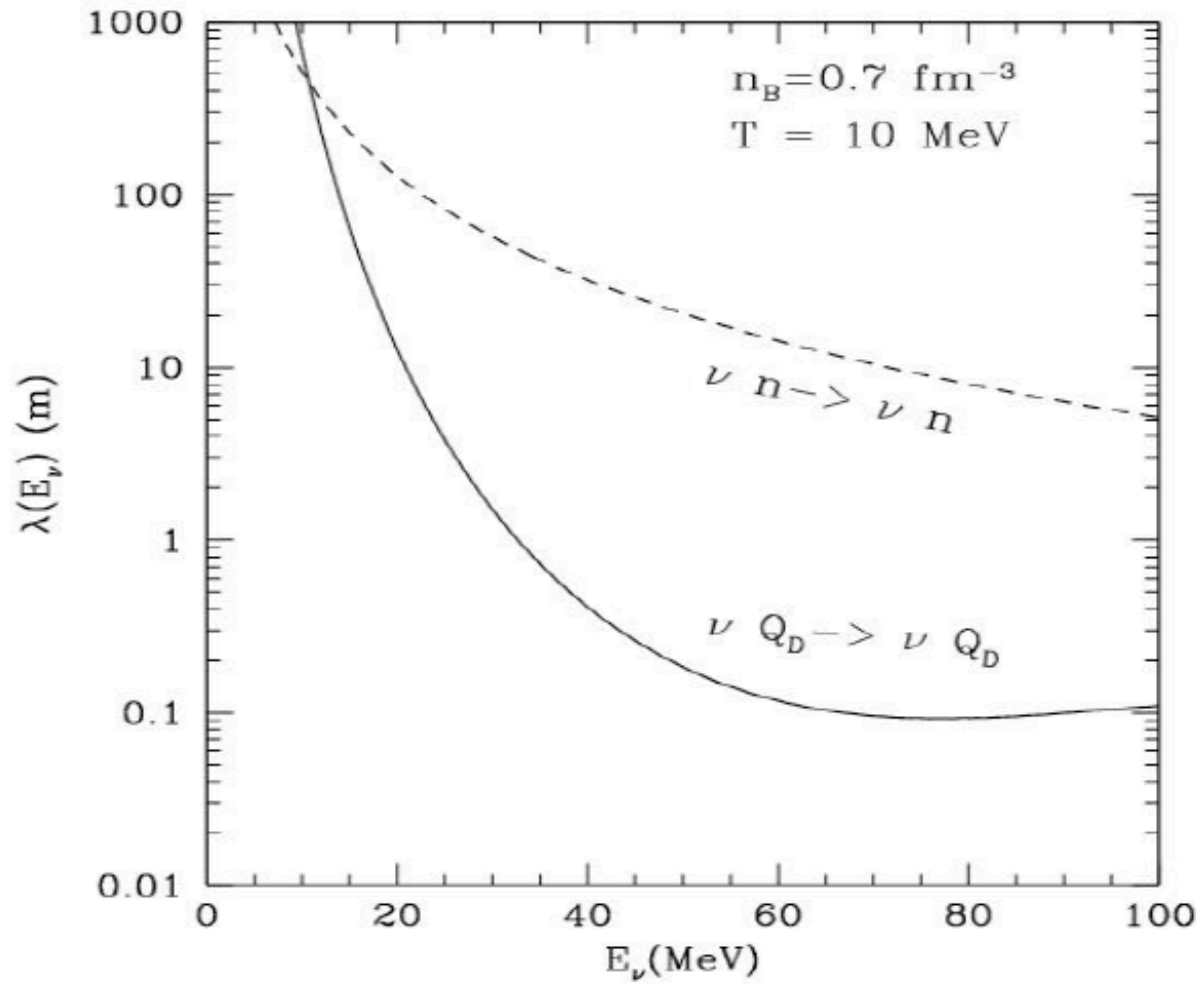

Coherent scattering from the droplets is large. Greatly reduces the neutrino mean free paths.

Neutrino Scattering in Superconducting Quark Matter.

$$\Pi_{\mu\nu}(q_0, q) = -i \int d^4p \; \mathrm{Tr}[G(p+q)\Gamma_\mu G(p)\Gamma_\nu]$$

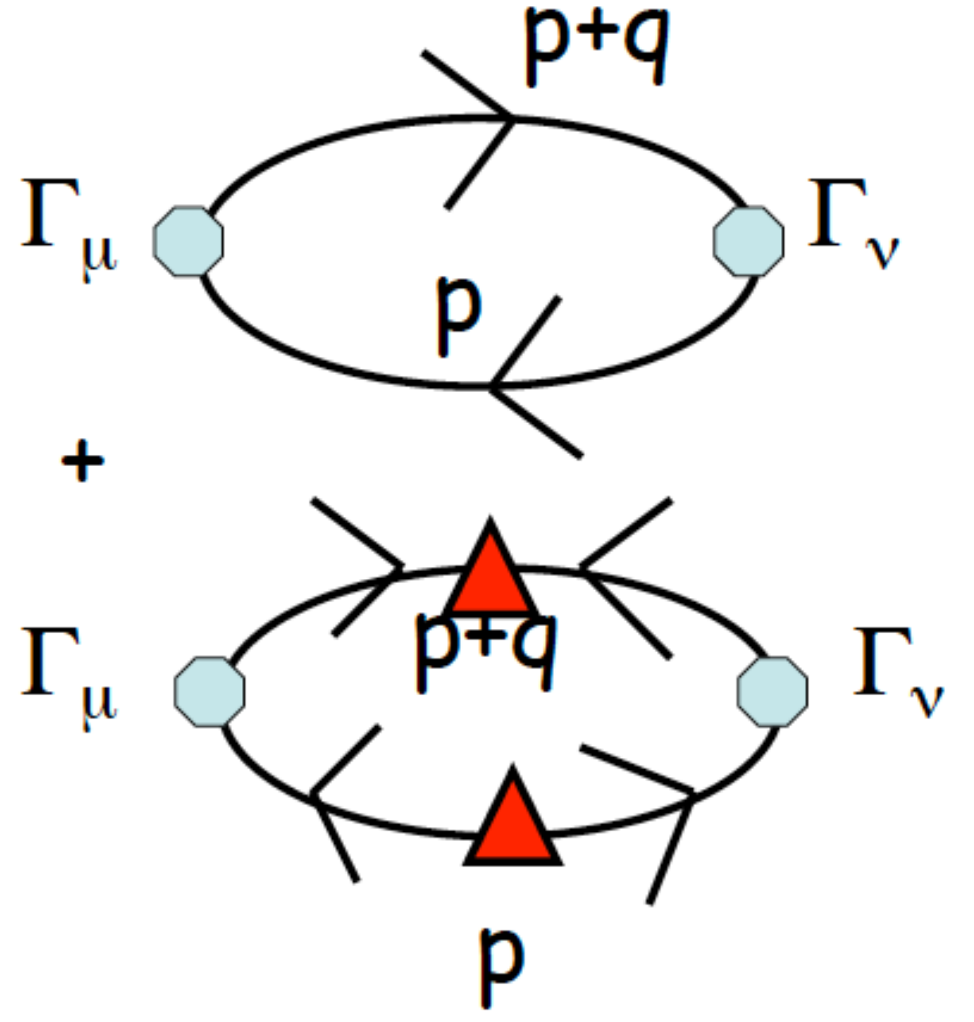

Pairing modifies particle propagation. Particles can be absorbed or emitted from the condensate.

Energy gap modifies the energy spectrum.

Response moves to high energy (time-like).
Neutrino scattering is exponentially suppressed.

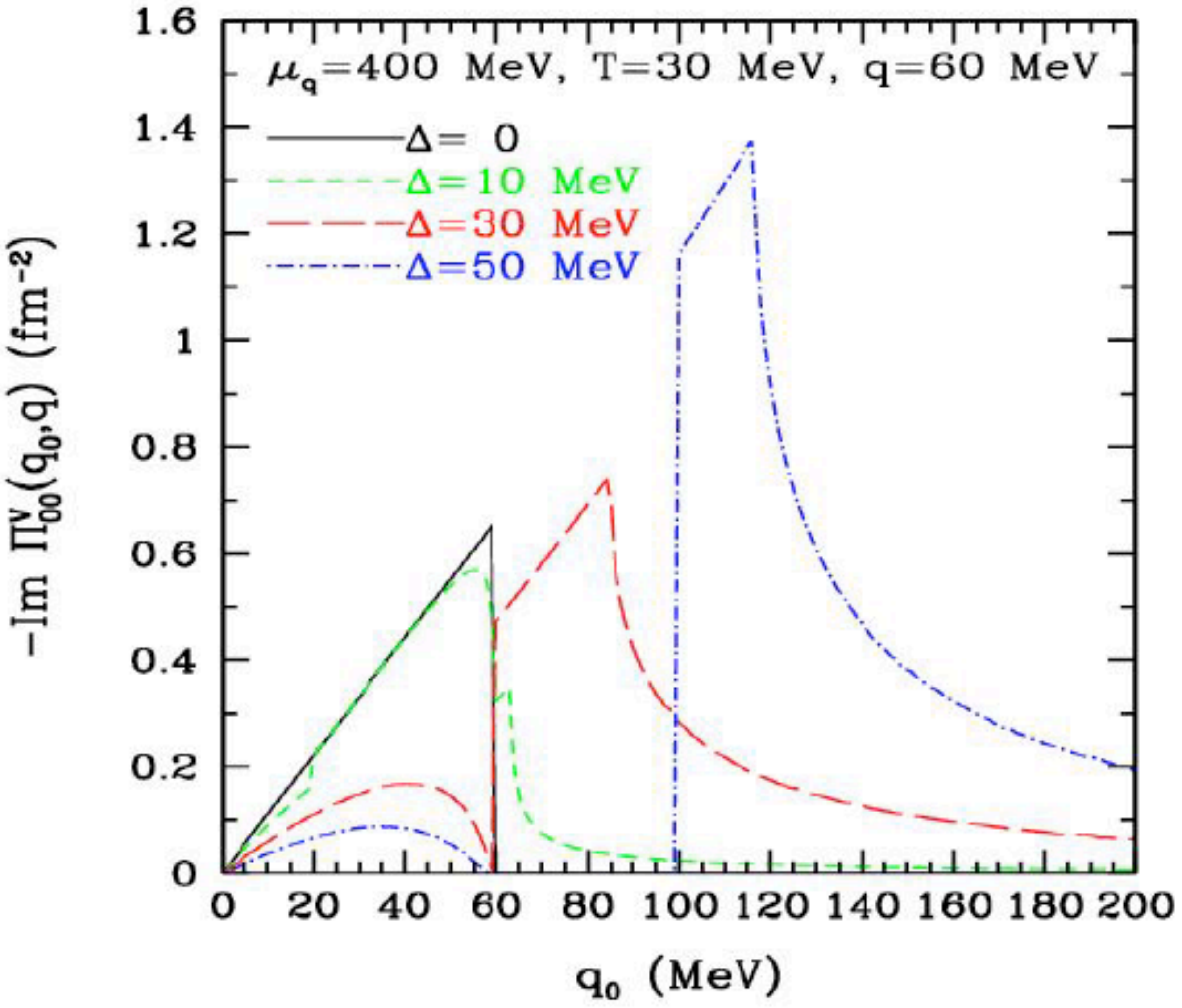

Carter & Reddy (2000)

Neutrino Scattering in Superconducting Quark Matter.

$$\Pi_{\mu\nu}(q_0, q) = -i \int d^4p \ \mathrm{Tr}[G(p+q)\Gamma_\mu G(p)\Gamma_\nu]$$

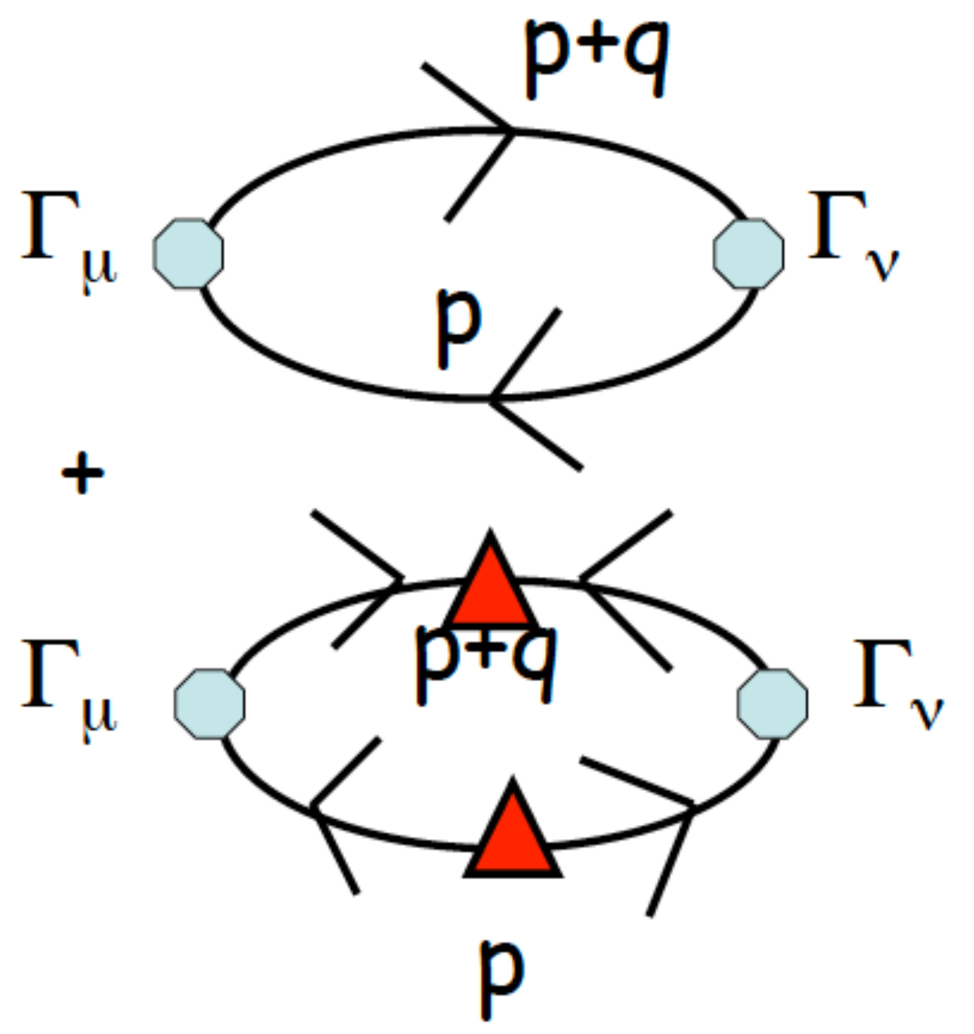

Pairing modifies particle propagation. Particles can be absorbed or emitted from the condensate.

Energy gap modifies the energy spectrum.

Response moves to high energy (time-like). Neutrino scattering is exponentially suppressed.

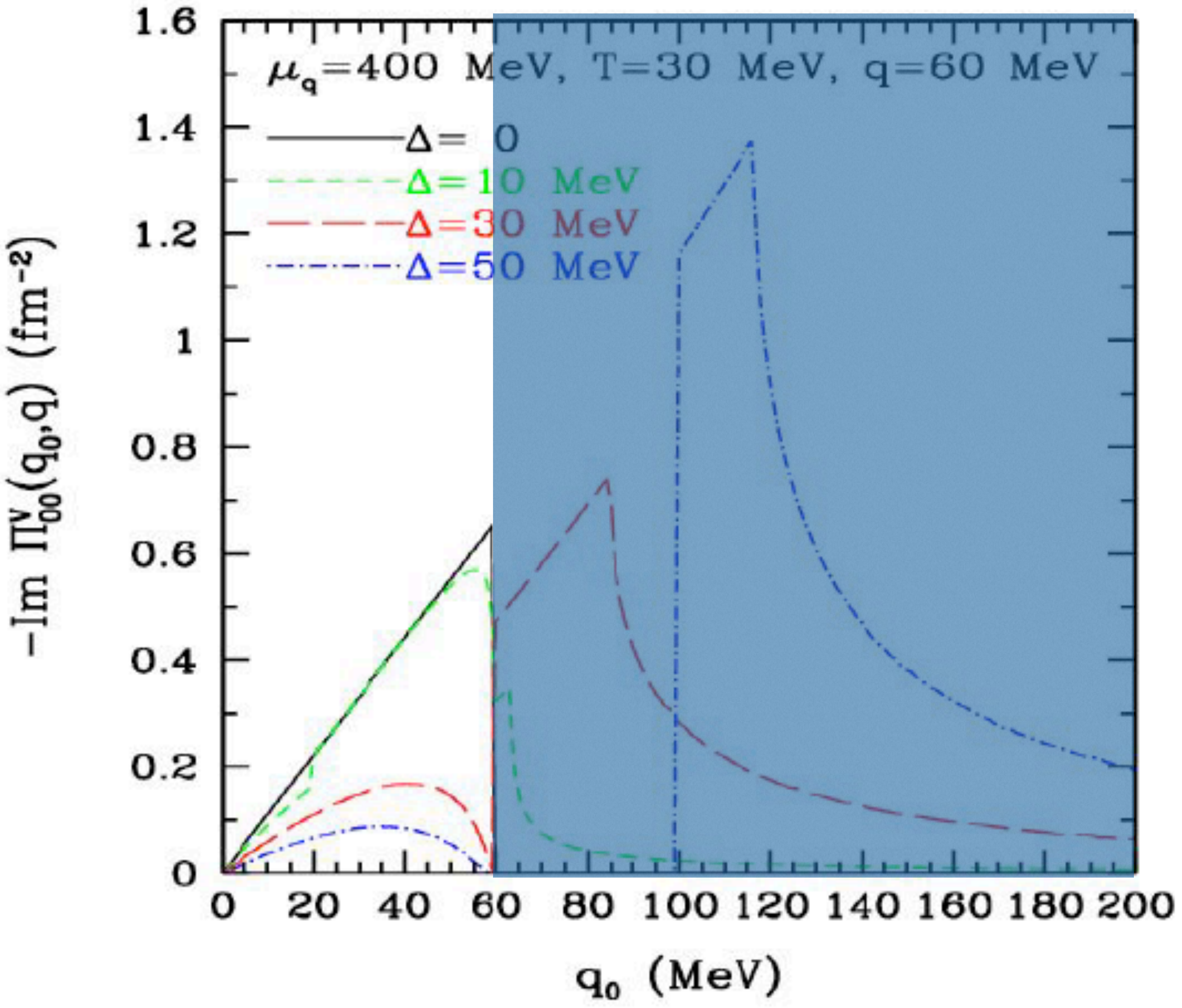

Carter & Reddy (2000)

Neutrino Scattering in Superfluid Quark Matter.

- Superfluid state has a Goldstone boson.
- Neutrinos couple to these modes.
- Arises naturally in RPA.
- At $T \ll T_c$ this is the only relevant mode for neutrino scattering.

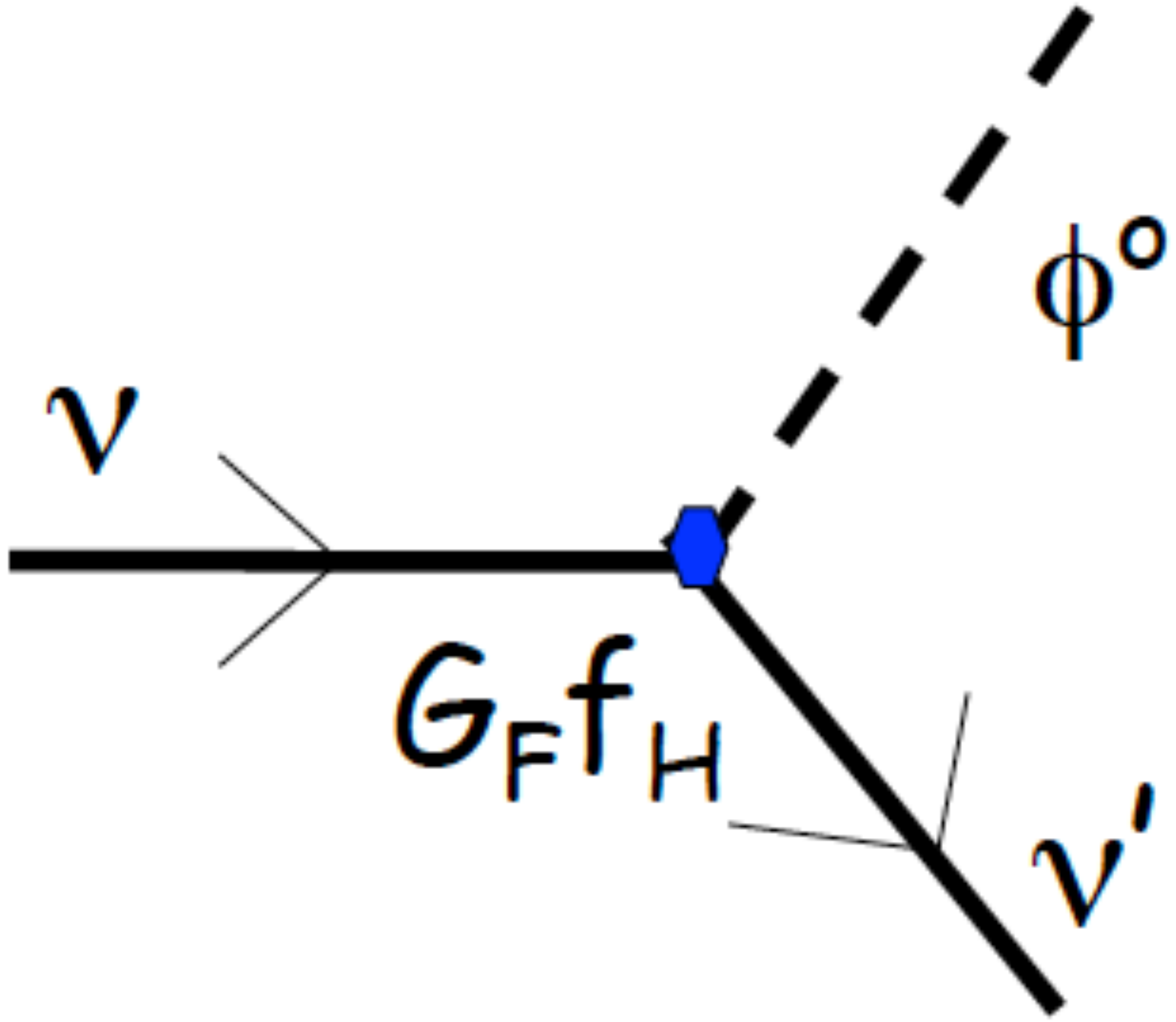

Ultra Dense Matter is Opaque to Neutrinos but Transparent to Photons!

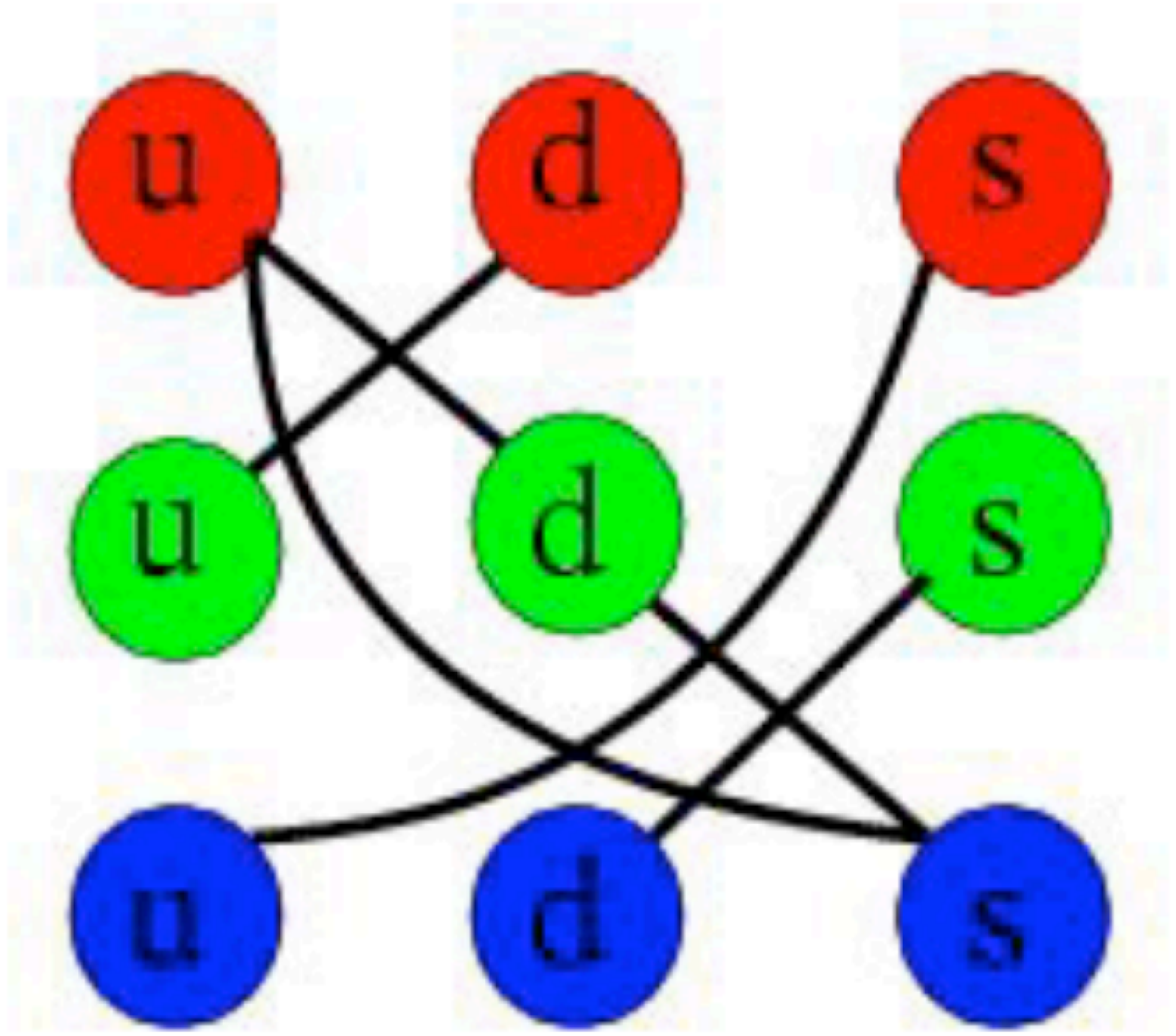

$$SU(3)_{color} \otimes SU(3)_L \otimes SU(3)_R \otimes U(1)_B$$
$$\Downarrow$$
$$SU(3)_{color+L+R} \otimes Z_2$$

Ultra Dense Matter is Opaque to Neutrinos but Transparent to Photons!

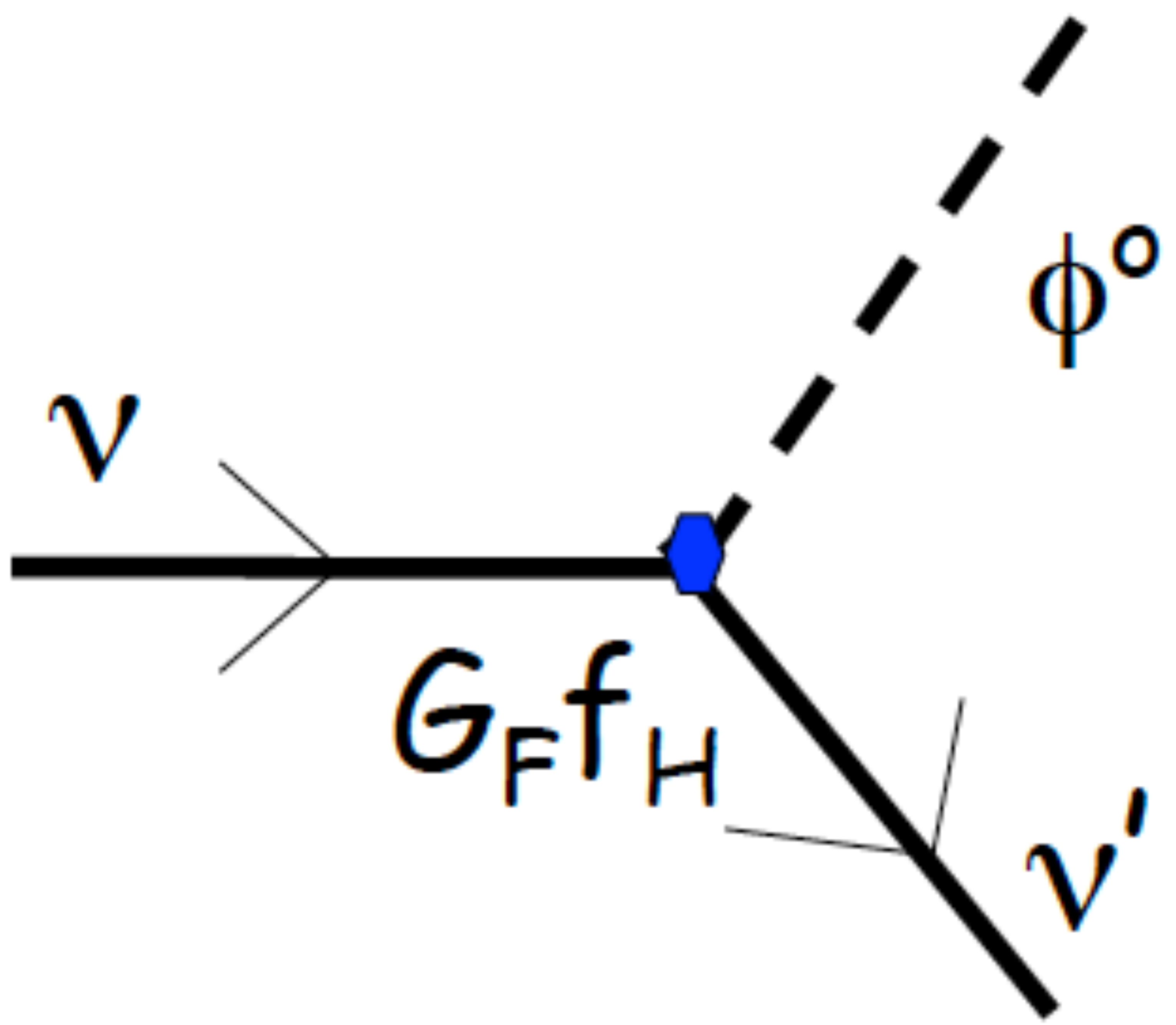

$$SU(3)_{color} \otimes SU(3)_L \otimes SU(3)_R \otimes U(1)_B$$
$$\Downarrow$$
$$SU(3)_{color+L+R} \otimes Z_2$$

Ultra Dense Matter is Opaque to Neutrinos but Transparent to Photons!

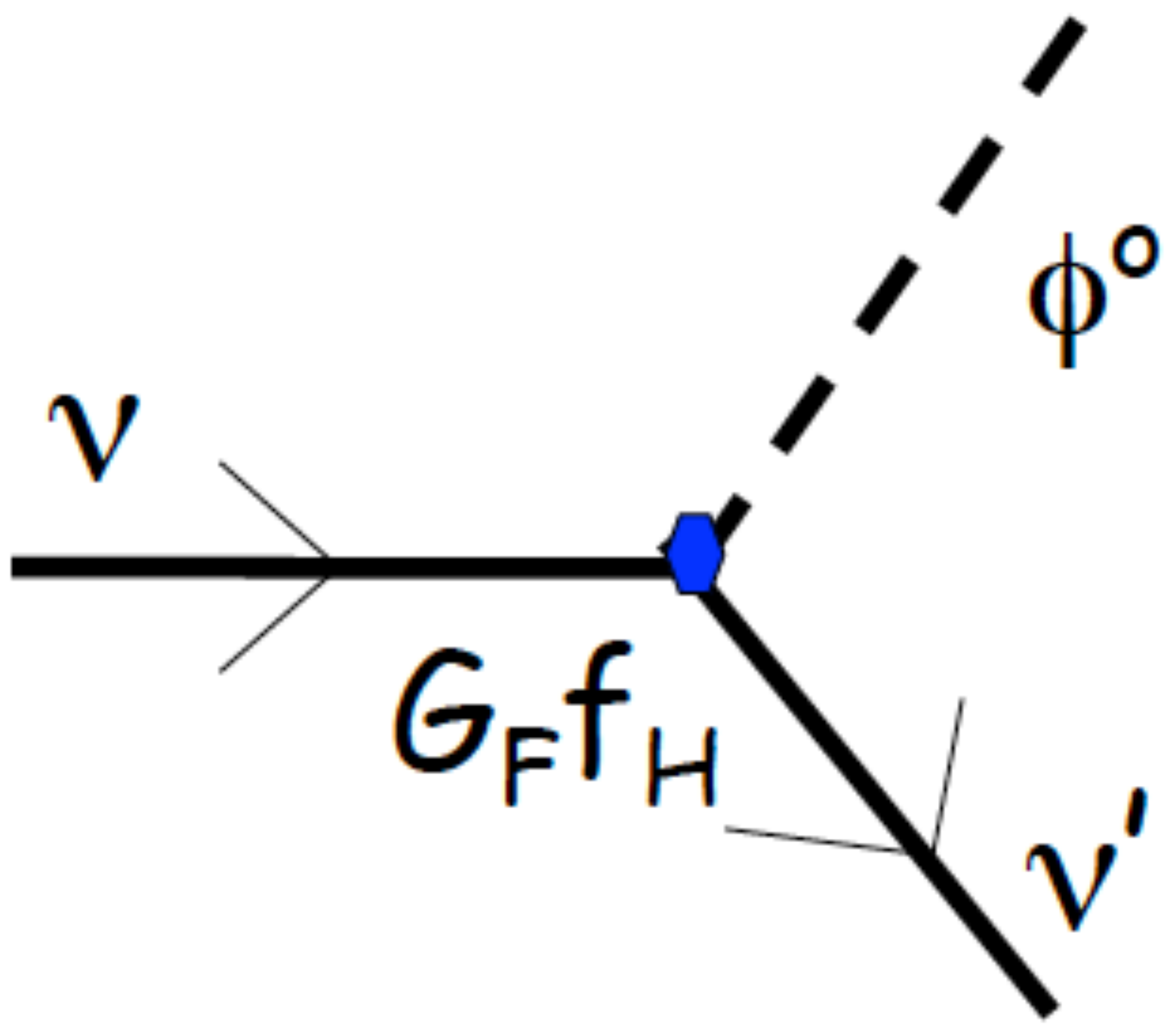

$$\frac{1}{\lambda_{\nu\to H\nu}(E_\nu)} = \frac{256}{45\pi}\left[\frac{v(1-v)^2(1+\frac{v}{4})}{(1+v)^2}\right] G_F^2\, f_H^2\;\, E_\nu^3$$

$$SU(3)_{color} \otimes SU(3)_L \otimes SU(3)_R \otimes U(1)_B$$
$$\Downarrow$$
$$SU(3)_{color+L+R} \otimes Z_2$$

Ultra Dense Matter is Opaque to Neutrinos but Transparent to Photons!

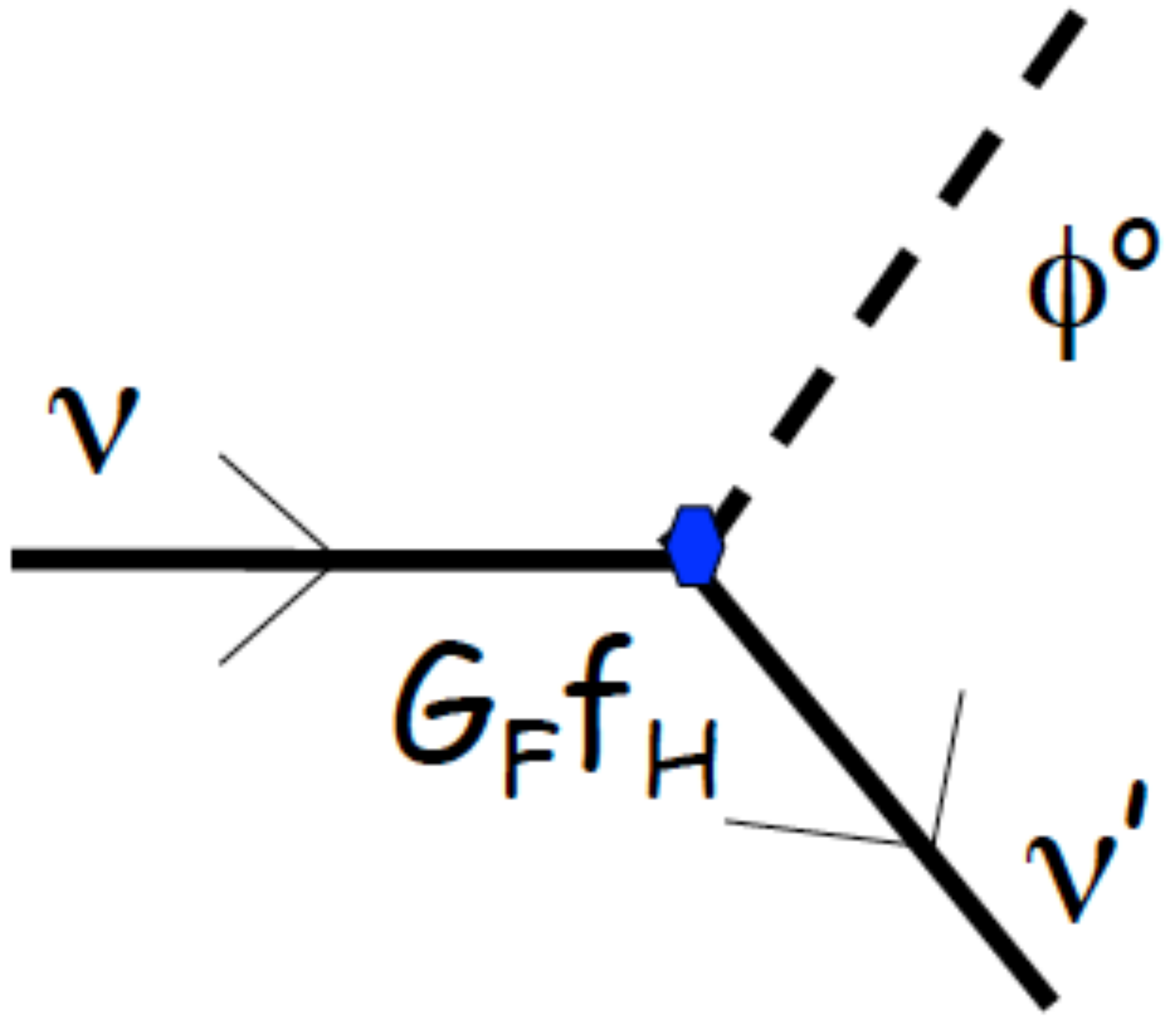

$$\frac{1}{\lambda_{\nu\to H\nu}(E_\nu)} = \frac{256}{45\pi}\left[\frac{v(1-v)^2(1+\frac{v}{4})}{(1+v)^2}\right] G_F^2\, f_H^2\;\; E_\nu^3$$

More Opaque than the Normal Phase !

phase	process	λ(T=5 MeV)	λ(T=30 MeV)
Nuclear	$\nu n \to \nu n$	200 m	1 cm
Matter	$\nu_e n \to e^- p$	2 m	4 cm
Unpaired	$\nu q \to \nu q$	350 m	1.6 m
Quarks	$\nu d \to e^- u$	120 m	4 m
CFL	λ_{3B}	100 m	70 cm
	$\nu\phi \to \nu\phi$	>10 km	4 m

$$SU(3)_{color} \otimes SU(3)_L \otimes SU(3)_R \otimes U(1)_B$$
$$\Downarrow$$
$$SU(3)_{color+L+R} \otimes Z_2$$

Neutron Star Tomography with Supernova Neutrinos

Temporal features in the late time neutrino signal contains valuable information about the core.

May be the only direct probe of the densest matter in the universe.

Its about time we had a galactic supernovae!

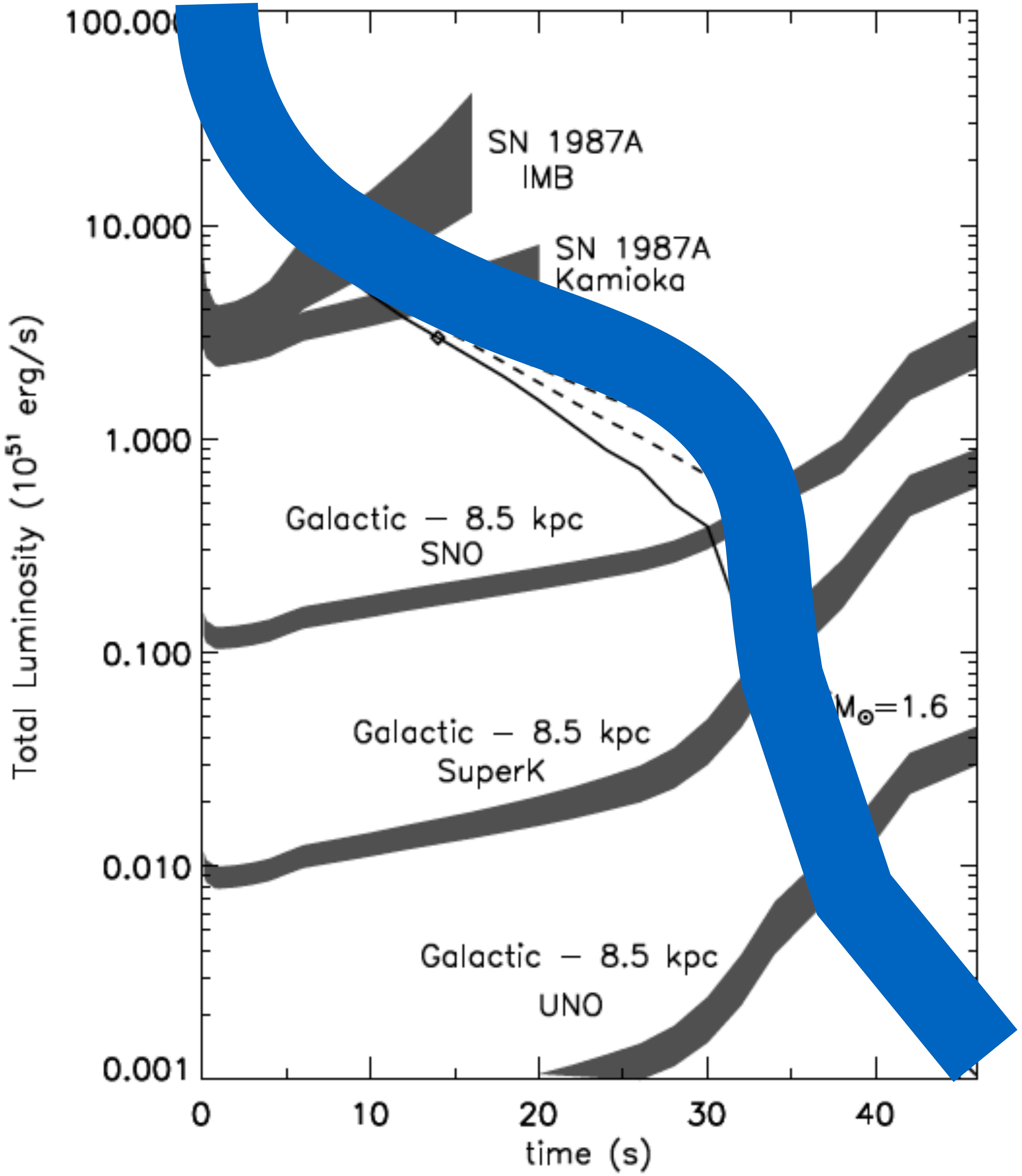

Neutron Star Tomography with Supernova Neutrinos

Temporal features in the late time neutrino signal contains valuable information about the core.

May be the only direct probe of the densest matter in the universe.

Its about time we had a galactic supernovae!